Breeding-aware Revenue Maximization for NFTs on Social Networks

Ya-Wen Teng
Institute of Information Science
Academia Sinica
Taipai, Taiwan
ywteng@iis.sinica.edu.tw

De-Nian Yang
Institute of Information Science
Academia Sinica
Taipai, Taiwan
dnyang@iis.sinica.edu.tw

Yishuo Shi
Statistics and Information Science
Wenzhou University
Zhejiang, China
yishuo@wzu.edu.cn

Guang-Siang Lee
Research Center for Information Technology Innovation
Academia Sinica
Taipai, Taiwan
gslee9822802@citi.sinica.edu.tw

Wang-Chien Lee
Computer Science and Engineering
Pennsylvania State University
Pennsylvania, USA
wlee@cse.psu.edu

Philip S. Yu
Computer Science
University of Illinois Chicago
Illinois, USA
psyu@uic.edu

Ming-syan Chen
Electrical Engineering
National Taiwan University
Taipei, Taiwan
mschen@ntu.edu.tw

Abstract

Non-fungible tokens (NFTs) have emerged as a transformative innovation in art and technology, relying heavily on social networks for promotion and revenue generation. The value of NFTs is profoundly influenced by their scarcity, rarity, and unique breeding mechanisms, which present novel challenges for viral marketing strategies. In this paper, we introduce a new research problem of *NFT Revenue Maximization (NRM)*, which focuses on maximizing revenue from the perspective of NFT marketplaces by optimally selecting users for viral marketing campaigns (NFT airdrops) and determining the ideal quantities of NFTs to release. We prove the hardness of NRM and propose an approximation algorithm named *Quantity and Offspring-Oriented Airdrops (QOOA)*. Our algorithm leverages the concepts of Scarcity-Conscious Revenue and Valuation-based Quantity Inequality to prune suboptimal airdrops and quantities at an early stage. To further enhance revenue through NFT breeding, QOOA identifies and incentivizes Rare Trait Collectors to acquire multiple NFTs with rare traits, facilitating the breeding of high-value offspring. Experimental results demonstrate that QOOA significantly outperforms baselines, achieving up to 3.8 times higher revenue in large-scale social networks.

Conference'17, Washington, DC, USA

ACM ISBN 978-x-xxxx-xxxx-x/YYYY/MM
https://doi.org/10.1145/nnnnnnn.nnnnnnn

CCS Concepts

• **Do Not Use This Code → Generate the Correct Terms for Your Paper**; *Generate the Correct Terms for Your Paper*; Generate the Correct Terms for Your Paper; Generate the Correct Terms for Your Paper.

Keywords

Social influence; optimization; viral marketing

ACM Reference Format:
Ya-Wen Teng, De-Nian Yang, Yishuo Shi, Guang-Siang Lee, Wang-Chien Lee, Philip S. Yu, and Ming-syan Chen. 2025. Breeding-aware Revenue Maximization for NFTs on Social Networks. In . ACM, New York, NY, USA, 34 pages. https://doi.org/10.1145/nnnnnnn.nnnnnnn

1 Introduction

The rise of Non-Fungible Tokens (NFTs) is a significant development at the intersection of art and technology. NFTs date back to 2017 when CryptoKitties, an innovative decentralized finance application utilizing Web3, pioneered trading virtual cats as unique digital assets. Since then, the NFT market has surged, with transactions reaching multimillion-dollar sums, exemplified by digital artist Beeple auctioning his NFT artwork for $69 million [6]. In light of this popularity, brands have increasingly turned to NFTs to boost customer engagement. NFT projects, consisting of limited digital assets verified by blockchain to ensure ownership, have emerged to form a hot market. They have gained traction across diverse categories, including luxury (e.g., Gucci's Gucci Vault Material [21], Louis Vuitton's VIA Treasure Trunk [49], Prada's Timecapsule [35], and Super PUMA [38]), art (e.g., Pudgy Penguins [37], Mutant Ape Yacht Club [28], and Moonbirds Mythic [40]), and entertainment (e.g., CryptoKitties [13] and Axie Infinity [5]), reflecting their

versatility and appeal. To sustain user interest, project creators enhance NFTs' utility by offering practical benefits, generating buzz, or *breeding* new NFT offspring, fostering deeper involvement. To ensure liquidity and revenue, these projects rely heavily on online social networks for promotion.[1]

NFT marketplaces like OpenSea, Blur, and Magic Eden leverage the *airdrop* strategy [7, 9, 33] for viral marketing.[2] Due to fierce competition, effective promotion strategies are required to attract brands and users to their marketplaces. Practicing the ideas of viral marketing well discussed in the literature, NFT airdrops distribute free NFTs to promote new projects, aiming to boost awareness, increase auction participation, and maximize revenue. However, these platforms typically use simple airdrop rules, such as random distribution (e.g., DoraHacks [8]), rewarding early users (e.g., zkSync [50]), or targeting users of the creator's other projects (e.g., ApeCoin [10] and Beanz [30]). The current practices lacks a sophisticated airdrop algorithm to maximize revenue by increasing transaction prices from NFT auctions and the potential values of their offspring. Thus, there is a research need to devise a new approach, different from conventional influence maximization, for NFT viral marketing by incorporating the unique characteristics of NFTs.

Compared with conventional viral marketing, NFTs exhibit unique characteristics and marketing features: 1) *Auction-based sales*: Most NFT marketplaces utilize auction mechanisms that emphasize *transaction prices* from highest bidders, based on their valuations of the NFTs and the *reserve price* (i.e., the lowest acceptable price). Hence, revenue depends on the highest bids, directly linked to the quantity of NFTs available for sale. 2) *Scarcity-, rarity- and ownership-driven valuation*: Unlike everyday necessities, scarcity, trait rarity, and notable ownership of NFTs significantly elevate their value [94, 109, 144]. A notable example of scarcity and rarity is CryptoPunks #5822, a one-of-a-kind NFT with the rare Alien trait (0.09%), sold for $23.7 million [17]. Meanwhile, ownership history also plays a crucial role, as seen in CryptoPunk #9997. Initially sold for $159,000, its value soared to $4.35 million after being acquired by renowned actor Shawn Yue [16]. 3) *NFT Breeding*: The innovation of NFT breeding, which allows NFTs to breed entirely new and unique offspring, enhances user engagement. These offspring are often rarer and more valuable than their parents, generating additional potential revenue. Axie Angel [2, 3] is a renowned offspring with three exceptionally rare traits: golden shell (0.01%), dreamy papi (0.02%), and pointy nyan (0.02%). Its sale for $1.1 million underscores the significant market value of breeding rare offspring.

Breeding mechanisms are widely used in NFT projects across various categories, including art projects (Heterosis [23] and Roaring Leaders [41]) and entertainment projects (STEPN [42], CryptoKitties [13], and Axie Infinity [5]). Note that as the traits of offspring are heavily influenced by their parents, it is a common practice to restrict the user *breeding quota* to maintain rarity. For instance, in MODragon, a user can generate up to five breeding pairs of NFTs concurrently [27]. Furthermore, users can breed their NFTs with friends' NFTs if available for siring. For example, Roaring Leaders users can engage in *social collaborative breeding*, creating diverse offspring from two users' NFTs [41]. None of the existing viral marketing approaches account for the unique characteristics and restrictions of NFT breeding in revenue maximization.

To the best knowledge of the authors, existing works on revenue maximization are not applicable for NFT viral marketing. Indeed, the unique characteristics of NFTs highlight several new challenges that arise in the pursuit of maximizing NFT revenue: 1) *Maximizing transaction prices*: The revenue from NFTs relies on transaction prices, which correspond to user valuations. To find maximal revenue/transaction prices, we need to consider various NFT quantities which incurs significant computational overhead. Prior works on IM [54, 66, 88, 113, 141, 148] (ignoring user valuations) and RM/PM [55, 61, 72, 73, 82, 90, 103, 129, 137, 138] (assuming fixed valuations) fail to accurately and efficiently evaluate revenue across varying quantities. 2) *Balancing scarcity and widespread adoption*: NFT viral marketing needs to jointly determining the for-sale quantity and selecting airdrops. While a larger quantity enables more transactions, it also reduces user valuations due to diminishing scarcity. This trade-off necessitates evaluating each quantity to determine the optimal solution, introducing substantial computational complexity. Previous works [54, 55, 61, 66, 72, 73, 82, 88, 90, 103, 113, 129, 137, 138, 141, 148] do not determine appropriate quantities for sale, making them inapplicable to addressing this trade-off. 3) *Leveraging NFT breeding*: Ensuring that users personally own multiple NFTs or have friends who hold NFTs is crucial for increasing breeding opportunities and maximizing revenue. Moreover, the rarity and ownership of NFT offspring significantly influence their value, underscoring the importance of strategically directing NFT viral marketing to facilitate breeding. However, preventing over-concentration of influence on specific user groups is essential, as such imbalances could leave many acquired NFTs unbred due to breeding quota limitations, ultimately reducing revenue. Previous works [54, 55, 61, 66, 72, 73, 82, 88, 90, 103, 113, 129, 137, 138, 141, 148], disregarding users' simultaneous influence from seed groups across multiple items, have limited ability to account for breeding and maximize revenue.

In this paper, we formulate a new problem, named *NFT Revenue Maximization (NRM)*. Given a social network in a marketplace, an NFT project with traits, reserve prices, and quantity limits, a user breeding quota, and a set of airdropping budgets, NRM aims to promote the project by determining NFT airdrops on the social network for viral marketing and the for-sale quantity of each NFT, to maximize revenue from the auctions of NFTs and the potential values of their offspring. The number of airdrops for each NFT is subject to the airdropping budget, and the quantity of each NFT is restricted by the quantity limit.

Example 1.1. Figure 1 illustrates an example for promoting a new NFT project consisting of three NFTs (denoted as n_1, n_2, and n_3) within a social network. Figure 1(a) shows the traits and (potential) assessments under different quantities of NFTs and their offspring. As shown in the project, the traits 'pink plaid' and 'flower' appear in only one NFT, making them rarer than 'leather,' which is found in two NFTs. As users may prefer different NFTs, their valuations of an NFT may be determined by multiplying their preferences for the NFT with its assessment. Figure 1(b) shows a social network where nodes represent users, edges represent friendships, edge weights

[1] Additional real-world examples for NFTs are provided in Appendix A.

[2] Since marketplaces earn commissions (e.g., a 2.5% service fee on the transaction prices at OpenSea), they are incentivized to promote hosted NFT projects.

		NFT project			New offspring
NFT		n_1 	n_2 	n_3 	
Traits		Leather, Flower	Leather	Pink plaid	Pink plaid, Flower
(Potential) Assessment under different quantities	1	11.02	6.05	8.17	11.02
	2	5.21	2.86	3.86	5.21
	3	4.06	2.23	3.00	4.06

(a) An NFT project and new offspring.

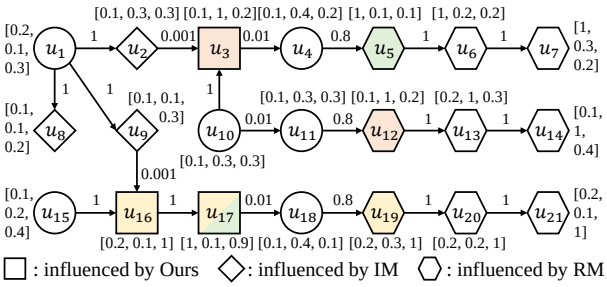

(b) A social network.

Figure 1: An illustrative example.

denote activation probabilities, and vectors near nodes indicate their preferences of NFTs. A promotion campaign for an NFT project is considered, where each NFT has an airdropping budget of 1 and a reserve price of 2.6. Based on the approach proposed in this paper, it airdrops n_1, n_2, and n_3 to u_{15}, u_{10}, and u_{15}, respectively, with quantities set at 1, 1, and 2. This results in an expected revenue of 28.72, including 4.32 contributed by an NFT offspring with rare traits (e.g., 'flower' and 'pink plaid') bred by u_{17}, who owns both n_1 and n_3 (bid winners indicated by squares, purchased NFTs by color). In contrast, RM/PM approaches, that disregard NFT supply and breeding, distribute NFTs to unrelated users (indicated by hexagons), limiting offspring revenue generation and resulting in an expected revenue of 20.19. Similarly, IM methods that overlook valuations lead to low transaction prices (indicated by diamonds), yielding an expected revenue close to 0 (detailed in Appendix B).

We prove that NRM is NP-hard and cannot be approximated within a factor of $|V|^{1/(\log\log|V|)^c}$ following the exponential time hypothesis (ETH), through a reduction from the Densest k-Subgraph problem, where $c > 0$ is a constant independent of $|V|$, and V is the set of users. To solve NRM, we design an approximation algorithm, named *Quantity and Offspring-Oriented Airdrops (QOOA)*, which incorporates several novel ideas: 1) To improve computational efficiency, QOOA introduces the notion of *Scarcity-Conscious Revenue (SCR)* to derive an upper bound on potential revenue with respect to a given set of users. SCR can be estimated efficiently for different quantities, enabling the rapid pruning of ineffective candidates. 2) To eliminate redundant searches over ineffective quantities, QOOA introduces *Valuation-based Quantity Inequality (VQI)* to derive upper bounds on revenue for different quantities, allowing QOOA to efficiently determine whether certain quantities can be pruned before performing a search for airdrops. 3) To increase revenue from NFT offspring, QOOA specifically targets users more likely to generate higher expected additional revenue, namely *Rare Trait Collectors (RTCs)*. QOOA introduces the notion of *Valuable Offspring Generation Utility Estimation (VOGUE)* to evaluate a user's potential to influence RTCs and their friends to hold rare NFTs and breed valuable offspring, and further leverages the *Breeding Index (B-Index)* to capture both individual and collaborative breeding potential while accounting for the user breeding quota. By tailoring the airdrops with high-VOGUE alternatives, QOOA increases the expected additional revenue across different breeding possibilities, thereby maximizing total revenue. We prove that QOOA is an approximation algorithm with a guaranteed performance bound and evaluate its performance on real NFT projects. In addition to promoting NFT projects, QOOA can be applied in various scenarios, such as *loyalty-aware marketing* and *demand-side economies of scale*. The contributions include:

- To the best of our knowledge, NRM, by considering auction-oriented viral marketing, NFT scarcity, trait rarity, and NFT breeding, has not been studied previously. We prove the hardness and inapproximability of NRM.
- We design an approximation algorithm QOOA for NRM. By exploiting SCR and VQI, QOOA efficiently finds airdrops that maximize revenue with a performance bound. Furthermore, QOOA identifies RTCs and tailors airdrops to enhance their potential for generating rare offspring.
- Experiments on data of real NFT projects demonstrate that QOOA achieves revenue up to 3.8 times over the baselines.

2 Related Work

Existing research on viral marketing has explored the problems of maximizing the influence, revenue, and profit of multiple products within a company. Previous studies [66, 148] assume that products are independent of each other and thus focus on optimizing the adoption of each product individually. Follow-up studies [54, 88, 113, 141] consider the interdependencies between product adoptions, such as complementary (positive impact) or substitutable (negative impact) relationships. Previous works on revenue/benefit maximization (RM/BM) [55, 61, 72, 73, 82, 103] introduce the concept of benefits related to influenced users or interactions among them, aiming to maximize revenue (derived from the total benefit) rather than focusing on the influence spread. Other studies on profit maximization (PM) [90, 129, 137, 138] further incorporate the cost of seeding to focus on maximizing the difference between revenue and cost.

We summarize the comparison between related work and NRM in Table 1 in Appendix C.1. 1) *Supply-constrained auction-base sale*: Instead of seeking to maximize either the number of influenced users or the total valuation of all influenced users, NRM targets the top valuations among those influenced users, reflecting the limited supply of NFTs. 2) *NFT breeding*: While breeding is entirely overlooked in the above studies, NRM specifically targets the potential transaction prices of offspring, evaluating the expected additional revenue generated by considering all breeding possibilities. The objective of NRM is fundamentally different from that of the above studies. 3) *Scarcity-driven valuation*: Unlike the above studies, where the quantity neither influences the set of influenced users nor their valuations, NRM jointly addresses seed selection

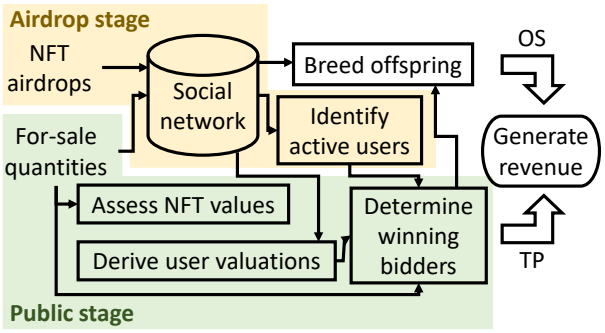

Figure 2: The workflow of NRM.

and quantity determination. Increasing the quantity facilitates more transactions but simultaneously reduces individual valuations due to diminished scarcity. Consequently, the quantity of an NFT for sale becomes a critical decision variable in NRM, directly shaping revenue generation—an aspect not addressed in the existing literature.[3]

3 Problem Formulation

The workflow of NRM is illustrated in Figure 2. We first introduce basic definitions related to NFTs and the social network. Then, we describe the airdrop stage (yellow-shaded region) and public stage (green-shaded region) in NFT marketplaces, followed by the unique breeding mechanisms of NFTs. Finally, we formally define the revenue function and NRM. Additional details are presented in the appendix, including examples (B), the elaboration of Figure 2 (D.1), complete definitions (D.2–D.5), parameter setting and derivation (D.6), discussions on broader applicability (D.7), and the proof of NP-Hard (E.1). Tables 2 and 3 (p. 16) summarize the notation and abbreviations used in this paper.

3.1 Problem Definition

For an NFT project $N = \{n_1, \ldots, n_k, \ldots, n_{|N|}\}$, it is characterized by a set of traits $T = \{t_1, \ldots, t_d, \ldots, t_{|T|}\}$, where a trait t_d is a feature associated with an NFT. Let $Q = \{q_1, \ldots, q_{|N|}\}$ denote the quantity set of N, where q_k is the quantity of n_k. The objective assessment of n_k under a quantity q_k, denoted as $A(n_k, q_k)$, can be obtained based on *scarcity* [94, 109, 144], *rarity* [85, 112], and *ownership* [107] (top-left box in the greed-shaded region in Figure 2). Specifically, $A(n_k, q_k)$ is likely to boost when q_k is small, traits in T_k are rare, and n_k is held by notable users.

In addition to the objective assessments of NFTs, we introduce users' subjective valuations on NFTs (bottom-left box in the greed-shaded region in Figure 2). Given a social network $G = (V, E)$ within the NFT marketplace, where V is the user set and E is the edge set, each user $u_i \in V$ has a personal preference for an NFT n_k, denoted as $w_{u_i,n_k} \in [0, 1]$, and each edge $e_{i,j} \in E$ indicates that $u_i \in V$ has an activation probability of $a_{i,j}$ to influence $u_j \in V$. Following [96, 97], a user u_i's valuation on an NFT n_k is derived according to u_i's subjective personal preference for n_k (i.e., w_{u_i,n_k}) and the objective value assessment of n_k (i.e., Equation (10)),

$$v_{u_i,n_k}(q_k) = w_{u_i,n_k} \cdot A(n_k, q_k). \tag{1}$$

In most NFT marketplaces, e.g., OpenSea [34], the launch process of NFTs consists of two stages: the *airdrop* stage for viral marketing and the *public* stage for auction. Let $S = \{(u_i, n_k), \ldots\}$ and $P = \{p_1, \ldots, p_{|N|}\}$ denote a set of NFT airdrops and the set of reverse prices of N, respectively, where (u_i, n_k) represents an NFT airdrop that provides a free NFT $n_k \in N$ to a user $u_i \in V$, and p_k is the reserve price of n_k.

The airdrop stage (yellow-shaded region in Figure 2) leverages a set of airdrops S to promote the NFT project N through diffusion over a social network, following a chosen model such as PTC, MF, TSC-HDM, LT, or IC [62, 81, 92, 126]. A user is considered an active user of n_k if they are successfully influenced by the airdrops $S_k \subseteq S$ of that specific NFT. The public stage (green-shaded region in Figure 2) then conducts an auction for n_k, targeting the top q_k bidders among its active users. Only those with valuations no less than the reserve price p_k are eligible. A user u_i who wins n_k pays a transaction price equal to their valuation $v_{u_i,n_k}(q_k)$, which satisfies $v_{u_i,n_k}(q_k) \geq p_k$. Note that n_k may remain partially unsold if fewer than q_k active users either meet the reserve price or are interested in purchasing it. Based on the airdrop and public stages, we first introduce the total transaction price function.

Definition 3.1 (Total Transaction Price Function). Given an NFT project N, the reserve prices P, and a social network G, the total transaction price generated from airdrops S for N with quantities Q is defined as follows (bottom-right arrow in Figure 2).

$$TP(S, Q) = \sum_{k=1}^{|N|} TP_k(S_k, q_k) = \sum_{k=1}^{|N|} \sum_{u_i \in V(S_k, q_k)} v_{u_i,n_k}(q_k), \tag{2}$$

where $TP_k(S_k, q_k)$ is the total transaction price of n_k influenced by S_k under the quantity q_k, $S_k \subseteq S$ is the set of airdrops of n_k, and $V(S_k, q_k)$ is the set of active users to hold the NFT n_k under the influence of S_k with the quantity q_k.[4]

Accordingly, the fundamental problem without breeding for promoting an NFT project N is to maximize the transaction price TP by finding a set of airdrops S and a set of NFT quantities Q for N, subject to the budget $B = \{b_1, \ldots, b_{|N|}\}$ and quantity limit $L = \{l_1, \ldots, l_{|N|}\}$ constraints, which restrict the number of airdrops (i.e., $|S_k| \leq b_k$) and the quantity for sale (i.e., $q_k \leq l_k$), respectively.[5]

However, as NFT breeding mechanisms allow the NFT holders to breed offspring after the airdrop and public stages (top-right box in Figure 2), potentially generating additional revenue, the aforementioned setting is insufficient to fully capture the dynamics of the NFT market. To address this limitation, we first introduce specific constraints and mechanisms related to breeding, inspired by prominent NFT projects such as CryptoKitties [14, 15], Roaring Leaders [41],

[3] The review of NFTs in social networks is presented in Appendix C.2.

[4] The set $V(S_k, q_k)$ depends on the influence diffusion of S_k and q_k. While it can be viewed as a random set in this context, for ease of illustration, we follow [135, 136] and adopt the concept of the live-edge graph, where each edge represents a realized influence pathway that deterministically determines whether a node can be reached from S_k. This ensures that $V(S_k, q_k)$ is uniquely determined by the connectivity of S_k in a live-edge graph and is therefore deterministic.

[5] Details on the airdrop and public stage as well as the formal definition of the fundamental problem without breeding is presented in Appendix D.4.

Axie Infinity [26], and MODragon [27], and then incorporate them into our problem formulation.[6]

Definition 3.2 (Breeding Constraints). The breeding process is subject to the following constraints: (1) Non-concurrent breeding: each NFT held by user u_i can participate in at most one breeding pair at a time; (2) User breeding quota: each user u_i can engage in at most c_{BQ} breeding pairs simultaneously; and (3) Inheritance: for each breeding pair (n_k, n_m), the offspring $o_{k,m}$ inherits all its traits from the parents, i.e., $\forall t \in T_{k,m}, t \in T_k \cup T_m$, where $T_{k,m}$ denotes the trait set of $o_{k,m}$.

Definition 3.3 (Breeding Mechanisms). Users can generate offspring NFTs through two mechanisms: individual breeding and collaborative breeding. In both cases, each user u_i initiates breeding with probability β_i and produces an offspring $o_{k,m}$ owned by u_i, i.e., $H_{k,m} = u_i$. In individual breeding, u_i selects two distinct NFTs from their own collection to form a breeding pair (n_k, n_m). In collaborative breeding, u_i selects one NFT n_k from their own collection and pairs it with a friend u_j's NFT n_m, which is chosen with probability γ_j from u_j's collection.

As the diffusion of airdrops S for the NFT project with Q reaches different users, it affects the potential breeding of NFT offspring (e.g., the total number of new NFT offspring and the owners of them). Following [85, 112, 127], the objective assessment of $o_{k,m}$, denoted as $A(o_{k,m}, S, Q)$, is also derived according to scarcity, rarity, and ownership.

Definition 3.4 (Offspring's Potential Transaction Price Function). Given an NFT project N, the reserve prices P, a social network G, and a user breeding quota c_{BQ}, the potential transaction prices of NFT offspring generated from airdrops S for N with quantities Q are defined as follows (top-right arrow in Figure 2).

$$OS(S,Q) = \sum_{u_i \in \bigcup_{k=1}^{|N|} V(S_k, q_k)} \sum_{z=1}^{c_{\mathrm{BQ}}} \mathbb{E}[\mathcal{V}(o_z^i, S, Q)], \tag{3}$$

where o_z^i is the z-th offspring bred by u_i within the quota c_{BQ} under the influence of S with quantities Q, and $\mathbb{E}[\mathcal{V}(o_z^i, S, Q)]$ is its expected transaction price (detailed in Appendix D.3).

As NFT marketplaces earn revenue from the service fees charged based on transaction prices [75], it is natural for the revenue function to take into account both the transaction prices of current NFTs and the potential transaction prices from NFT offspring. The revenue function is thus defined as follows.

Definition 3.5 (Revenue Function). Given an NFT project N, the reserve prices P, a social network G, and a user breeding quota c_{BQ}, the revenue generated from airdrops S for N with quantities Q consists of the transaction prices of *NFTs in N* (i.e., Definition 3.1) and the potential transaction prices of *NFT offspring generated from N* (i.e., Definition 3.4) as follows (right-most box in Figure 2).

$$f(S,Q) = TP(S,Q) + \lambda \cdot OS(S,Q), \tag{4}$$

where λ is associated with the liquidity of N to adjust the weighting of OS by following [36, 116].[7]

Formally, we formulate *NFT Revenue Maximization (NRM)* as follows. Note that it can also be applied in various scenarios, such as *loyalty-aware marketing* and *demand-side economies of scale*.

Problem: *NFT Revenue Maximization (NRM)*[8]
Instance: An NFT project $N = \{n_1, n_2, \ldots, n_{|N|}\}$ with traits T and their reserve prices P, a social network G, a user breeding quota c_{BQ}, a set of airdrop budgets B for N, and a set of quantity limits L.
Task: To promote the NFT project N by finding a set of airdrops S and a set of NFT quantities Q for N, such that the non-concurrent breeding, user breeding quota, inheritance, budget, and quantity limit constraints hold. The objective is to maximize revenue $f(S,Q)$.

Theorem 3.1. *NRM is NP-hard and cannot be approximated within a factor of* $|V|^{1/(\log\log|V|)^c}$ *assuming the exponential time hypothesis (ETH), where* $c > 0$ *is a constant independent of* $|V|$.

Proof. Please refer to Appendix E.1 for the details. □

4 Approximation Algorithm

4.1 Algorithm Overview

To efficiently solve NRM, we design an approximation algorithm, namely *Quantity and Offspring-Oriented Airdrops (QOOA)*, based on the following new ideas.[9] 1) To identify the best set of airdrop recipients who can effectively influence potential buyers and maximize revenue, it is essential to efficiently filter out unlikely candidates. Thus, we propose the notion of *Scarcity-Conscious Revenue (SCR)* to evaluate possible revenue w.r.t. a set of users selected for airdrops. Given an NFT and a specific quantity for it, let *reserve-price acceptors* (*acceptors* for short) be the users with valuations no smaller than its reserve price. QOOA first finds the likelihood for each user in the social network to influence the acceptors. As such, SCR can be exploited to derive the upper bound of revenue from a set of candidate airdrop users by calculating the likelihood they influence the acceptors and evaluating their valuations. Equipped with SCR, QOOA efficiently prunes ineffective users for airdrops. Due to limited quantities, TP (Equation (2)) is not submodular (proven in Lemma E.3), making pruning strategies [63, 68, 76] (relying on submodularity) inapplicable.

2) To increase revenue from NFT offspring, we target users with high impact (who can elevate the offspring's assessment) and their friends (who may leverage collaborative breeding) to produce offspring with rare traits within the user breeding quota. QOOA identifies *Rare Trait Collectors (RTCs)* as users who may acquire at least one NFT with the rarest traits. For each such rare-trait NFT, QOOA introduces *Valuable Offspring Generation Utility Estimation (VOGUE)* to evaluate a user's potential to influence RTCs and their friends to hold this NFT and breed valuable offspring. We also design *Breeding Index (B-Index)* to measure the likelihood for RTCs and their friends to participate in breeding rare offspring. Users with

[6] More details and complete definitions of breeding, along with the flexibility of NRM to accommodate various breeding mechanisms, such as boosters and only individual breeding, are provided in Appendix D.5. Meanwhile, our proposed approach, QOOA, also supports these mechanisms, as detailed in Appendix G.1.

[7] High liquidity enhances the likelihood of newly generated offspring being sold, leading to a higher λ. The liquidity of an NFT project can be predicted based on social network engagement [36] and transaction intervals [116].

[8] Discussions on problem parameters are presented in Appendix D.6.

[9] Table 1 (p. 15) demonstrates that prior works are inadequate to solve NRM.

greater B-Index exhibit great breeding probabilities and significant impacts, or possess great siring probabilities if they are friends of RTCs and potentially engaged in collaborative breeding, while likely contributing to high TP. Consequently, QOOA finds alternative airdrops with high VOGUE to replace the original airdrops, leading to the breeding of more valuable NFT offspring.

3) To deal with the trade-off between scarcity and widespread adoption, we derive *Valuation-based Quantity Inequality (VQI)* to efficiently find the upper bound of revenue subject to the NFT quantity. Specifically, the active users with the highest valuations are vital since their bids set the transaction prices and revenue. However, due to the reserve price restriction, the highest bidders do not always win the auction. When a larger quantity is available, user valuations drop as the NFT becomes less scarce, though revenue may rise due to additional transactions generated. If user valuations fall below the reserve price, no additional transaction is achieved. Hence, VQI carefully finds the exact number of acceptors under various quantities, in order to establish tight upper bounds on revenue to efficiently prune redundant searches for the quantities producing low revenue.

In summary, QOOA consists of two steps: Quantity-driven Airdrop Selection (QAS) and Offspring Revenue Enhancement (ORE). For each NFT, QAS evaluates SCR w.r.t. different sets of users to efficiently find airdrops that maximize TP. It iteratively evaluates revenue with increasing quantities until no more revenue can be increased while efficiently trimming redundant searches, by exploiting the upper bound of revenue derived by VQI. As the best NFT airdrops and quantities identified in QAS do not account for breeding, QOOA leverages ORE to improve revenue from breeding by encouraging RTCs and their friends to purchase multiple rare-trait NFTs. The theoretical analyses of QOOA's correctness, approximation ratio, and time complexity are provided in Appendix E.2. Additional details are presented in the appendix, including illustrative examples (B), pseudo-code and workflow (F.1), detailed deviations (F.2–F.4), and discussions on various breedings, dynamic social networks, and real-world issues (G).

4.2 Algorithm Description

4.2.1 Quantity-driven Airdrop Selection (QAS). QAS aims to maximize revenue by finding the best airdrops and NFT quantities. Let $S_k^{q_k}$ denote the set of airdrops for NFT n_k identified by QAS under quantity q_k. Specifically, for each NFT n_k, QAS starts from $q_k = 1$ and finds S_k^1 that maximizes the total transaction price $TP_k(S_k^1, 1)$. Then, QAS iteratively increases q_k by 1 until q_k reaches the quantity limit l_k. Finally, QAS identifies the best quantities and the corresponding airdrops that maximize TP_k.

To improve efficiency, QAS is equipped with two pruning strategies realized by *Scarcity-Conscious Revenue (SCR)* and *Valuation-based Quantity Inequality (VQI)*. Specifically, SCR is the upper bound of TP_k for a set of airdrops S_k under a specific quantity (proved in Lemma E.2), which prunes ineffective airdrops that generate a smaller TP_k than the best airdrops identified so far. On the other hand, VQI infers the upper bound of TP_k under a specific q_k, irrespective of the airdrop set S_k, to facilitate effective pruning of redundant quantities.

SCR-based pruning. Specifically, for each quantity $q_k = x$ and NFT n_k, to maximize TP_k, QAS iteratively selects the best airdrop and adds it to the current set S_k^x of airdrops. To efficiently prune ineffective airdrops, given a candidate airdrop (u_i, n_k), QAS first evaluates SCR of $\hat{S}_k^x = S_k^x \cup \{(u_i, n_k)\}$ and compares it with TP_k of S_k^x, as SCR serves as the upper bound of TP_k. If SCR of $\hat{S}_k^x$ is smaller than $TP_k(S_k^x, x)$, adding (u_i, n_k) to S_k^x does not yield a greater TP_k. Otherwise, QAS carefully evaluates the marginal gain of TP_k by adding (u_i, n_k) to S_k^x, i.e., $TP_k(\hat{S}_k^x, x) - TP_k(S_k^x, x)$. When the budget is sufficient, i.e., $\left|S_k^x\right| < b_k$, QAS adds (u_i, n_k) to S_k^x if it has the largest positive marginal gain among candidates.[10]

The idea behind SCR w.r.t $\hat{S}_k^x$ is to extract those users who generate the top-x expected revenue of n_k (where $q_k = x$), while being influenced by $\hat{S}_k^x$. The sum of these top-x expected revenue serves as the SCR of $\hat{S}_k^x$. Thus, we define and identify the *reserve-price acceptors* as those who have the potential to generate revenue.

Definition 4.1 (Reserve-price acceptors). Reserve-price acceptors (or acceptors for short) of an NFT n_k are those with the valuations of n_k no smaller than its reserve price. Specifically, for NFT n_k under a specific quantity $q_k = x$ with the reserve price p_k, the set of acceptors is defined as $V_k^{\mathrm{a}}(x) = \{u : v_{u,n_k}(x) \geq p_k\}$.

For each acceptor u, QAS evaluates its *Reserve Reachable Revenue (RR-Rev)* in n_k under the influence of $\hat{S}_k^x$ with quantity $q_k = x$, denoted as $\mathcal{R}_k(u, \hat{S}_k^x, x)$. It takes into account u's valuation on n_k and the likelihood for every user in $\hat{S}_k^x$ to influence u through reverse reachable sets, serving as the upper bound of the expected revenue in n_k when $\hat{S}_k^x$ successfully influences u. Equipped with RR-Rev, QAS evaluates the SCR of a set of users, in order to derive the upper bound of TP_k for $\hat{S}_k^x = S_k^x \cup \{(u_i, n_k)\}$ to decide if (u_i, n_k) is an ineffective airdrop. For NFT n_k with $q_k = x$, SCR of $\hat{S}_k^x$ is defined as the sum of RR-Rev of the acceptors with the top-x RR-Rev.

$$SCR_k(\hat{S}_k^x, x) = \sum_{u \in V_k^{\mathcal{R}}(\hat{S}_k^x, x)} \mathcal{R}_k(u, \hat{S}_k^x, x), \tag{5}$$

where $V_k^{\mathcal{R}}(\hat{S}_k^x, x)$ is the set of acceptors with the top-x RR-Rev in NFT n_k under the influence of $\hat{S}_k^x$. Note that $TP_k(\hat{S}_k^x, x)$ is no greater than $SCR_k(\hat{S}_k^x, x)$. QAS thus skips the evaluation of $TP_k(\hat{S}_k^x, x)$ when $SCR_k(\hat{S}_k^x, x)$ is no greater than $TP_k(S_k^x, x)$, i.e., the greatest total transaction price achieved by the best airdrops identified so far.

VQI-based pruning. After $q_k = x$ is examined, QAS continues to find $S_k^{q_k}$ for $q_k = x + 1$. Before the search for $q_k = x + 1$ starts, QAS derives VQI under the premise that users winning the bid must have valuations no smaller than the reserve price p_k, in order to find the upper bound of TP_k for $q_k = x + 1$, denoted as $UB_k(x + 1)$. If the upper bound $UB_k(x + 1)$ is no greater than the best TP_k generated so far, QAS skips the search for $q_k = x + 1$. After all quantities are examined, QAS assigns $q_k = x'$ and $S_k = S_k^{x'}$, where $TP_k(S_k^{x'}, x')$ is the greatest among all examined quantities.

Ideally, the upper bound $UB_k(x + 1)$ under $q_k = x + 1$ is the sum of the transaction prices of the top-$(x + 1)$ user valuations, assuming that all acceptors with the top-$(x + 1)$ valuations are influenced. Nevertheless, in reality, the number of acceptors under $q_k = x + 1$

[10] Since $TP_k(S_k^x, x)$ is not monotonically increasing (proved in Lemma E.3), adding (u_i, n_k) with a negative marginal gain to S_k^x decreases the revenue, because the total transaction price will be lowered.

may be smaller than $x+1$ due to the reserve price p_k. Therefore, to obtain a more accurate $UB_k(x+1)$, VQI derives the exact number of acceptors under $q_k = x+1$, by carefully examining whether users with the top-$(x+1)$ preferences for n_k have valuations no smaller than p_k. For $q_k = x+1$, $UB_k(x+1)$ is thus derived by considering only the acceptors with top-$(x+1)$ preferences for n_k.

$$UB_k(x+1) = \sum_{y=1}^{\min\{x+1, |V_k^{\mathrm{a}}(x+1)|\}} W_k(y) A(n_k, x+1), \quad (6)$$

where $W_k(y)$ is the y-th largest user preference for n_k, and $A(n_k, x+1)$ is the assessment of n_k with quantity $x+1$. Consequently, if there exists $x' \leq x$ leading to $UB_k(x+1) \leq TP_k(S_k^{x'}, x')$, i.e., $TP_k(S_k^{x+1}, x+1)$ for every possible S_k^{x+1} cannot be greater than TP_k obtained so far, QAS skips the search for $q_k = x+1$.

4.2.2 Offspring Revenue Enhancement (ORE). After QAS identifies the best NFT airdrops and quantities, ORE aims to further increase revenue by encouraging the breeding of rare NFT offspring. It recognizes the NFTs with the rarest traits as *treasures* to serve as the parents in the breeding. Specifically, let $T^{\mathrm{R}} \subseteq T$ denote the set of rarest traits according to the trait rarity in Equation (8).[11] Based on T^{R}, ORE defines the treasures of NFTs (with at least one trait in T^{R}) as $N^{\mathrm{T}} = \{n_k : T_k \cap T^{\mathrm{R}} \neq \emptyset\}$. Accordingly, ORE identifies users purchasing at least one treasure as *Rare Trait Collectors (RTCs)*. Our idea is to encourage RTCs and their friends to purchase more treasures, within the user breeding quota, to breed rare (more valuable) offspring by tailoring the airdrops of the treasures.[12] The treasures are examined sequentially by prioritizing those with more rare traits, since their offspring are more inclined to be highly valuable.

During the examination for each treasure $n_k \in N^{\mathrm{T}}$, ORE introduces the *Valuable Offspring Generation Utility Estimation (VOGUE)* of every user, indicating the potential of a user to influence acceptors to hold treasures and breed valuable offspring. It identifies users with low VOGUE in the original airdrops (i.e., those less helpful for breeding, as the original airdrops identified by QAS do not account for breeding), and finds users with high VOGUE as alternative airdrops to replace them. Particularly, VOGUE prioritizes those alternative airdrops who have potential to influence acceptors that may breed valuable offspring, by targeting i) RTCs with great breeding probabilities (more likely to breed), significant impacts (breeding offspring assessed higher due to ownership), and high aggregated transaction prices of n_k under their influence (avoiding reducing TP significantly), ii) friends of the aforementioned RTCs with great siring probabilities (more likely to participate in breeding) and high aggregated transaction prices of n_k (also avoiding reducing TP significantly), and iii) RTCs holding fewer treasures than c_{BQ} (adhering to the user breeding quota).[13] Thus, the user with the highest VOGUE replaces the originally selected user with the lowest VOGUE in airdrops to improve revenue.

According to the above three criteria, VOGUE is evaluated by considering both the probability of influencing acceptors and the extent to which they are prioritized as targets for purchasing n_k with quantity q_k. We first introduce the *Breeding Index (B-Index)* of an acceptor u_{a} for n_k, denoted as $\mathcal{B}_k(u_{\mathrm{a}}, S, Q)$. An acceptor with a larger B-Index for n_k indicates a greater likelihood of participating in breeding valuable offspring from n_k. Then, based on B-Index, VOGUE of a user $u \in V$ is the sum of the B-Indices of acceptors influenced by u, weighted by their likelihood of being influenced, in order to capture the potential of u to jointly facilitate purchases and collaborative breeding of the treasure n_k under quantity q_k.

$$VOGUE_k(u, q_k) = \sum_{u_{\mathrm{a}} \in V_k^{\mathrm{Val}}(q_k)} \mathcal{B}_k(u_{\mathrm{a}}, S, Q) \cdot oc(u, u_{\mathrm{a}}), \quad (7)$$

where $V_k^{\mathcal{B}}(q_k)$ is the set of acceptors with the top-q_k B-Index, and $oc(u, u_{\mathrm{a}})$ is the likelihood for u to influence u_{a}. A user with a larger VOGUE is more inclined to be chosen as an alternative airdrop, since it enhances the likelihood of breeding valuable offspring.

ORE iteratively tailors the set of airdrops identified by QAS by replacing them with alternative airdrops who have higher VOGUE. This replacement occurs only if it leads to an improvement in expected revenue, considering both TP and OS; otherwise, the current airdrop remains unchanged, ensuring that each adjustment in ORE consistently optimizes overall expected revenue. To this end, ORE first extracts the user u^* not selected for airdrops by QAS (i.e., $u^* \notin \{u : (u, n_k) \in S_k\}$) but having the largest VOGUE. Let $\underline{u} \in \{u : (u, n_k) \in S_k\}$ denote the user identified by QAS for airdrops with the smallest VOGUE. If $\underline{u}$'s VOGUE is smaller than that of u^*, i.e., $VOGUE_k(\underline{u}, q_k) < VOGUE_k(u^*, q_k)$, $\underline{u}$ is less likely to influence acceptors to generate valuable offspring from n_k (compared with u^*). Therefore, ORE opts to airdrop n_k to u^* instead of $\underline{u}$ (i.e., replacing $(\underline{u}, n_k)$ with (u^*, n_k)), to facilitate breeding of rare traits. It updates S as $(S \setminus \{(\underline{u}, n_k)\}) \cup \{(u^*, n_k)\}$ if the above replacement improves total revenue, with both TP and OS, i.e., $f\big((S \setminus \{(\underline{u}, n_k)\}) \cup \{(u^*, n_k)\}, Q\big) > f(S, Q)$.

Theorem 4.1. *QOOA is $\frac{1}{ea(1+c)}$-approximation in $O(l_{\max} b_{\max} |V| |N|)$ time for NRM, where $a = \max_{1 \leq k \leq |N|} \frac{r(\hat{S}_k, 1)}{p_k}$, $c = \frac{\lambda q_{\max} c_{\mathrm{BQ}} \mathcal{V}_{\max}}{p_{\min}}$, $\mathcal{V}_{\max}$ is the maximum potential transaction price of offspring, $p_{\min}$ is the minimum reserve price, $l_{\max} = \max_{l_k \in L} l_k$ is the maximum quantity limit, and $b_{\max}$ is the maximum budget in B.*[14]

Proof. Please refer to Appendix E.2 for details. □

5 Experiments

We conduct experiments on NFT projects: Defimons Characters (Defi) [18], Lascaux (Las) [25], Timpers Pixelworks (Tim) [46], and Gutter Cat Gang (GCG) [22], and social networks: NBA [29], EthereumWAX [115], and Moralis [51].[15] We compare QOOA with state-of-the-art approaches for selecting airdrops: Dysim [141], BGRD [54], RMA [82], TipTop [103], and AG [72]. Additional details are presented in Appendix, including experimental settings (H.1), additional results on the large-scale NFT project (GCG) and execution time (H.2), and case studies (H.3).

[11] Following [112], the top 10% rarest ones are usually discussed.
[12] ORE optimizes expected revenue by increasing the probability of breeding rare offspring, rather than assuming deterministic user behavior, detailed in Appendix F.5.
[13] ORE also supports Only Individual Breeding and Booster, detailed in Appendix F.4.
[14] The relation between NRM's inapproximability and QOOA's approximation ratio is detailed in Appendix E.2.
[15] The rationale of choosing the datasets and baselines is detailed in Appendix H.1.

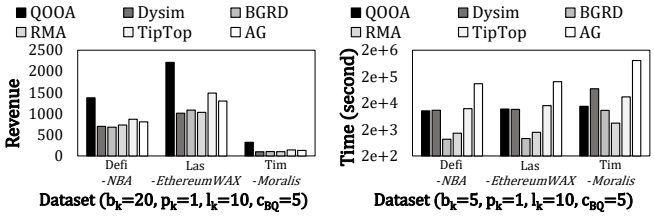

(a) f vs dataset. (b) Time vs dataset.

Figure 3: Comparisons on Defi-*NBA*, Las-*EthereumWAX*, and Tim-*Moralis*.

5.1 Main Results

Figure 3(a) compares the revenues of examined approaches on different datasets. Among them, QOOA achieves the highest revenue by leveraging QAS to maximize TP, instead of focusing on influence spread or total valuation. Specifically, QAS exploits SCR to obtain airdrop candidates, considering their influence on the expected revenue from the top acceptors up to the for-sale quantity, factoring in influence probability, user valuation, and for-sale quantity. Among different datasets, promoting Timpers Pixelworks generates the least revenue due to its significantly lower number of NFTs compared to other projects. Although the numbers of NFTs in Defimons Characters and Lascaux are similar, QOOA achieves considerably higher revenue on Las-*EthereumWAX* than on Defi-*NBA*. This is attributed to the higher NFT rarity in Lascaux and a greater proportion of NFTs with the rarest traits, allowing QOOA to effectively utilize ORE to generate substantial revenue from offspring.

Figure 3(b) compares the execution time on different datasets. As shown, QOOA outperforms all baselines, especially in large-size Tim-*Moralis* dataset, except for BGRD and RMA. BGRD and RMA are faster because they do not spend time optimizing for breeding and identifying airdrops for different quantities, resulting in at most 35% of the revenue by QOOA (as shown in Figure 3(a)). QOOA examines various quantities but leverages VQI to effectively prune redundant quantities, making it faster than TipTop, AG and even the quantity-agnostic Dysim. It is also worth noting that on Tim-*Moralis* which has more users than the other two datasets, the execution time of QOOA does not increase as significantly as other baselines, because QOOA utilizes SCR as an upper bound of revenue to efficiently filter ineffective airdrop candidates, which mitigates the impact of a larger user base. In summary, QOOA significantly outperforms all baselines in terms of revenue with low execution time on multiple datasets of different characteristics, demonstrating superior performance and robustness.

5.2 Sensitivity Tests

Figure 4(a) evaluates the revenue for varied user breeding quotas c_{BQ} on Defi-*NBA*. As c_{BQ} increases, all approaches achieve higher revenue. However, the gap between QOOA and the baselines becomes more pronounced with the growth of the quota. The strength of QOOA is attributed to ORE, which judiciously balances the treasures (rare-trait NFTs) held by RTCs and their friends, ensuring that they optimize the breeding of valuable offspring within the quota. Next, Figure 4(b) compares the revenue of evaluated algorithms on

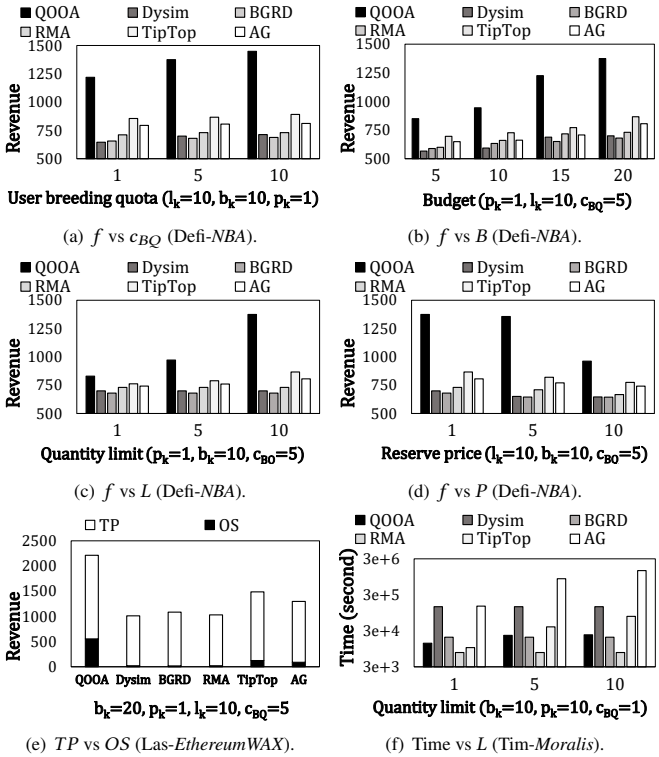

(a) f vs c_{BQ} (Defi-*NBA*). (b) f vs B (Defi-*NBA*).

(c) f vs L (Defi-*NBA*). (d) f vs P (Defi-*NBA*).

(e) TP vs OS (Las-*EthereumWAX*). (f) Time vs L (Tim-*Moralis*).

Figure 4: Sensitivity tests on examined approaches.

Defi-*NBA*, by increasing budget b_k for each NFT n_k. QOOA consistently achieves the highest revenue compared to the baselines, under all budgets. As b_k increases, all approaches yield higher revenue, but the increments from QOOA are the most obvious, followed by TipTop and AG. In addition to different budgets, Figure 4(c) presents the revenue under increasing quantity limits l_k for each NFT n_k. As l_k increases, the revenue obtained by all approaches grows, manifesting that more quantities provide greater opportunities for breeding, subsequently boosting OS. Figure 4(d) shows the revenue with respect to different reserve prices p_k for each n_k. As p_k grows, the revenue for all approaches drops. This is because a higher reserve price reduces the number of acceptors, which not only lowers TP but also diminishes the opportunities for offspring breeding, thereby decreasing OS. In contrast to QOOA, the revenue differences obtained by all baselines under varying c_{BQ}, b_k, l_k, and p_k are insignificant, since they are unable to identify effective airdrops tailored to different breedings to maximize revenue.

Figure 4(e) evaluates the revenue generated by original NFTs (TP) and offspring (OS) on Las-*EthereumWAX*. As shown, QOOA is most effective at achieving high OS because ORE meticulously tailors the airdrops of rare-trait NFTs, encouraging RTCs and their friends with high B-Indices to purchase them simultaneously. Figure 4(f) illustrates the execution time on Tim-*Moralis* under varying quantity limits l_k. As shown, the impact of the growing quantity limit on QOOA's execution time is minor, because QOOA leverages VQI for pruning and thus avoid exhaustive examination.

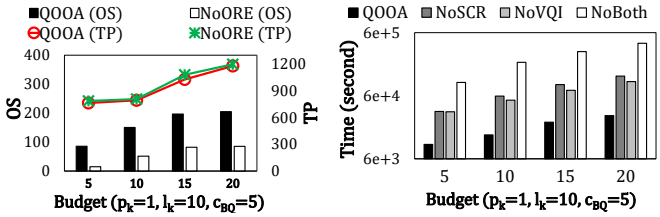

(a) *OS*/*TP* vs *B* (Defi-*NBA*). (b) Time vs *B* (Defi-*NBA*).

Figure 5: Ablation study on QOOA.

5.3 Ablation Study

To evaluate the efficacy of SCR, VQI, and ORE, we compare four QOOA variants: NoSCR, NoVQI, NoBoth, and NoORE. Specifically, NoSCR skips SCR to prune unlikely airdrop recipients; NoVQI omits VQI to prune quantities unnecessary; NoBoth excludes both SCR and VQI; NoORE forgoes airdrop adjustments. Figure 5(a) compares QOOA and NoORE in terms of *TP* and *OS* across varied budgets. Note that NoSCR, NoVQI, and NoBoth are excluded since SCR and VQI, aiming to reduce running time, do not impact revenue. As shown, QOOA consistently outperforms NoORE in *OS* because ORE effectively promotes rare-trait NFTs to RTCs and their friends, facilitating both individual and collaborative breeding. Figure 5(b) compares the execution times of QOOA, NoSCR, NoVQI, and NoBoth across different budgets. QOOA harnesses VQI to effectively avoid redundant searches across different quantities, leading to a considerable decrease in execution time, by 30% compared to NoVQI. When seeking airdrops under a specific quantity, QOOA leverages SCR to prune unlikely airdrop candidates. The advantages of SCR become particularly evident as the budget increases. The results indicate that both SCR and VQI substantially enhance the efficiency of QOOA. In contrast, NoBoth without any pruning strategy requires the most time.

6 Conclusion

To the best of our knowledge, this work is the first attempt to investigate revenue maximization via viral marketing for NFTs. By considering unique characteristics such as breeding, scarcity, and rarity, we formulate a new problem, named NRM, to find NFT airdrops and determine the quantities for viral marketing. We prove the hardness of NRM and design an approximation algorithm QOOA, which effectively tackles NRM by efficiently identifying airdrops under varying quantities and increasing revenue from offspring, with the new ideas of SCR, VQI, and RTCs. Experiments on real NFT projects and social networks demonstrate that QOOA achieves up to 3.8 times of the revenue compared to state-of-the-art approaches. In future work, we plan to recommend appropriate actions (either breeding or selling) to users in order to maximize revenue.

Acknowledgement

This work is supported in part by NSF under grants III-2106758 and POSE-2346158, by the Ministry of Education, Taiwan, under grant 114L9009, by the NSTC, Taiwan, under grants 111-2221-E-002-135-MY3, 113-2223-E-002-011, 113-2221-E-001-016-MY3, 112-2221-E-001-010-MY3, and by Academia Sinica, Taiwan, under Academia Sinica Investigator Project Grant AS-IV-114-M06. We thank the NCHC for providing computational and storage resources.

References

[1] 2025. APENFT Airdrop. https://airdrops.io/apenft/.
[2] 2025. Axie Angel. https://app.axieinfinity.com/marketplace/axies/1046/.
[3] 2025. Axie Angel. https://opensea.io/assets/ethereum/0xf5b0a3efb8e8e4c201e2a935f110eaaf3ffecb8d/1046.
[4] 2025. Axie Breeding Guide. https://support.axieinfinity.com/hc/en-us/articles/7225771030555-Axie-Breeding-Guide.
[5] 2025. Axie Infinity. https://axieinfinity.com/.
[6] 2025. Beeple: The First 5000 Days. https://onlineonly.christies.com/s/beeple-first-5000-days/beeple-b-1981-1/112924.
[7] 2025. Binance Introduces CR7 NFT Airdrop. https://www.altcoinbuzz.io/cryptocurrency-news/binance-introduces-cr7-nft-airdrop/.
[8] 2025. bitsCrunch Hackathon: Unlocking the Future with Web3 Data. https://dorahacks.io/hackathon/bitscrunch-data/detail.
[9] 2025. Blur Airdrop. https://blur.io/airdrop.
[10] 2025. Claim ApeCoin. https://apecoin.com/claim.
[11] 2025. Collect Trump Cards. https://collecttrumpcards.com/.
[12] 2025. Crypto Unicorns: Breeding. https://whitepaper.cryptounicorns.fun/intro/assets/unicorn-nfts/breeding.
[13] 2025. CryptoKitties. https://www.cryptokitties.co/.
[14] 2025. CryptoKitties: Cooldown Speed. https://guide.cryptokitties.co/guide/cat-features/cooldown-speed.
[15] 2025. CryptoKitties: Siring. https://www.cryptokitties.co/search?include=sire.
[16] 2025. CryptoPunk #9997. https://onlineonly.christies.com/s/no-time-present/larva-labs-est-2005-2/129415?sc_lang=en.
[17] 2025. A CryptoPunk NFT Was Recently Sold for $23.7 Million. https://finance.yahoo.com/news/cryptopunk-nft-recently-sold-23-161710404.html.
[18] 2025. Defimons Characters. https://rarible.com/collection/0xea462af52ceb68de674d5eaf1d681a44af0b00dc/items.
[19] 2025. EtherScan API. https://docs.etherscan.io/.
[20] 2025. Fat Ape Club. https://linktr.ee/Fatapeclub.
[21] 2025. Gucci Vault Material. https://opensea.io/assets/ETHEREUM/0x7daec605e9e2a1717326eedfd660601e2753a057/7.
[22] 2025. Gutter Cat Gang. https://opensea.io/collection/guttercatgang.
[23] 2025. Heterosis. https://og.art/collections/heterosis/.
[24] 2025. How do timed auctions work? https://support.opensea.io/en/articles/8867012-how-do-timed-auctions-work.
[25] 2025. Lascaux: The Future. https://opensea.io/collection/lascauxfuture.
[26] 2025. Mating Club (siring) is Live! https://medium.com/axie-infinity/mating-club-siring-is-live-b25874112135.
[27] 2025. MODragon: Breeding. https://mobox.gitbook.io/modragon.
[28] 2025. Mutant Ape Yacht Club. https://opensea.io/collection/mutant-ape-yacht-club.
[29] 2025. NBA Top Shot Transactions. https://www.kaggle.com/datasets/chigorin/nba-topshot-transactions/data.
[30] 2025. New Dapps Report: BEANZ – Surprise Airdrop from Azuki. https://dappradar.com/blog/new-dapps-report-beanz-surprise-airdrop-from-azuki.
[31] 2025. NFT Marketing Campaign in 2023: Building Community, Creating Hype, and Achieving a Successful NFT Sale. https://icoda.io/blog/nft-marketing-campaign-in-2023-building-community-creating-hype-and-achieving-a-successful-nft-sale/.
[32] 2025. OpenSea API. https://docs.opensea.io/reference/api-overview.
[33] 2025. OpenSea Drops. https://opensea.io/drops.
[34] 2025. Part 2: Prepare your drop schedule. https://support.opensea.io/en/articles/8867049-part-2-prepare-your-drop-schedule.
[35] 2025. Prada Timecapsule. https://www.prada.com/us/en/pradasphere/special-projects/2024/prada-timecapsule.html.
[36] 2025. Predicting NFT Liquidity. https://medium.com/@nftstatistics/predicting-nft-liquidity-925d72f6f767.
[37] 2025. Pudgy Penguins. https://pudgypenguins.com/.
[38] 2025. Puma's Super PUMA mascot is the hero of a playful new streetwear capsule. https://www.prada.com/us/en/pradasphere/special-projects/2024/prada-timecapsule.html.
[39] 2025. Rarible–Terminology. https://help.rarible.com/hc/en-us/articles/4408194060685-Terminology.
[40] 2025. Rise of Mythics: A Moonbirds Legend. https://www.proof.xyz/mythics.
[41] 2025. Roaring Leaders. https://linktr.ee/roaringleaders.
[42] 2025. STEPN. https://stepn.com/.
[43] 2025. STEPN: Shoe-Minting. https://whitepaper.stepn.com/game-fi-elements/shoe-minting.
[44] 2025. Super PUMA. https://opensea.io/collection/super-puma.
[45] 2025. Super PUMA #10. https://opensea.io/assets/ethereum/0x283c0bba69ebd4643cfce761b34b0206e75b2091/10.

[46] 2025. Timpers Pixelworks. https://rarible.com/timperspixelworks/items.
[47] 2025. Tiny World. https://docs.tinyworlds.io/tiny-nft/bnb-chain/tinymon-nfts.
[48] 2025. The Ultimate NFT Marketing Guide: How to Promote NFTs in 2023? https://proleo.io/how-to-promote-nfts-in-2023/.
[49] 2025. VIA Treasure Trunk. https://opensea.io/zh-TW/collection/via-treasure-trunk-lv.
[50] 2025. ZKsync to airdrop 3.6 billion ZK tokens next week. https://www.theblock.co/post/299404/zksync-airdrop-zk-tokens.
[51] S. Alizadeh, A. Setayesh, A. Mohamadpour, and B. Bahrak. 2023. A network analysis of the non-fungible token (NFT) market: Structural characteristics, evolution, and interactions. *Applied Network Science* (2023).
[52] D. W. E. Allen, C. Berg, and A. M. Lane. 2023. Why airdrop cryptocurrency tokens? *Journal of Business Research* (2023).
[53] M.-F. Balcan, A. Daniely, R. Mehta, R. Urner, and V. V. Vazirani. 2014. Learning economic parameters from revealed preferences. In *WINE*.
[54] P. Banerjee, W. Chen, and L. V. S. Lakshmanan. 2019. Maximizing welfare in social networks under a utility driven influence diffusion model. In *ACM SIGMOD*.
[55] S. Banerjee and B. Pal. 2022. Budgeted influence and earned benefit maximization with tags in social networks. *Social Network Analysis and Mining* (2022).
[56] N. Bansal, A. Blum, S. Chawla, and A. Meyerson. 2004. Approximation algorithms for deadline-TSP and vehicle routing with time-windows. In *ACM STOC*.
[57] S. Bhagat, A. Goyal, and L. V. S. Lakshmanan. 2012. Maximizing product adoption in social networks. In *ACM WSDM*.
[58] Y. Cao, X. Yang, M. Xia, H. Liu, K. Shigyo, W. Zeng, F. Cheng, Y. Wang, Q. Yu, and H. Qu. 2023. NFTeller: Dual centric visual analytics of NFT transactions. In *IEEE BigComp*.
[59] S. Casale-Brunet, M. Zichichi, L. Hutchinson, M. Mattavelli, and S. Ferretti. 2022. The impact of NFT profile pictures within social network communities. In *ACM GoodIT*.
[60] T. Chakraborty and R. Narayanam. 2016. Cross-layer betweenness centrality in multiplex networks with applications. In *IEEE ICDE*.
[61] T. Chen, J. Guo, and W. Wu. 2022. Adaptive multi-feature budgeted profit maximization in social networks. *Social Network Analysis and Mining* (2022).
[62] X. Chen, Y. Zhao, G. Liu, R. Sun, X. Zhou, and K. Zheng. 2022. Efficient similarity-aware influence maximization in geo-social network. *IEEE TKDE* (2022).
[63] S. Cheng, H. Shen, J. Huang, G. Zhang, and X. Cheng. 2013. Staticgreedy: Solving the scalability-accuracy dilemma in influence maximization. In *ACM CIKM*.
[64] A Colicev. 2023. How can non-fungible tokens bring value to brands. *International Journal of Research in Marketing* (2023).
[65] D. Costa, L. La Cava, and A. Tagarelli. 2023. Show me your NFT and I tell you how it will perform: Multimodal representation learning for NFT selling price prediction. In *ACM WWW*.
[66] S. Datta, A. Majumder, and N. Shrivastava. 2010. Viral marketing for multiple products. In *IEEE ICDM*.
[67] X. Deng, F. Long, B. Li, D. Cao, and Y. Pan. 2019. An influence model based on heterogeneous online social network for influence maximization. *IEEE TNSE* (2019).
[68] V. E. do Carmo, V. da F. Vieira, R. S. Oliveira, and C. R. Xavier. 2023. FastCELF++: A novel and fast heuristic for influence maximization in complex networks. In *ICCSA*.
[69] Nicholas Economides. 1996. The economics of networks. *International Journal of Industrial Organization* (1996).
[70] G. Farnad, B. Babaki, and M. Gendreau. 2020. A unifying framework for fairness-aware influence maximization. In *WWW*.
[71] M. Feldman, J. Naor, and R. Schwartz. 2011. A unified continuous greedy algorithm for submodular maximization. In *IEEE FOCS*.
[72] C. Gao, S. Gu, R. Yang, H. Du, S. Ghosh, and H. Wang. 2019. Robust profit maximization with double sandwich algorithms in social networks. In *IEEE ICDCS*.
[73] C. Gao, S. Gu, J. Yu, H. Du, and W. Wu. 2022. Adaptive seeding for profit maximization in social networks. *Journal of Global Optimization* (2022).
[74] D. Garcia, P. Mavrodiev, D. Casati, and F. Schweitzer. 2017. Understanding popularity, reputation, and social influence in the Twitter society. *Policy & Internet* (2017).
[75] L. Goodman. 2022. How Do NFT Marketplaces Make Money? https://nftclub.com/how-do-nft-marketplaces-make-money/.
[76] A. Goyal, W. Lu, and L. V. S. Lakshmanan. 2011. Celf++: Optimizing the greedy algorithm for influence maximization in social networks. In *WWW*.
[77] M. Grande, F. Borondo, and J. Borondo. 2023. The predictive power of the Blockhain transaction networks: Towards a new generation of network science market indicators. *arXiv preprint arXiv:2401.01379* (2023).
[78] M. Grande and J. Borondo. 2025. Trust as a driver in the DeFi market: Leveraging TVL/MCAP bands as confidence indicators to anticipate price movements. *Finance Research Letters* (2025).
[79] A. Gulati and M. Eirinaki. 2018. Influence propagation for social graph-based recommendations. In *IEEE Big Data*.
[80] C. Guo, W. Li, J. Wang, X. Yu, X. Liu, A. M. Luvembe, C. Wang, and Q. Jin. 2024. Heterogeneous network influence maximization algorithm based on multi-scale propagation strength and repulsive force of propagation field. *Knowledge-Based Systems* (2024).
[81] J. Guo, T. Chen, and W. Wu. 2020. A multi-feature diffusion model: Rumor blocking in social networks. *IEEE/ACM Transactions on Networking* (2020).
[82] K. Han, B. Wu, J. Tang, S. Cui, C. Aslay, and L. V. S. Lakshmanan. 2021. Efficient and effective algorithms for revenue maximization in social advertising. In *ACM SIGMOD*.
[83] T. Hayashi, T. Akiba, and Y. Yoshida. 2015. Fully dynamic betweenness centrality maintenance on massive networks. *VLDB* (2015).
[84] K. Hayawi, S. Mathew, N. Venugopal, M. M. Masud, and P.-H. Ho. 2022. DeeProBot: a hybrid deep neural network model for social bot detection based on user profile data. *Social Network Analysis and Mining* (2022).
[85] K.-H. Ho, Y. Hou, T.-T. Chan, and H. Pan. 2022. Analysis of non-fungible token pricing factors with machine learning. In *IEEE SMC*.
[86] Z. Hu, Y. Dong, K. Wang, and Y. Sun. 2020. Heterogeneous graph transformer. In *WWW*.
[87] Z. Huang, X. Gu, J. Hu, and X. Chen. 2024. UPI-LT: Enhancing Information Propagation Predictions in Social Networks Through User Influence and Temporal Dynamics. *Applied Sciences* (2024).
[88] H.-J. Hung, H.-H. Shuai, D.-N. Yang, L.-H. Huang, W.-C. Lee, J. Pei, and M.-S. Chen. 2016. When social influence meets item inference. In *ACM SIGKDD*.
[89] A. Iacob, B. Cautis, and S. Maniu. 2023. Sequential Learning Algorithms for Contextual Model-Free Influence Maximization. In *ACM SIGKDD*.
[90] T. Jin, Y. Yang, R. Yang, J. Shi, K. Huang, and X. Xiao. 2021. Unconstrained submodular maximization with modular costs: Tight approximation and application to profit maximization. *VLDB* (2021).
[91] A. Kapoor, D. Guhathakurta, M. Mathur, R. Yadav, M. Gupta, and P. Kumaraguru. 2022. Tweetboost: Influence of social media on NFT valuation. In *WWW*.
[92] D. Kempe, J. Kleinberg, and É. Tardos. 2003. Maximizing the spread of influence through a social network. In *ACM SIGKDD*.
[93] D. Kempe, J. Kleinberg, and É. Tardos. 2005. Influential nodes in a diffusion model for social networks. In *ICALP*.
[94] H. Kim, H.-S. Kim, and Y.-S. Park. 2023. Decentralized valuation and inflation control for NFTs in incentivized play-to-earn web3 applications. *arXiv:2306.13672* (2023).
[95] S. Kim and J. Han. 2020. Detecting engagement bots on social influencer marketing. In *SocInfo*.
[96] N. K. Klein, F. Lattermann, and D. Schiereck. 2023. Investment in non-fungible tokens (NFTs): The return of Ethereum secondary market NFT sales. *Journal of Asset Management* (2023).
[97] D.-R. Kong and T.-C. Lin. 2021. Alternative investments in the Fintech era: The risk and return of Non-Fungible Token (NFT). *Available at SSRN 3914085* (2021).
[98] A. Krause and D. Golovin. 2014. Tractability: Practical approaches to hard problems. In *Submodular Function Maximization*. Cambridge Univ. Press Cambridge, UK.
[99] A. Krause and C. Guestrin. 2005. *A note on the budgeted maximization of submodular functions*. Citeseer.
[100] V. Kumar and W. Reinartz. 2018. *Customer relationship management*. Springer.
[101] H. Lee, G.-C. Lee, and H.-Y. Koo. 2024. Exploring the relationship between rarity and price of profile picture NFT: A formal concept analysis on the BAYC NFT collection. *Blockchain: Research and Applications* (2024).
[102] J. Li, C. Li, J. Liu, J. Zhang, L. Zhuo, and M. Wang. 2019. Personalized mobile video recommendation based on user preference modeling by deep features and social tags. *Applied Sciences* (2019).
[103] X. Li, J. D. Smith, T. N. Dinh, and M. T. Thai. 2019. Tiptop: (Almost) exact solutions for influence maximization in billion-scale networks. *IEEE/ACM Transactions on Networking* (2019).
[104] Z. Li, X. Wang, C. Yang, L. Yao, J. McAuley, and G. Xu. 2023. Exploiting explicit and implicit item relationships for session-based recommendation. In *ACM WSDM*.
[105] X. Liang, Z. Yang, B. Wang, S. Hu, Z. Yang, D. Yuan, N. Z. Gong, Q. Li, and F. He. 2021. Unveiling fake accounts at the time of registration: An unsupervised approach. In *ACM SIGKDD*.
[106] H. Lu, M. Zhang, W. Ma, Y. Shao, Y. Liu, and S. Ma. 2019. Quality effects on user preferences and behaviors in mobile news streaming. In *WWW*.
[107] J. Luo, Y. Jia, and X. Liu. 2023. Understanding NFT price moves through tweets keywords analysis. In *ACM GoodIT*.
[108] L. Lv, P. Hu, Z. Zheng, D. Bardou, T. Zhang, H. Wu, S. Niu, and G. Yu. 2023. A community-based centrality measure for identifying key nodes in multilayer networks. *IEEE TCSS* (2023).

[109] B. R. Mandel. 2009. Art as an investment and conspicuous consumption good. *American Economic Review* (2009).

[110] P. Manurangsi. 2017. Almost-polynomial ratio ETH-hardness of approximating densest k-subgraph. In *ACM STOC*.

[111] Q. Mao, Z. Liu, C. Liu, and J. Sun. 2023. Hinormer: Representation learning on heterogeneous information networks with graph transformer. In *WWW*.

[112] A. Mekacher, A. Bracci, M. Nadini, M. Martino, L. Alessandretti, L. M. Aiello, and A. Baronchelli. 2022. Heterogeneous rarity patterns drive price dynamics in NFT collections. *Scientific Reports* (2022).

[113] X. Miao, H. Peng, K. Chen, Y. Peng, Y. Gao, and J. Yin. 2022. Maximizing time-aware welfare for mixed items. In *IEEE ICDE*.

[114] S. H. Moghaddam and M. Abbaspour. 2022. Friendship preference: Scalable and robust category of features for social bot detection. *IEEE TDSC* (2022).

[115] M. Nadini, L. Alessandretti, F. Di Giacinto, M. Martino, L. M. Aiello, and A. Baronchelli. 2021. Mapping the NFT revolution: Market trends, trade networks, and visual features. *Scientific Reports* (2021).

[116] R. Nourmohammadi, M. Arabian, M. Ghorbanpour, M. M. Nazemi, and N. Nezhadsistani. 2022. NFT scoring: An analysis of the considerable features. In *ICBTA*.

[117] T. Pan, X. Li, A. Kuhnle, and M. T. Thai. 2020. Influence diffusion in online social networks with propagation rate changes. *IEEE Transactions on Network Science and Engineering* (2020).

[118] Y. Pang, L. Wu, Q. Shen, Y. Zhang, Z. Wei, F. Xu, E. Chang, B. Long, and J. Pei. 2022. Heterogeneous global graph neural networks for personalized session-based recommendation. In *ACM WSDM*.

[119] N. H. Park, H. Kim, C. Lee, C. Yoon, S. Lee, and S. Shin. 2023. A deep dive into NFT whales: A longitudinal study of the NFT trading ecosystem. *arXiv:2303.09393* (2023).

[120] T.-T. Pham and T.-D. Trinh. 2023. Scoring model for NFT evaluation. In *SOICT*.

[121] D. Piyadigama and G. Poravi. 2022. An analysis of the features considerable for NFT recommendations. In *IEEE HSI*.

[122] Z. Qiang, E. L. Pasiliao, and Q. P. Zheng. 2019. Model-based learning of information diffusion in social media networks. *Applied Network Science* (2019).

[123] K. V. Rao and C. R. Chowdary. 2022. CBIM: Community-based influence maximization in multilayer networks. *Information Sciences* (2022).

[124] S. A. Rios, F. Aguilera, J. D. Nuñez-Gonzalez, and M. Graña. 2019. Semantically enhanced network analysis for influencer identification in online social networks. *Neurocomputing* (2019).

[125] R. Sawhney, M. Thakkar, R. Soun, A. Neerkaje, V. Sharma, D. Guhathakurta, and S. Chava. 2022. Tweet based reach aware temporal attention network for NFT valuation. In *EMNLP*.

[126] B. Saxena, V. Saxena, N. Anand, V. Hassija, V. Chamola, and A. Hussain. 2023. A Hurst-based diffusion model using time series characteristics for influence maximization in social networks. *Expert Systems* (2023).

[127] L. Schaar and S. Kampakis. 2022. Non-fungible tokens as an alternative investment: Evidence from cryptopunks. *The Journal of The British Blockchain Association* (2022).

[128] R. Schuchard, A. Crooks, A. Stefanidis, and A. Croitoru. 2018. Bots in nets: Empirical comparative analysis of bot evidence in social networks. In *CNA*.

[129] P. Sharma and S. Banerjee. 2022. Profit maximization using social networks in two-phase setting. In *Advanced Data Mining and Applications*.

[130] Q. Shi, C. Wang, J. Chen, Y. Feng, and C. Chen. 2019. Location driven influence maximization: Online spread via offline deployment. *Knowledge-Based Systems* (2019).

[131] X. Shi, H. Ling, Y. Pang, W. Hu, P. Chu, and J. Xing. 2019. Rank-1 tensor approximation for high-order association in multi-target tracking. *International Journal of Computer Vision* (2019).

[132] S. Sidana, M. Trofimov, O. Horodnytskyi, C. Laclau, Y. Maximov, and M.-R. Amini. 2021. User preference and embedding learning with implicit feedback for recommender systems. *Data Mining and Knowledge Discovery* (2021).

[133] A.-A. Stoica and A. Chaintreau. 2019. Fairness in social influence maximization. In *WWW*.

[134] K. Sun, T. Qian, T. Chen, Y. Liang, Q. V. H. Nguyen, and H. Yin. 2020. Where to go next: Modeling long-and short-term user preferences for point-of-interest recommendation. In *AAAI*.

[135] L. Sun, W. Huang, P. S. Yu, and W. Chen. 2018. Multi-round influence maximization. In *ACM SIGKDD*.

[136] L. Sun, X. Rui, and W. Chen. 2023. Scalable Adversarial Attack Algorithms on Influence Maximization. In *ACM WSDM*.

[137] J. Tang, X. Tang, and J. Yuan. 2018. Profit maximization for viral marketing in online social networks: Algorithms and analysis. *IEEE TKDE* (2018).

[138] J. Tang, X. Tang, and J. Yuan. 2018. Towards profit maximization for online social network providers. In *IEEE INFOCOM*.

[139] Y. Tang, X. Xiao, and Y. Shi. 2014. Influence maximization: Near-optimal time complexity meets practical efficiency. In *ACM SIGMOD*.

[140] Y.-W. Teng, H.-W. Chen, D.-N. Yang, Y.-A. Pignolet, T.-W. Li, and L. Chen. 2021. On influencing the influential: Disparity seeding. In *ACM CIKM*.

[141] Y.-W. Teng, Y. Shi, C.-H. Tai, D.-N. Yang, W.-C. Lee, and M.-S. Chen. 2021. Influence maximization based on dynamic personal perception in knowledge graph. In *IEEE ICDE*.

[142] A. Tsang, B. Wilder, E. Rice, M. Tambe, and Y. Zick. 2019. Group-fairness in influence maximization. In *IJCAI*.

[143] D. Varshney, S. Kumar, and V. Gupta. 2017. Predicting information diffusion probabilities in social networks: A Bayesian networks based approach. *Knowledge-Based Systems* (2017).

[144] C. Velasco, M. Pombo, and F. Barbosa-Escobar. 2021. Value in the age of non-fungible tokens (NFTs). *BI Business Review* (2021).

[145] G. Wang, T. Konolige, C. Wilson, X. Wang, H. Zheng, and B. Y. Zhao. 2013. You are how you click: Clickstream analysis for sybil detection. In *USENIX*.

[146] Y. Wu, K. Li, G. Zhao, and X. Qian. 2022. Personalized long-and short-term preference learning for next POI recommendation. *IEEE TKDE* (2022).

[147] Y. Yang, Y. Xu, E. Wang, K. Lou, and D. Luan. 2018. Exploring influence maximization in online and offline double-layer propagation scheme. *Information Sciences* (2018).

[148] H. Zhang, H. Zhang, A. Kuhnle, and M. T. Thai. 2016. Profit maximization for multiple products in online social networks. In *IEEE INFOCOM*.

[149] S. Zhang, Y. Huang, J. Sun, W. Lin, X. Xiao, and B. Tang. 2023. Capacity constrained influence maximization in social networks. In *ACM SIGKDD*.

[150] X. Zhang, H. Xie, P. Yi, and J. C. S. Lui. 2022. Enhancing Sybil detection via social-activity networks: A random walk approach. *IEEE TDSC* (2022).

A NFT Background with Practical Examples

The section provide a detailed explanation of NFTs, NFT auctions, NFT viral marketing, and NFT breeding, supplemented with concrete examples.

1) Non-fungible tokens (NFTs): They are unique digital assets, each characterized by distinctive traits that define its appearance, attributes, or functionalities. Within an NFT project N, creators curate a limited collection of such digital assets, typically maintaining a cohesive aesthetic while incorporating variations in traits, thereby forming a collective trait set T. In recent years, major brands such as Gucci [21], Louis Vuitton (LV) [49], Prada [35], and Puma [38] have adopted NFTs to expand their digital presence and enhance user engagement. A notable example is the Super PUMA NFT project [44], where each NFT exhibits a range of distinctive traits. Among them, the most viewed NFT, Super PUMA #10 [45], features seven traits: green, cool, calico, beanie, motorsport helmet, white shirt, and easy rider.

2) NFT viral marketing: It leverages the social network $G = (V, E)$ within the NFT marketplace to distribute airdrops (u_i, n_k) for an NFT project N, subject to a budget constraint B that limits the number of free airdrops. In the airdrop stage, these airdrops diffuse information across the social network, activating users who develop an interest in specific NFTs and potentially driving higher engagement. Major marketplaces such as OpenSea [33], Blur [9], and Binance [7] have employed NFT viral marketing to broaden their audience and enhance customer loyalty. However, many NFT marketplaces provide only basic rules for project creators to configure airdrop distributions, leading to simplistic heuristics such as targeting early adopters (e.g., zkSync [50]), distributing to users of affiliated NFT projects (e.g., ApeCoin [10], Beanz [30]), or allocating airdrops randomly (e.g., DoraHacks [8]). These approaches often fail to optimize engagement and revenue, highlighting the need for an algorithmic approach to strategically selecting airdrops for more effective NFT viral marketing.

3) NFT Auctions: These auctions incorporate multiple interrelated factors that influence the final transaction price of each NFT. Scarcity is determined by the limited quantity q_k available for sale, rarity reflects the uniqueness of specific traits, and ownership considers the prominence of previous holders. These factors, combined with users' individual preferences, collectively shape their valuations for an NFT. A reserve price establishes the minimum acceptable bid, ensuring that only users whose valuations meet or exceed this threshold can participate in the auction. During the public stage, up to q_k top bidders secure the NFT, provided their valuations meet the reserve price. NFT auctions offer high transparency, as blockchain records enable public verification of bidding history and final sale prices. Additionally, APIs like Etherscan [19] and OpenSea [32] provide accessible transaction data, supporting in-depth research on NFT viral marketing strategies and their impact on market dynamics. Leading marketplaces, such as OpenSea [24] and Blur [39], employ auction-based mechanisms for NFT sales. A notable example illustrating the impact of scarcity and rarity is CryptoPunks #5822, a one-of-a-kind NFT featuring the rare Alien trait (0.09%), which was sold for USD 23.7 million [17]. Meanwhile, ownership history has also played a crucial role in NFT valuations, as demonstrated by CryptoPunk #9997. Initially sold for approximately USD 159,000, its value skyrocketed to USD 4.35 million after being acquired by renowned actor Shawn Yue [16]. These cases highlight how scarcity, rarity, and ownership influence the perceived value of NFTs in auctions.

4) NFT breeding: It involves generating offspring from parent NFTs while adhering to constraints related to non-concurrent breeding, user breeding quotas, and trait inheritance. Users can participate in individual breeding, forming breeding pairs exclusively from their own NFTs, or collaborative breeding, partnering with friends to expand breeding opportunities. Leading projects such as Mutant Ape Yacht Club [28], Moonbirds Mythic [40], Roaring Leader [41], CryptoKitties [15], Axie Infinity [5], and StepN [43] have adopted NFT breeding to foster user engagement and expand their digital ecosystems. Axie Angel [2, 3] is a renowned offspring featuring three exceptionally rare traits: golden shell (0.01%), dreamy papi (0.02%), and pointy nyan (0.02%). Its sale for $1.1 million underscores the substantial market value associated with breeding rare offspring.

B Examples

Example B.1 (A detailed version of Example 1.1). Figures 6(a) and 6(b) illustrates an example for promoting a new NFT project consisting of three NFTs (denoted as n_1, n_2, and n_3) within a social network. Figure 6(a) shows the traits and (potential) assessments under different quantities of NFTs and their offspring. As shown in the project, the traits pink plaid and flower appear in only one NFT, making them rarer than leather, which is found in two NFTs. As users may prefer different NFTs, their valuations of an NFT may be determined by multiplying their preferences for the NFT with its assessment. Figure 6(b) shows a social network where nodes represent users, edges represent friendships, edge weights denote activation probabilities, and vectors near nodes indicate their preferences of NFTs. An NFT promotion campaign starts by airdropping some NFTs to selected users who may trigger influence propagation on the social network to activate user interests in the NFTs. After the campaign ends, the influenced users may bid on NFTs of interest with their valuations (estimated based on various factors).

Given that each NFT has an airdropping budget of 1 and a reserve price of 2.6, based on the approach proposed in this paper, airdropping n_1, n_2, and n_3 to u_{15}, u_{10}, and u_{15}, respectively, with the quantities set as 1, 1, and 2 may yield an expected revenue of 28.72, where the influenced users u_3, u_{16}, and u_{17} (represented by square shapes) win the auctions and the NFTs they purchase are indicated by colors. Since u_{17} possesses both n_1 and n_3, she has the opportunity to generate an new NFT offspring. The NFT offspring inherits the rare traits flower and pink plaid from its parents, making it a one-of-a-kind NFT that does not exist within the current project. This uniqueness contributes to an additional revenue of 4.32.

By contrast, an existing viral marketing algorithm based on influence maximization (IM) [54], which seeks to identify seed users to maximize the number of influenced users, may airdrop all NFTs to u_1, due to its expected influence spread of 3, where the influenced users u_2, u_8, and u_9 are represented by diamond shapes. However, as the users influenced by u_1 do not have high valuations of NFTs, the expected revenue is almost 0 when the quantity of each NFT is one. On the other hand, a classical revenue maximization (RM)

		NFT project			New offspring
NFT					
Traits		Leather, Flower	Leather	Pink plaid	Pink plaid, Flower
(Potential) Assessment under different quantities	1	11.02	6.05	8.17	11.02
	2	5.21	2.86	3.86	5.21
	3	4.06	2.23	3.00	4.06

(a) An NFT project and new offspring.

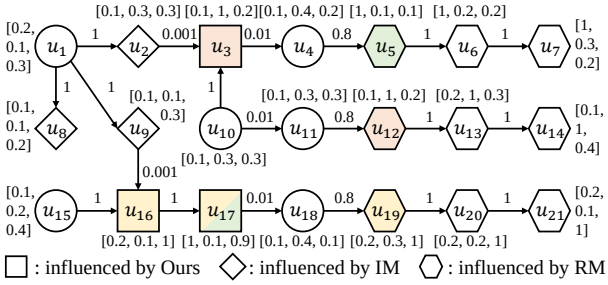

(b) A social network.

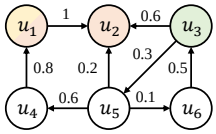

Preference	u_1	u_2	u_3	u_4	u_5	u_6
n_1	0.6	0.5	0.8	0.3	0.7	0.2
n_2	0.8	0.8	0.7	0.6	0.7	0.9
n_3	0.9	0.6	0.9	0.7	0.5	0.4

(c) An example for QOOA.

Figure 6: Illustrative examples.

algorithm [103] may designate u_4, u_{11}, and u_{18} as the airdrop recipients for n_1, n_2, and n_3, respectively, thereby maximizing the total expected revenue of 60.57 without considering the limited supply of NFTs, where the influenced users are represented by hexagonal shapes. Nevertheless, when the quantity of each NFT is limited to one, the expected revenue is reduced to 20.19, where the NFTs they purchase are indicated by colors. In addition, for both cases, no user can breed NFT offspring to generate additional revenue. On the other hand, when the quantity of each NFT increases, the valuations of influenced users decline significantly, with many falling below the reserve prices. The revenue obtained is thus smaller compared to the case where the quantity is one. As a result, both approaches of maximizing influence and revenue fall short in the marketing goal of NFT viral marketing, as they do not consider the features of NFTs, including breeding, scarcity, and trait rarity, and the need to determine NFT quantities. ■

Example B.2. Follow Example B.1, where the set of airdrops is $S = \{(u_{15}, n_1), (u_{10}, n_2), (u_{15}, n_3)\}$, the quantities are $Q = \{1, 1, 2\}$, and the reserve prices are $P = \{2.6, 2.6, 2.6\}$. Given the user breeding quota $c_{\mathrm{BQ}} = 1$, the breeding probability $\beta_i = 1$ for each user u_i, and the siring probability $\gamma_i = 0$ for each user u_i, under the influence of S with Q, n_1 is sold to u_{17}, n_2 is sold to u_3, and n_3 is sold to u_{16} and u_{17}, as shown in Figure 6(b). Since the siring probabilities of all users are 0, only u_{17} breeds offspring from n_1 and n_3 with a probability $1 \times 1 = 1$. The NFT generated can be n_1, n_2, n_3, and a new offspring (as shown in the last column in Figure 6(a)).

On the other hand, another case is considered in which u_{17} does not want to breed offspring but is inclined to provide NFTs for siring, i.e., $\gamma_{17} = 0.7$ and $\beta_{17} = 0$. In this case, u_{16} will breed offspring with u_{17}'s siring-ready NFT with a probability $\beta_{16} \times \gamma_{17} = 1 \times 0.7 = 0.7$. The offspring generated based on two n_3 (from u_{16} and u_{17}) can only result in n_3, whereas the offspring generated based on n_3 (from u_{16}) and n_1 (from u_{17}) can be n_1, n_2, n_3, and a new offspring (i.e., the same as described in the preceding paragraph). ■

Example B.3. Following Example B.2, given that $\lambda = 1$, $\beta_i = 1$ and $\gamma_i = 0$ for each user u_i, and the inheritance probabilities of leather, flower, and pink plaid are $\frac{2}{3}$, $\frac{1}{3}$, and $\frac{1}{3}$, respectively, under the influence of S under Q, the total transaction price $TP(S, Q) = (1 \times 11.02 \times 1) + (1 \times 6.05 \times 1) + (1 \times 3.86 \times 1 + 1 \times 3.86 \times 2.7) = 24.4$. For the potential transaction prices of offspring, since u_{17} generates offspring n_1, n_2, n_3, and the new offspring with probabilities $\frac{2}{3} \cdot \frac{1}{3} = 0.22$, $\frac{2}{3} \cdot \frac{2}{3} = 0.44$, $\frac{2}{3} \cdot \frac{1}{3} = 0.22$, and $\frac{1}{3} \cdot \frac{1}{3} = 0.11$, respectively, $OS(S, Q) = 0.22 \times 5.21 + 0.44 \times 2.86 + 0.22 \times 3 + 0.11 \times 11.02 = 4.32$. Therefore, the revenue $f(S, Q) = 28.72$. ■

Example B.4. Unlike the previous example, this example features a distinct social network structure and parameter configuration. Specifically, we consider an NFT project $N = \{n_1, n_2, n_3\}$, as depicted in Figure 6(a), to be promoted in the social network in Figure 6(c). Given that $B = \{2, 2, 2\}$, $L = \{2, 2, 2\}$, $P = \{1.8, 1.8, 1.8\}$, $\eta_0 = 0$, $\eta_1 = 1.5$, $\eta_2 = 0.2$, and $\eta_3 = 0.5$, QAS starts from n_1 subject to $q_1 = 1$. At first, QAS examines all users and chooses u_1 for an airdrop to maximize the total transaction price, i.e., $S_1^1 = \{(u_1, n_1)\}$ and $TP_1(S_1^1, 1) = 5.51$. Next, QAS derives SCR as follows.

$$SCR_1(S_1^1 \cup \{(u_2, n_1)\}, 1) = 4.32,$$
$$SCR_1(S_1^1 \cup \{(u_3, n_1)\}, 1) = 4.32,$$
$$SCR_1(S_1^1 \cup \{(u_4, n_1)\}, 1) = 7.73,$$
$$SCR_1(S_1^1 \cup \{(u_5, n_1)\}, 1) = 7.44,$$
$$SCR_1(S_1^1 \cup \{(u_6, n_1)\}, 1) = 8.64.$$

Since both $SCR_1(S_1^1 \cup \{(u_2, n_1)\}, 1)$ and $SCR_1(S_1^1 \cup \{(u_3, n_1)\}, 1)$ are smaller than $TP_1(S_1^1, 1) = 5.51$, QOOA prunes u_2 and u_3, and evaluates the total transaction prices considering only u_4, u_5, and u_6. As airdropping n_1 to u_6 leads to the greatest total transaction price, i.e., $TP_1(S_1^1 \cup \{(u_6, n_1)\}, 1) = 7.1$, QAS then updates $S_1^1 = \{(u_1, n_1), (u_6, n_1)\}$ and finishes the search for $q_1 = 1$ because $|S_1^1| = b_1 = 2$. ■

Example B.5. Following Example B.4, before the search for $q_1 = 2$ begins, QAS extracts $W_1(1) = 0.8$ and $W_1(2) = 0.7$ and computes $\frac{p_k}{\eta^*} \cdot e^{-\frac{\eta_1}{q_k}} = \frac{1.8}{e^{0.2 \times 4.5}} \cdot e^{-\frac{1.5}{2}} = 0.35$. Since both $W_1(1) = 0.8 > 0.35$ and $W_1(2) = 0.7 > 0.35$, the corresponding users (i.e., u_3 and u_5, respectively) are valid acceptors. As a result, QAS derives $UB_1(2) = W_1(1) \cdot A(n_1, 2) + W_1(2) \cdot A(n_1, 2) = 7.81$. Since $UB_1(2) = 7.81 > TP_1(S_1^1, 1) = 7.1$, QAS continues the search under $q_1 = 2$. ■

Example B.6. Following Example B.5, QOOA obtains $S = \{(u_1, n_1), (u_6, n_1), (u_4, n_2), (u_3, n_2), (u_4, n_3), (u_6, n_3)\}$ and $Q = \{1, 2, 1\}$, with $f(S, Q) = 25.93$. Given that $\lambda = 1$, and $c_{\mathrm{BQ}} = 3$, since flower and

pink plaid are the rarest traits, ORE identifies $N^{\mathrm{T}} = \{n_1, n_3\}$. For n_3, ORE examines VOGUE as follows.

$$\begin{aligned} \text{Airdrops:} \quad & VOGUE_3(u_4, 1) = 0.51, \\ & VOGUE_3(u_6, 1) = 0.26. \\ \text{Non-airdrops:} \quad & VOGUE_3(u_3, 1) = 0.37, \\ & VOGUE_3(u_5, 1) = 0.36, \\ & VOGUE_3(u_1, 1) = 0, \\ & VOGUE_3(u_2, 1) = 0. \end{aligned}$$

Accordingly, ORE attempts to replace u_6 with u_3 for airdrops of n_3 because $VOGUE_3(u_3, 1) = 0.37 > VOGUE_3(u_6, 1) = 0.26$. Since $f\big((S \setminus \{(u_6, n_3)\}) \cup \{(u_3, n_3)\}, Q\big) = 26.97 > f(S, Q) = 25.93$, ORE updates $S = (S \setminus \{(u_6, n_3)\}) \cup \{(u_3, n_3)\}$. As $VOGUE_3(u_5, 1) = 0.36 < VOGUE_3(u_4, 1) = 0.51$, ORE terminates the enhancement for n_3. Consequently, the solution is $S = \{(u_1, n_1), (u_6, n_1), (u_4, n_2), (u_3, n_2), (u_4, n_3), (u_3, n_3)\}$ and $Q = \{1, 2, 1\}$, with $f(S, Q) = 26.97$. ■

C Detailed Comparisons with Related Work

C.1 Key Differences, New Challenges, and Novel Ideas

This section elaborates on the key differences from related work, the emerging challenges, and the novel ideas proposed to address them. Table 1 summarizes the comparison between our work and related studies based on several key factors: *obj. to maximize* (the primary goal of the study, such as influence, revenue, or profit), *seeding budget* (whether a budget constraint is considered), *multiple seed groups as output* (whether multiple seed groups are identified), *additional output* (whether the study provides outputs beyond seed selection), *benefit* (whether benefits vary across users, interactions, or products), and *breeding* (whether holding multiple products provides additional benefits). Based on obj. to maximize, studies can be categorized into influence maximization (IM) [54, 66, 88, 113, 141, 148] (Rows 1–6 of Table 1), which focuses on maximizing influence spread; revenue/benefit maximization (RM/BM) [55, 61, 72, 73, 82, 103] (Rows 7–12 of Table 1), which aims to maximize revenue from influenced users and interactions; and profit maximization (PM) [90, 129, 137, 138] (Rows 13–16 of Table 1), which incorporates seeding costs to maximize net profit.

1) *NFT breeding*: Unlike existing IM problems [54, 66, 88, 113, 141, 148], which focus solely on maximizing user reach, and prior RM/BM/PM studies [55, 61, 72, 73, 82, 90, 103, 129, 137, 138], which primarily consider single-item revenue—while even multi-item approaches fail to account for additional revenue from simultaneous purchases—our NRM introduces a set of novel breeding definitions (Definitions **??**–3.4 and D.10–D.14) specifically designed for NFT breeding, an aspect entirely overlooked in classical IM, RM, and PM. In particular, NRM targets both the total transaction price TP (Definition 3.1 and Equation (2)), and the potential transaction prices of offspring OS (Definition 3.4 and Equation (3). Here, OS evaluates the expected additional revenue generated by considering all breeding possibilities, representing a fundamentally different objective from that of traditional IM.

This difference gives rise to new challenges, which we address with the following ideas. Unlike existing IM/RM/BM/PM studies [54, 55, 61, 66, 72, 73, 82, 88, 90, 103, 113, 129, 137, 138, 141, 148], which do not consider whether users are simultaneously influenced by seed groups from multiple items, NRM incorporates individual and collaborative breeding mechanisms (Definitions D.13 and D.14). As a result, it is important to ensure that users either personally own multiple NFTs or that their friends also hold NFTs to increase breeding opportunities and enhance OS. Furthermore, the rarity and ownership history of NFT offspring significantly impact their assessment (Definitions D.7, D.8, and D.10), highlighting the need to strategically influence which users acquire NFTs to initiate breeding. Additionally, since NRM considers the user breeding quota constraint (Definition **??**), it must prevent excessive concentration of influence on a specific group of users, as this could result in many acquired NFTs remaining unbred due to breeding quota limitations, leading to a lower OS.

The Offspring Revenue Enhancement (ORE) step in QOOA specifically targets users more likely to generate higher expected additional revenue, namely Rare Trait Collectors (RTCs). QOOA introduces the notion of Valuable Offspring Generation Utility Estimation (VOGUE) to evaluate a user's potential to influence RTCs and their friends to hold this NFT and breed valuable offspring, and further leverages the Breeding Index (B-Index) to capture both individual and collaborative breeding potential while accounting for the user breeding quota. This enables QOOA to focus on users most likely to produce valuable offspring and strategically replace original airdrops with high-VOGUE alternatives, thereby enhancing NFT offspring value. By ensuring that RTCs are influenced by airdrops of multiple NFTs, QOOA can potentially increase the expected additional revenue across different breeding possibilities, thereby maximizing total revenue. Prior studies on influence and revenue maximization that overlook breeding fail to tailor airdrops for generating additional revenue.

2) *Supply-constrained auction-base sales*: Traditional IM approaches [54, 66, 88, 113, 141, 148] focus solely on maximizing the number of influenced users, while conventional RM/BM/PM methods [55, 61, 72, 73, 82, 90, 103, 129, 137, 138] aim to maximize the aggregate valuation of all influenced users. In contrast, our NRM introduces a set of key definitions (Definitions **??**–3.1) for supply-constrained auction-based sales, which is not addressed by either IM or RM. Instead of seeking to maximize either the number of influenced users or the total valuation of all influenced users, NRM specifically targets the top q_k valuations among those influenced users in TP (Definition D.6 and Equation (2)), thereby reflecting the limited supply of NFTs.

We present the new challenges caused by this difference and the corresponding ideas we propose to solve them. In contrast to IM methods [54, 66, 88, 113, 141, 148] that ignore user valuations and RM/BM/PM approaches [55, 61, 72, 73, 82, 90, 103, 129, 137, 138] that assume user valuations remain fixed, NRM focuses on user valuations that vary with quantities (Definitions D.6, D.9, and **??**) when selecting airdrops S_k for each NFT n_k. Because varying q_k affects revenue even under the same S_k (Definitions 3.1 and 3.5), repeatedly evaluating the revenue of the same S_k across varying quantities incurs significant computational overhead.

To improve computational efficiency, QOOA introduces the notion of Scarcity-Conscious Revenue (SCR) to derive an upper bound on potential revenue with respect to a given set of users. SCR can be

Table 1: Comparison to related work on influence, revenue, benefit, and profit maximization.

	Obj. to maximize	Seeding budget	Multiple seed groups as output	Additional output	Benefit	Breeding
[66]	influence	✓	1 for each product	✗	✗	✗
[148]	influence	✓	1 for each product	✗	✗	✗
[141]	influence	✓	1 for each product	✗	✗	✗
[88]	influence	✓	1 for each product	✗	✗	✗
[54]	welfare	✓	✗	✗	✗	✗
[113]	welfare	✓	1 for each product	✗	✗	✗
[103]	benefit	✓	✗	✗	on user	✗
[61]	benefit	✓	✗	✗	on user	✗
[82]	revenue	✓	1 for each advertiser	✗	on advertiser	✗
[55]	benefit	✓	✗	tags	on user	✗
[73]	benefit	✓	✗	✗	on edge	✗
[72]	worst-case ratio of benefit	✓	✗	✗	on edge	✗
[137]	influence − cost	✗	✗	✗	✗	✗
[138]	benefit − cost	✗	✗	✗	on user	✗
[90]	revenue − cost	✗	✗	✗	✗	✗
[129]	benefit − cost	✓	1 for each phase	✗	on user	✗
NRM	revenue	✓	1 for each NFT	quantities	on user, varying due to quantities	✓

estimated efficiently for different quantities, enabling the rapid pruning of ineffective candidates. However, because the number of NFTs for sale is limited, the total transaction price function is not submodular (proven in Lemma E.3 in Appendix E.2.3), rendering pruning strategies from prior works [63, 68, 76] (relying on submodularity) inapplicable.

3) *Scarcity-driven valuation*: Unlike in traditional IM/RM/BM/PM problems [54, 55, 61, 66, 72, 73, 82, 88, 90, 103, 113, 129, 137, 138, 141, 148], where the quantity q_k neither influences the set of influenced users nor their valuations, our NRM introduces a set of new definitions (Definitions D.6–D.9, and **??**) to jointly address seed selection and quantity determination. In NRM, increasing q_k allows more users' valuations to be incorporated into TP (Definition D.6 and Equation (2)), yet it simultaneously reduces individual valuations due to diminished scarcity (Definitions D.6, D.9, and **??** as well as Equations (10) and (1)). Consequently, q_k serves as a critical decision variable that directly shapes revenue generation.

The following are the new challenges arising from this difference and the ideas we propose to address them. Unlike IM/RM/PM approaches [54, 55, 61, 66, 72, 73, 82, 88, 90, 103, 113, 129, 137, 138, 141, 148] that do not simultaneously determine seeds and quantities, NRM aims to jointly identify q_k and the corresponding airdrops S_k for each NFT n_k. To balance the trade-off between scarcity and widespread adoption—where restricting supply preserves scarcity, while increasing availability to promote adoption reduces user valuations (Definitions D.6, D.9, and **??**)—NRM must examine multiple quantity settings to identify the optimal solution, introducing substantial computational complexity.

To eliminate redundant searches over ineffective quantities, QOOA introduces Valuation-based Quantity Inequality (VQI) to derive upper bounds on revenue for different quantities. This allows QOOA to efficiently determine whether certain quantities can be pruned before performing a search for airdrops. Compared to prior revenue and profit maximization works [55, 61, 72, 73, 82, 90, 103, 129, 137, 138] that do not incorporate product quantity into consideration, the pruning based on VQI effectively leverages the quantity-dependent revenue characteristic of NFTs to trim off low-revenue quantities.

C.2 Review of NFTs in Social Networks

NFTs, as digital assets, are well-suited for viral marketing on social networks. Recent studies [91, 125] highlight the significant influence of Twitter user engagement metrics, such as likes and replies, on NFT trends and prices. Other research [65, 112] predicts NFT prices using features like images, texts, and rarity. Casale-Brunet et al. [59] examine how NFT holders in prominent projects shape large social communities. While these works explore the link between user behavior and the NFT market, they overlook strategies for promoting NFTs through viral marketing on social networks, which are increasingly in demand [31, 48]. Our work builds upon the insights gained from these studies to formulate NRM that closely reflects real-world dynamics in the NFT market.

D Details on Problem Formulation

Tables 2 and 3 summarize the notation and abbreviations used in this paper.

D.1 Workflow

The workflow of NRM comprises two primary stages: the airdrop stage and the public stage, which together facilitate NFT dissemination, auction participation, offspring breeding, and revenue generation. The airdrop stage (as the yellow-shaded region in Figure 7) initiates the process by distributing airdrops to propagate information about the NFT project through the social network. Utilizing a diffusion model, this stage identifies active users who become potential participants in the subsequent auction. Once the influence of the airdrops is established, the workflow transitions into the public stage (as the green-shaded region in Figure 7), where the auction process takes place. Given the designated for-sale quantity, NFT

Table 2: Notation table.

Notation	Description
	Section 3
N; n_k	NFT project; an NFT
T; t_d; T_k	Universal set of traits; a trait; trait set of n_k
P; p_k	Set of reserve prices of N; reserve price of n_k
Q; q_k	Set of NFT quantities; quantity of n_k
$\phi(t_d)$; $\Phi(n_k)$	Rarity of trait t_d; rarity of n_k
H_k; h_k	Ownership history of n_k; impact of H_k
$A(n_k, q_k)$	Assessment of n_k under q_k
G; u_i	Social network; a user
$a_{i,j}$	Activation probability of u_i to u_j
$v_{u_i,n_k}(q_k)$; w_{u_i,n_k}	u_i's valuation of n_k when the quantity of n_k is q_k; u_i's preference for n_k
β_i; γ_i	Breeding probability of u_i; siring probability of u_i
c_{BQ}	User breeding quota
S; (u_i, n_k)	Set of NFT airdrops; an NFT airdrop
S_k	Set of NFT airdrops for n_k
$o_{k,m}$	NFT offspring generated from n_k and n_m
$A(o_{k,m}, S, Q)$	Assessment of offspring $o_{k,m}$ given S and Q
$f(S, Q)$	Revenue of S and Q
$TP(S_k, q_k)$; $OS(S, Q)$	Total transaction price of n_k generated by S_k subject to q_k; potential transaction prices of NFT offspring under the influence of S subject to Q
λ	Parameter to adjust the weighting of OS
$V(S_k, q_k)$	Set of influenced users holding n_k under the influence of S_k with the quantity q_k
B; b_k	Set of budgets; budget for n_k
L; l_k	Set of quantity limits; quantity limit for n_k
	Section 4
$V_k^{\text{a}}(x)$	Reserve-price acceptors of n_k under reserve price x
$\mathcal{R}_k(u, \hat{S}_k^x, x)$	u's RR-Rev in n_k under the influence of $\hat{S}_k^x$ and reserve price x
$SCR_k(\hat{S}_k^x, x)$	SCR of $\hat{S}_k^x$ for n_k with $q_k = x$
$V_k^{\mathcal{R}}(\hat{S}_k^x, x)$	Set of acceptors with the top-x RR-Rev in n_k under the influence of $\hat{S}_k^x$
$W_k(y)$	The y-th largest user preference for n_k
$UB_k(x+1)$	Upper bound on n_k's revenue under $q_k = x + 1$
$\mathcal{B}_k(u_a, S, Q)$	B-Index of u_a for n_k under S with Q
$\Theta(u_a, S, Q)$	Number of treasures held by u_a given S and Q
$VOGUE_k(u, q_k)$	VOGUE of u for n_k with quantity q_k
$V_k^{\text{Val}}(q_k)$	Set of acceptors with the top-q_k valuations

values are assessed, user valuations are derived, and winning bidders among the active users are thus determined. Beyond the auction, the workflow extends to "breed offspring," where winning bidders can generate new assets through NFT breeding. Finally, the process culminates in "generate revenue," integrating total transaction price (TP) from winning bidders and offspring's potential transaction price (OS) from bred NFTs to compute the overall revenue.

D.2 NFT Terminology

Definition D.1 (NFT). An NFT, denoted as n_k, is a unique digital asset verified on a blockchain. Each NFT is characterized by a set of traits, denoted as T_k, that define its visual appearance, attributes, or functionalities.

Table 3: Abbreviation table.

Abbreviation	Description (where it is defined)
NRM	NFT Revenue Maximization (p. 5)
QOOA	Quantity and Offspring-Oriented Airdrops (p. 5)
QAS	Quantity-driven Airdrop Selection (p. 6)
ORE	Offspring Revenue Enhancement (p. 7)
RR-Rev	Reverse Reachable Revenue (p. 6)
SCR	Scarcity-Conscious Revenue (p. 6)
VQI	Valuation-based Quantity Inequality (p. 6)
RTC	Rare Trait Collector (p. 7)
B-Index	Breeding Index (p. 7)
VOGUE	Valuable Offspring Generation Utility Estimation (p. 7)

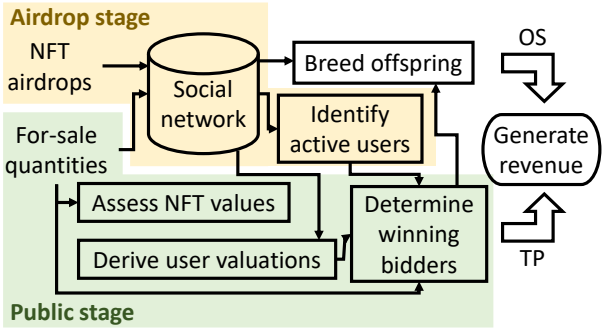

Figure 7: The workflow of NRM.

Definition D.2 (NFT project). An NFT project, denoted as $N = \{n_1, \ldots, n_{|N|}\}$, also known as an NFT collection, is a curated set of limited digital assets designed by a creator and verified via blockchain technology to ensure ownership. These NFTs typically share a consistent artistic style but exhibit variations in traits such as appearance or background, collectively forming a universal set of traits $T = \bigcup_{n_k \in N} T_k$.

For example, the Super PUMA NFT project [44] consists of 10000 NFTs, with T containing 202 distinct traits. Among them, the most viewed NFT is #10, which features seven traits: green, cool, calico, beanie, motorsport helmet, white shirt, and easy rider.

Definition D.3 (Social network). A social network $G = (V, E)$ within the NFT marketplace consists of a user set V and an edge set E. Each user $u_i \in V$ has a personal preference for an NFT n_k, denoted as $w_{u_i,n_k} \in [0, 1]$, while each edge $e_{i,j} \in E$ indicates that $u_i \in V$ has an activation probability of $a_{i,j} \in (0, 1]$ to influence $u_j \in V$.[16]

Definition D.4 (Airdrop). An airdrop, denoted as (u_i, n_k), designates the free distribution of a digital asset n_k, such as a token or a coin, to a user u_i. NFT airdrops aim to incentivize users to engage in viral marketing on social networks by giving complimentary

[16]The user preference can be derived from learning models, such as HG-GNN [118] and DGNN [104], according to the purchase history of the user and the traits of the NFT. Moreover, it can also account for both personal and global economic conditions [132], detailed in Appendix D.6

gifts. Let S_k denote the set of all airdrops for n_k. Note that each element in S_k is of the form (u_i, n_k) for some user u_i. Thus, it is clear that $S_k \cap S_m = \emptyset$ for any $k, m \in \{1, 2, \ldots, |N|\}$ with $k \neq m$. Let $S = \bigcup_{n_k \in N} S_k$ represent the set of all airdrops used in NFT viral marketing.

Definition D.5 (Reserve price). The reserve price of an NFT n_k, denoted as p_k, represents the lowest acceptable price at which n_k can be sold.[17] A user u_i with a valuation $v_{u_i,n_k}(q_k) < p_k$ is unable to purchase n_k, as the price is set beyond their willingness to pay. For an NFT project N, let $P = \{p_1, \ldots, p_{|N|}\}$ denote the set of reserve prices for all NFTs in N.

D.3 Details on NFT Assessment

The value of an NFT can be assessed based on its scarcity, rarity, and ownership [85, 94, 109, 112, 115, 127, 144].

Definition D.6 (Scarcity). Following [94, 109, 144], the scarcity of an NFT n_k refers to the quantity of n_k available for sale, i.e., q_k. The value of an NFT n_k is likely to boost if it is scarce, i.e., q_k is small. For an NFT project N, let $Q = \{q_1, \ldots, q_{|N|}\}$ denote the set of quantities for all NFTs in N.

Definition D.7 (Rarity). Following [85, 112], the rarity of *a trait* t is inversely proportional to its occurrence in the set N, i.e.,

$$\phi(t) = \frac{|N|}{Occ(t, N)}, \tag{8}$$

where $Occ(t, N)$ represents the number of NFTs in N possessing the trait t. The rarity of *an NFT* n_k is the sum of the rarity of its traits, i.e.,

$$\Phi(n_k) = \sum_{t \in T_k} \phi(t), \tag{9}$$

where T_k is the set of traits for NFT n_k.

Definition D.8 (Ownership). The ownership history of n_k, especially when held by notable users (e.g., celebrities) [107], usually increases its value. Ownership primarily affects the assessment of offspring, as the breeder becomes the initial holder. Let H_k denote the set of all previous and current owners of n_k. The impact imparted by H_k, denoted as h_k, can be evaluated by the prominence of users in H_k.[18]

Definition D.9 (NFT assessment). Following [85], the objective assessment of n_k under a quantity q_k is defined as follows.

$$A(n_k, q_k) = e^{\eta_0 + \eta_1 \frac{1}{q_k} + \eta_2 \Phi(n_k) + \eta_3 h_k}, \tag{10}$$

where η_0, η_1, η_2, and η_3 are weight parameters.[19] As shown, n_k is assessed by *scarcity* ($e^{\eta_1 \frac{1}{q_k}}$, assessed higher as n_k becomes scarcer), *rarity* ($e^{\eta_2 \Phi(n_k)}$, assessed higher when n_k possesses more rare traits [85, 112]), and *ownership* ($e^{\eta_3 h_k}$, assessed higher when n_k has been held by more notable users [107]). Meanwhile, for all $n_k \in N$, e^{η_0} represents the assessment related to the whole NFT project, e.g., the reputation of the creator [91] and the market trend (detailed in Appendix D.6.2).

Next, we turn to assess the value of the offspring. Similar to the assessment of NFTs, the offspring are also assessed according to scarcity, rarity, and ownership.

Definition D.10 (Offspring assessment). As the diffusion of S with Q reaches different users and subsequently influences the breeding of NFT offspring, the assessment of an offspring should also take S and Q into account. For an offspring $o_{k,m}$, following [85, 112, 127], its objective assessment of $o_{k,m}$ is derived similarly to Equation (10) as follows.

$$A(o_{k,m}, S, Q) = e^{\eta_0 + \eta_1 \frac{1}{q_{k,m}(S,Q)} + \eta_2 \sum\limits_{t \in T_{k,m}} \frac{|N \cup O(S,Q)|}{Occ\left(t, N \cup O(S,Q)\right)} + \eta_3 h_{k,m}}, \tag{11}$$

where $q_{k,m}(S, Q)$ is the quantity of $o_{k,m}$ given S and Q, $O(S, Q)$ is the set of all NFT offspring given S and Q, and $h_{k,m}$ is the impact of u_i since $H_{k,m} = \{u_i\}$.[20] Similar to Equation (10), $o_{k,m}$ is assessed at $e^{\eta_1 \frac{1}{q_{k,m}(S,Q)}}$, $e^{\eta_2 \sum\limits_{t \in T_{k,m}} \frac{|N \cup O(S,Q)|}{Occ\left(t, N \cup O(S,Q)\right)}}$, and $e^{\eta_3 h_{k,m}}$ according to scarcity, rarity, and ownership, respectively, while e^{η_0} indicates the assessment related to the NFT project.

In addition, let $\mathbb{E}[\mathcal{V}(o_{k,m}, S, Q)]$ denote the expected transaction price of $o_{k,m}$. $\mathbb{E}[\mathcal{V}(o_z^i, S, Q)]$ is derived from 1) the probability, denoted as $Pr(o_z^i = o_{k,m})$, that u_i breeds the offspring $o_{k,m}$ by selecting a breeding pair (n_k, n_m), where each eligible pair is chosen with equal likelihood, 2) the assessment of $o_{k,m}$ (i.e., $A(o_{k,m}, S, Q)$ derived from Equation (11)) and 3) the expected preference of users across the entire social network, denoted as ω, which is derived from the engagement rate in [74, 120] and accounts for the uncertainty of future winning bidders. Hence, $\mathbb{E}[\mathcal{V}(o_z^i, S, Q)]$ is formulated as follows.

$$\mathbb{E}[\mathcal{V}(o_z^i, S, Q)] = \sum_{(n_k, n_m) \in \mathcal{P}_i} Pr(o_z^i = o_{k,m}) \cdot A(o_{k,m}, S, Q) \cdot \omega, \tag{12}$$

where $\mathcal{P}_i$ denotes the set of all eligible breeding pairs for user u_i, $Pr(o_z^i = o_{k,m}) = \frac{1}{|\mathcal{P}_i|}$ reflects the uniform selection probability among eligible breeding pairs, $A(o_{k,m}, S, Q)$ represents the assessment of the offspring, and ω captures the expected preference of users across the social network.

D.4 Details on the Airdrop and Public Stages

Initially, in the airdrop stage, all users are inactive in all NFTs, except for those in the set of NFT airdrops S who are active for their respective NFT.[21] Following the diffusion model, a user who is

[17] The determination of the reserve prices is detailed in Appendix D.6.1.

[18] Generally, the popularity of celebrities on social networks can be measured by various approaches [60, 83]. For the NFT market, it can be further enhanced by the number of NFTs they hold and the frequency of their transactions [58, 119]. When n_k has not been held by any user, i.e., $H_k = \emptyset$, then $h_k = 0$.

[19] The weight parameters can be learned from previous NFT projects with ordinary least square regression in [85].

[20] $q_{k,m}(S, Q)$ and $O(S, Q)$ are determined by S and Q, as S influences the set of active users, while Q determines which users acquire the NFTs, collectively shaping the composition of NFT holders. Variations in holder composition affect the feasible offspring combinations, influencing $O(S, Q)$ and altering the quantity of identical offspring $q_{k,m}(S, Q)$.

[21] A user active in an NFT n_k is said to be interested in n_k. Following most diffusion models [62, 81, 92, 126], user states are progressive; that is, active users do not revert to being inactive.

active in an NFT n_k may influence her inactive friend u_j to become active in n_k. Once u_j is successfully influenced by her active friend, she too becomes active in n_k.[22] The influence thus propagates until no more users can be influenced.

In the public stage, the active users bid on NFTs based on their valuations of NFTs. In most NFT marketplaces, such as OpenSea and Blur, each n_k is sold to its top q_k bidders.[23] Specifically, each of the active users of n_k who have the top q_k highest valuations acquires a single NFT n_k, where the valuations are no smaller than the reserve price p_k. For a user u_i winning an NFT n_k, the *transaction price* is equal to her offer according to her valuation $v_{u_i,n_k}(q_k)$, where $v_{u_i,n_k}(q_k) \geq p_k$. Note that n_k may not be sold out if there are fewer than q_k users with valuations of at least p_k.

Definition D.11 (Budget Constraint). Let $B = \{b_1, \ldots, b_{|N|}\}$ denote the set of budgets for the NFTs in N, where each b_k represents the maximum number of airdrops that can be distributed for NFT n_k, i.e., $|S_k| \leq b_k$.[24]

Definition D.12 (Quantity Limit Constraint). Let $L = \{l_1, \ldots, l_{|N|}\}$ denote the set of quantity limits for the NFTs in N, where each l_k limits the maximum quantity of NFT n_k that can be offered for sale, i.e., $q_k \leq l_k$.[25]

Based on the airdrop and public stages, a basic problem setting for promoting an NFT project is to maximize the transaction price TP subject to the budget and quantity limit constraints.

Problem: *NFT Revenue Maximization (NRM) without breeding*
Instance: An NFT project N with traits T and their reserve prices P, a social network G, a set of airdrop budgets B for N, and a set of quantity limits L.
Task: To promote the NFT project N by finding a set of airdrops S and a set of NFT quantities Q for N, such that the budget and quantity limit constraints hold. The objective is to maximize the total transaction price $TP(S, Q)$.

D.5 Details on Breeding

The breeding mechanisms prevalent in various NFT projects are elaborated as follows.

1) *Breeding constraints*: An NFT breeding mechanism usually has some constraints to maintain the NFTs' rarity and regulate breeding frequency. Almost all NFT projects enforce a cooldown period, ensuring *non-concurrent breeding* [4, 12, 14, 23, 43]. Besides, users are restricted by a breeding quota c_{BQ}, i.e., the maximum number of simultaneous breeding pairs owned by a user. For example, in MODragon, $c_{\mathrm{BQ}} = 5$ [27]. Each NFT may also have a breeding limit that defines the maximum number of times it can engage in breeding. For example, in STEPN, the maximum breeding limit is 7, and the cooldown period grows longer as the breed count of NFTs approaches 7. In addition, inbreeding restrictions may be in place to protect genetic diversity, e.g., MODragon also prohibits the breeding of sibling NFTs.

2) *Genetic mechanisms*: Generally, offspring inherit traits from their parent NFTs, but rarer traits have lower inheritance chances. Boosters can raise the inheritance probability of a specific trait by c_{BT}. For example, in Crypto Unicorns, using a berry (booster) associated with a trait increases its inheritance probability by 10% [12]. Besides, mutations introduce an element of unpredictability by occasionally endowing offspring with entirely novel traits, thereby enhancing their rarities. For example, in Tiny World [47], offspring have a greater chance of mutation when the breed counts of their parents increase.

3) *Collaborative breeding*: This mechanism, which facilitates community interaction, is prominently adopted by Roaring Leader [41], Axie Infinity [26], and CryptoKitties [15]. An NFT holder u_j has a siring probability, denoted as γ_j, to designate his NFTs as available for siring, indicating a willingness to collaborate with friends' NFTs in the breeding process.[26] Let u_j's friend u_i, desiring to breed her NFTs, have a breeding probability, denoted as β_i. Besides breeding with her own NFTs, u_i can choose to engage with u_j's siring-ready NFTs. It is noteworthy that the initiator of the breeding (i.e., u_i) is the legal owner of the offspring.

4) *NFT maturation*: The lifecycle of NFT offspring may follow a distinct evolutionary path of multiple stages, including egg, baby, and adult. Until the phase of hatching, the traits of an NFT offspring are typically concealed. At this point, holders have the option to trade, and the inherent uncertainty often boosts the NFT's assessment. After hatching, certain NFT projects, such as Crypto Unicorns, reach the baby stage. As they attain the adult stage of development, they have the opportunity to mutate and acquire rare traits. Notably, these NFTs cannot breed offspring until they have reached the adult stage.

5) *Fusion breeding*: This mechanism requires parent NFTs to be surrendered (i.e., sacrificing parent NFTs) to potentially breed offspring with upgraded rarity. The likelihood of fusing traits from parent NFTs to generate offspring with an upgraded (i.e., rarer) trait increases from 0 to c_{F}, potentially enhancing the value of the offspring. In Fat Ape Club, for example, fusion breeding produces new and stronger apes [20].

Accordingly, we present the detailed definitions of individual and collaborative breeding mechanisms as follows.

Definition D.13 (Individual Breeding Mechanism). This mechanism enables users to form multiple breeding pairs concurrently, subject to the non-concurrent breeding and the user breeding quota constraints. For each NFT owned by a user u_i, there is a probability β_i that u_i is willing to initiate breeding. When initiating breeding, u_i may select any two distinct NFTs from their collection to form a breeding pair, thereby producing offspring. Under the non-concurrent breeding and the user breeding quota constraints, each NFT can participate in at most one breeding pair at a time, and they may form up to c_{BQ} pairs simultaneously. Users determine the formation of breeding pairs based on their individual inclinations. In practice, rational users tend to select pairs composed of NFTs with rare traits, as such combinations are more likely to yield rare

[22] For the promotional relationship between different NFTs, when a user influenced by an NFT n_k is more likely to be influenced by another NFT n_m ($m \neq k$), diffusion models for multiple correlated items [54, 88, 141] can be adopted for the proposed problem.

[23] Following research on influence, revenue, and profit maximization [57, 92, 137], the seed users (i.e., those who receive free samples, referred to as airdrops in the context of NFTs) have already obtained the products. Hence, there is no need for them to participate in the bidding process to acquire the NFTs.

[24] The determination of budgets is detailed in Appendix D.6.1.

[25] The determination of quantity limits is detailed in Appendix D.6.1.

[26] Offering NFTs for siring usually enhances one's reputation within the NFT community and may also earn siring fees.

offspring. Finally, for any breeding pair (n_k, n_m) formed by u_i, the resulting offspring $o_{k,m}$ is owned by u_i; that is, the ownership history of $o_{k,m}$, denoted as $H_{k,m}$, is $\{u_i\}$.

Definition D.14 (Collaborative Breeding Mechanism). This mechanism enables users to collaborate with their friends to breed offspring. Specifically, for each NFT owned by a user u_i, there is a probability β_i that the NFT is selected for breeding. Concurrently, for each friend u_j of u_i, each NFT held by u_j is chosen for siring with probability γ_j. Note that an NFT contributed for siring remains owned by its original holder. Subsequently, u_i forms a breeding pair by selecting one of the NFTs designated for breeding from their collection and one of the NFTs designated for siring from one of their friends. The formation of these breeding pairs is subject to the non-concurrent breeding and user breeding quota constraints; that is, each NFT can participate in at most one breeding pair simultaneously, and u_i may form at most c_{BQ} breeding pairs concurrently. Similar to the individual breeding mechanism, breeding pairs are determined by individual inclinations in practice. Finally, for any breeding pair (n_k, n_m) formed by u_i, the resulting offspring $o_{k,m}$ is owned by u_i, even if n_m is contributed by one of u_i's friends, i.e., $H_{k,m} = \{u_i\}$.

D.6 Discussion on Problem Parameters

D.6.1 Tractability Enhancement of NRM. This subsection discusses how to obtain or simplify parameters to make NRM tractable.

We first elaborate on the acquisition of the following parameters. 1) *Activation probability*: The activation probability $a_{i,j}$ represents the likelihood that user u_i successfully influences user u_j. Following [122, 143], which employ Bayesian networks and mixed-integer programming to learn activation probabilities from historical cascades that capture the propagation of information or influence within a network (such as social media interactions, product shares, or retweets), these probabilities can be derived accordingly. 2) *Preference*: The preference v_{u_i,n_k} quantifies the extent to which user u_i favors a particular NFT n_k. Following [104, 118, 134, 146], which utilize RNN, LSTM, HG-GNN, and DGNN to learn personal preferences from purchasing history, incorporating details such as NFTs bought, prices paid, user demographic information, and NFT traits, the user preferences can be derived accordingly. 3) *Reserve price*: The reserve price of an NFT represents the minimum acceptable selling price and can be set at the discretion of the project creators based on their strategic objectives or market preferences. One common approach is to reference existing similar NFTs. For instance, Trump's fourth NFT series maintained consistency with the previous three series, setting the reserve price for each NFT at $99 [11]. 4) *Budget*: The budget for each NFT defines the maximum number of airdrops that can be distributed and is determined by the project creator based on their allocation strategy or financial constraints. Alternatively, data-driven approaches, such as leveraging blockchain transaction data and tokenomics models to analyze similar projects [52], offer a systematic basis for budget determination. 5) *Quantity limit*: The quantity limit for each NFT specifies the maximum number available for sale and can be adjusted by the project creator to align with supply constraints or market positioning. Following [101], which employs formal concept analysis to examine the relationship between trait sets and price fluctuations in NFTs, the quantity limits could also be derived based on the rarity of the trait sets.

On the other hand, we discuss the problem parameters that can be simplified to improve tractability. 1) *Activation probability*: Following [81, 103, 117], the activation probability of u_i to influence u_j can be set to $\frac{1}{\deg(u_j)}$, where $\deg(u_j)$ denotes the in-degree of u_j. Unlike the activation probability, the following parameters in NRM reflect practical constraints: reserve prices set a minimum bid, quantity limits control supply, and breeding quotas regulate resource use. However, when these constraints are unnecessary, they can be set to specific values to simplify the problem, representing an unconstrained scenario. This practice is common in optimization problems; for example, in the Deadline Traveling Salesman Problem [56], when there is no practical need for a deadline, setting the deadlines to infinity effectively simplifies the problem. 2) *Reserve price*: The reserve prices can be set to 0, removing any minimum bidding requirements. This ensures that all users, regardless of their valuation, can place bids without restriction. 3) *Quantity limit*: The quantity limits can be set to the total number of users in the social network, i.e., $|V|$. This removes constraints on the quantity search space, as any quantity exceeding $|V|$ yields the same outcome as setting it to $|V|$. 4) *User breeding quota*: The user breeding quota, which limits the maximum number of concurrent breeding pairs a user can engage in, can be set to unlimited. This allows users to form an unrestricted number of breeding pairs, provided that each NFT participates in only one breeding pair at a time.

While the above parameters can be simplified to enhance tractability, key parameters such as the ownership impact h_k of NFT n_k, the breeding probability β_i of user u_i, and the siring probability γ_i of user u_i remain essential, as they capture the defining characteristics of NFTs, including ownership-driven valuations, individual breeding, and collaborative breeding. Removing these parameters would weaken NRM's ability to accurately model the fundamental properties of NFTs.

D.6.2 Additional Real-world Considerations. This subsection generalizes our formulation to accommodate additional real-world factors, such as market trends and economic conditions.

1) *Market trends*: The valuation of NFTs is influenced by various market factors, including the popularity of different NFT categories (e.g., profile picture NFTs, utility NFTs, gaming NFTs), shifts in investor sentiment (e.g., speculative trading vs. long-term holding), and prevailing demand patterns (e.g., blue-chip collections vs. emerging projects). In Equation (10), the term e^{η_0} represents the overall assessment of an NFT project. To incorporate market trends, η_0 should explicitly account for: i) creator reputation, where well-established projects (e.g., Bored Ape Yacht Club) typically receive higher assessments; ii) NFT category popularity, as certain types of NFTs (e.g., profile picture NFTs) may experience higher demand at a given time; and iii) liquidity and trading volume, where projects with greater transaction activity tend to be valued more favorably. These factors refine the assessment of all NFTs within a project, ensuring that user valuations align with prevailing market conditions rather than assuming universal desirability. By integrating these elements into η_0 with market-driven modeling techniques that account for liquidity, investor sentiment, and transaction activity,

as explored in cryptocurrency and DeFi market analyses [77, 78], NRM enhances its alignment with real-world investor behavior.

2) *Economic conditions*: Users' disposable income levels, overall crypto market stability (e.g., Ethereum price fluctuations), and prevailing investor sentiment (e.g., risk aversion vs. speculative behavior) significantly impact their willingness to invest in NFTs. In Equation (1), the user preference w_{u_i,n_k} can be adjusted to further incorporate these economic factors, including: i) income levels, where higher-income users may exhibit stronger preferences for premium NFTs; ii) market sentiment, as risk-averse investors are more likely to favor established NFT projects over speculative assets; and iii) the crypto wealth effect, wherein users whose cryptocurrency holdings have appreciated (e.g., due to an increase in ETH prices) may demonstrate higher valuations for NFTs. Following [53], which learns utility functions from revealed preferences, different economic conditions, such as users' available financial resources and crypto market volatility (e.g., ETH price fluctuations), can be incorporated into user preference/status modeling through utility-based analysis of purchasing behavior. By integrating economic conditions into w_{u_i,n_k}, NRM ensures that user valuations reflect real-world financial constraints and investment behavior rather than assuming uniform preferences across all individuals.

D.7 Other Application Scenarios of NRM

NRM is not limited to NFT applications but is general and capable of addressing prior IM and RM problems, as well as various scenarios such as loyalty-aware marketing and demand-side economies of scale. The revenue function f can be tailored to fit the objectives of these applications.

1) *Influence maximization on complementary products.* Prior influence maximization considers products with complementary relationships [88, 141], where users often purchase multiple products together. NRM can address this by tailoring the objective f, with TP representing the total number of users influenced by these products, OS representing the number of users simultaneously influenced by complementary products, and λ indicating the strength of the complementary relationship between the products.

2) *Maximizing interactions.* Prior work [72, 73] focuses on maximizing interactions among activated nodes. NRM addresses this by tailoring the objective f to focus exclusively on OS (with $\lambda = 1$), where OS represents the number of interactions between influenced users.

3) *Loyalty-aware marketing.* According to customer relationship management [100], in addition to acquiring new customers, loyalty and repeat business are long-term goals. For example, Apple's ecosystem strategy seamlessly integrates its products, such as the iPhone, iPad, Mac, and Apple Watch. It fosters high customer loyalty, as users are incentivized to remain within the Apple ecosystem for compatibility and enhanced functionality. Similarly, Tesla's ecosystem of electric vehicles, energy storage solutions, and solar panels encourages customers to invest in multiple Tesla products, reinforcing brand loyalty through interconnected benefits. The objective is to maximize f by considering TP as the revenue earned from the sales of all products, OS as the additional benefits from loyalty, and λ as the weighting on these additional benefits. Specifically, in TP, v_{u_i,n_k} is the revenue earned from user u_i's purchase of product n_k. For instance, in Apple's ecosystem, when a user u_i purchases an iPhone, the revenue from that sale corresponds to $v_{u_i,\text{iPhone}}$. In OS, a user is regarded as loyal when they purchase multiple products within the ecosystem, such as an iPhone and an Apple Watch, which together enhance the user's experience. The benefit from loyalty, $\mathbb{E}[\mathcal{V}(o^i_{k,m}, S, Q)]$, represents the added value derived from owning both products n_k (e.g., iPhone) and n_m (e.g., Apple Watch) simultaneously. In such cases, c_{BQ} is considered infinite to ensure the focus remains on maximizing the interconnected value.

4) *Demand-side economies of scale.* This phenomenon occurs when the utility a user derives from a good or service increases with the number of friends or collaborators using compatible products [69]. For example, in electronic payment systems like PayPal, a user can use the platform to make purchases at merchants. When friends also use PayPal, the utility increases significantly, as it enables peer-to-peer transfers, making it easier to split bills, lend money, or settle debts directly within their network. Similarly, Slack offers personal task management and integration with other tools. Its utility is amplified when an entire team adopts the platform, allowing for real-time collaboration, group messaging, and streamlined communication across the team, which are only possible when all relevant participants are active users. The objective is to maximize f by considering TP as the user utility derived from the product, OS as the additional utility from demand-side economies of scale, and λ as the weighting for this phenomenon. Specifically, in TP, $v_{u_i,n}$ represents user u_i's utility from independently using product n. For instance, a user may derive basic utility from using PayPal for purchases at merchants or Slack for personal organization and integrations. In OS, $\mathbb{E}[\mathcal{V}(o^{i,j}, S, Q)]$ reflects the additional utility for user u_i when using the product with her friend u_j. For example, PayPal's utility increases significantly when u_i can also engage in peer-to-peer transfers with u_j, or Slack's value is enhanced when both u_i and u_j are part of the same team, enabling collaborative communication and shared workflows. In these cases, c_{BQ} is infinite, ensuring that the focus remains on maximizing utility derived from network interactions.

E Theoretical Analysis

E.1 NRM's Hardness

Theorem E.1. *NRM is NP-hard and cannot be approximated within a factor of* $|V|^{1/(\log\log|V|)^c}$ *assuming the exponential time hypothesis (ETH), where* $c > 0$ *is a constant independent of* $|V|$.

Proof. We prove this theorem with a reduction from the Densest k-Subgraph problem (DkS), which is NP-hard and cannot be approximated within a factor of $|V|^{1/(\log\log|V|)^c}$ assuming the exponential time hypothesis (ETH), where $c > 0$ is a constant independent of $|V|$ [110]. Given a graph G and two integers k and h, where h is set to a sufficiently large integer, the decision version of DkS is to decide whether there exists an induced subgraph of G with k vertices and h edges.[27] Given an instance (G, k, h) of

[27]The parameter h is set to a sufficiently large interger, ensuring that any induced subgraph of G with k vertices has no more than h edges. In fact, in theoretical analysis, there is no need to know the exact value of h. Instead, it is necessary to examine whether the logical inference holds true. With the setting of h (i.e., ensuring that any induced subgraph of G with k vertices has no more than h edges), our goal is to determine whether there exists an induced subgraph of G with k vertices and *exactly* h edges.

DkS, where $V(G) = \{v_1, v_2, \ldots, v_{|G|}\}$, we construct an instance of NRM as follows. i) Let $W = \{w_1, w_2, \ldots, w_{|G|}\}$, where w_i is a copy of v_i for any $i \in \{1, 2, \ldots, |G|\}$. The social network of the NRM instance is a graph with vertex set $V(G') \cup W$ and edge set $E(G') \cup \{e_{w_1,v_1}, e_{w_2,v_2}, \ldots, e_{w_{|G|},v_{|G|}}\}$, where G' is an orientation of G, i.e., G' is obtained from G by assigning exactly one direction to each edge of G. The activation probability a_{v_i,v_j} is set to 0 for any edge $e_{v_i,v_j} \in E(G')$, and a_{w_i,v_i} is set to 1 for any $i \in \{1, 2, \ldots, |G|\}$. ii) The NFT project $N = \{n_1\}$, reserve price $p_1 = 1$, seed budget $b_1 = k$ and valuation $v_{u,n_1}(q_1) = 1$ for each user $u \in V(G') \cup W$ and any quantity q_1 of NFT n_1.[28] Let $\beta_i = 1$ and $\gamma_i = 1$ for any user $u_i \in V(G') \cup W$, i.e., in the constructed instance, the NFT offspring can be created only when two activated users are friends, and each of them provides a parent NFT, since there is only one NFT involved. Thus, the creation of an offspring corresponds to the existence of an edge between two activated users. Let $\mathcal{V}(o, S, Q) = 1$ for any NFT offspring o under the diffusion of any S and Q.[29] iii) Let $\lambda = 1$.

To complete the proof, we show that there exists an induced subgraph with k vertices and h edges in DkS if and only if there is a set of NFT airdrops S of size k and a set of NFT quantity $Q = \{q_1 = \infty\}$ such that $f(S, Q) = k + h$ in NRM. We first prove the necessary condition. Suppose that there exists an induced subgraph with k vertices and h edges in DkS. Let the k corresponding users in W form the set of NFT airdrops S, and let $Q = \{q_1 = \infty\}$. By the construction, exactly k users in $V(G')$ are activated, and exactly h offspring are created. Thus (S, Q) is a solution such that $f(S, Q) = k + h$. We then prove the sufficient condition. Suppose that there is a set of NFT airdrops S of size k and a set of NFT quantity $Q = \{q_1 = \infty\}$ such that $f(S, Q) = k + h$ in NRM. Since the activation probability $a_{v_i,v_j} = 0$ for $e_{v_i,v_j} \in E(G')$ and $a_{w_i,v_i} = 1$ for $i = \{1, 2, \ldots, |G|\}$, if any user receiving one of the k NFT airdrops is not selected from W, this user cannot activate anyone, resulting in fewer than k users being activated to acquire the NFT. Moreover, the number of edges induced by these activated users (fewer than k) is no more than h. The reason is as follows. Recall that, by the setting of h, any induced subgraph of G with k vertices has no more than h edges. Hence, any induced subgraph with fewer than k vertices also has no more than h edges. Therefore, we conclude that the k NFT airdrops must be chosen from the set W, otherwise $f(S, Q) \leq (k - 1) + h < k + h$. Thus the corresponding vertices in $V(G)$ form an induced subgraph with k vertices and h edges in DkS. Therefore, NRM is NP-hard and cannot be approximated within a factor of $|V|^{1/(\log\log|V|)^c}$ assuming ETH, where $c > 0$ is a constant independent of $|V|$. The theorem follows. □

E.2 QOOA's Performance Guarantee

E.2.1 Correctness of QAS. QAS ensures that each time a seed group is identified under quantity q_k for NFT n_k, the solution is retained only if it generates higher revenue than previous ones (lines 20-21 in Algorithm 1). If the final solution (S_k, q_k) can be further improved by QAS, implying that there is a solution (S'_k, q'_k) with higher revenue than it. According to the operation of QAS, (S_k, q_k) should be replaced, indicating that it should not be the final solution. Therefore, q_k is incrementally increased by 1 to search (S'_k, q'_k). Please note that q'_k will not be smaller than q_k; otherwise (S'_k, q'_k) is updated as a solution in the earlier time, and it is impossible that the operation of QAS updates (S_k, q_k) as a new solution.[30] Therefore, the approximation ratio is ensured according to Lemma E.5 and Theorem 4.1.

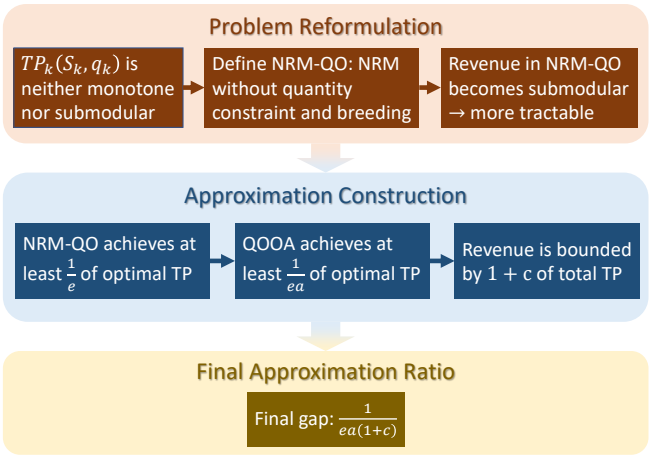

Figure 8: The logic flow of the proof strategy.

E.2.2 Correctness of SCR.

Lemma E.2. *For a set of airdrops S_k for n_k under a quantity q_k, $SCR_k(S_k, q_k) \geq TP_k(S_k, q_k)$.*

Proof. Recall $TP_k(S_k, q_k) = \sum_{u_j \in V(S_k,q_k)} v_{u_j,n_k}(q_k)$, where $V(S_k, q_k)$ is the set of users influenced by S_k to hold the NFT n_k under the quantity q_k. For each $u_j \in V(S_k, q_k)$, her expected revenue on NFT n_k is no greater than $\mathcal{R}_k(u_j, S_k, q_k)$. As SCR has taken RR-Rev of the users in $V_k^{\mathcal{R}}(S_k, q_k)$ into account, for any user $u_j \in V(S_k, q_k)$, if $u_j \in V_k^{\mathcal{R}}(S_k, q_k)$, her RR-Rev is already counted in SCR; otherwise, her RR-Rev must be no greater than $\mathcal{R}_k(u_{\min}, S_k, q_k)$, where $u_{\min}$ is the user with the least RR-Rev in $V_k^{\mathcal{R}}(S_k, q_k)$. Therefore, $SCR_k(S_k, q_k)$ is the upper bound of $TP_k(S_k, q_k)$. The lemma follows. □

E.2.3 Approximation Ratio. We first provide the proof strategy for each derivation step, where the logic flow is illustrated in Figure 8.

1) Formulate a simplified problem, i.e., NRM without the quantity constraint and breeding (NRM-QO) (as shown in the Problem Reformulation layer in Figure 8): We show that the total transaction price function $TP_k(S_k, q_k)$ of an NFT n_k is neither monotonically increasing nor submodular in NRM (Lemma E.3, as shown in the leftmost box in the Problem Reformulation layer in Figure 8), where S_k denotes the set of airdrops for n_k and q_k represents the quantity of n_k available for sale. Hence, we consider an unconstrained problem,

[28] For each $u \in V$, $v_{u,n_1}(q_1)$ can be set to 1 by letting the personal preference $w_{u,n_1} = 1$ and the parameters $\eta_0 = \eta_1 = \eta_2 = \eta_3 = 0$, i.e., $v_{u,n_1}(q_1) = w_{u,n_1} \times e^{\eta_0 + \eta_1 \frac{1}{q_1} + \eta_2 \Phi(n_1) + \eta_3 h_1} = 1 \times e^0 = 1$.

[29] $\mathcal{V}(o, S, Q)$ can be set to 1 by letting the parameters $\eta_0 = \eta_1 = \eta_2 = \eta_3 = 0$, i.e., $\mathcal{V}(o, S, Q) = e^0 = 1$.

[30] For uncorrelated influence propagation between NFTs, QAS independently determines the quantity and airdrops for each NFT, making the order of examination irrelevant.

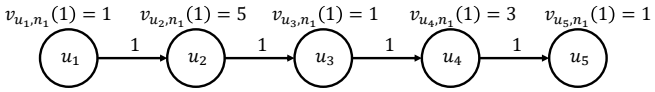

Figure 9: An example for Lemma E.3.

NRM-QO, similar to NRM but without the quantity constraint and NFT breeding (as shown in the middle box in the Problem Reformulation layer in Figure 8). In this unconstrained problem, we show that the revenue function is still non-monotonically increasing but becomes submodular (Lemma E.4), making it more tractable for analysis (as shown in the rightmost box in the Problem Reformulation layer in Figure 8).

2) Use NRM-QO to approximate NRM (as shown in the Approximation Construction layer in Figure 8): To construct the connection between NRM and NRM-QO, we show that the revenue of NRM-QO is at least $\frac{1}{e}$ times of the optimal total transaction price function (Lemma E.5, as shown in the leftmost box in the Approximation Construction layer in Figure 8). We then prove that the total transaction price function of QOOA is at least $\frac{1}{ea}$ times of the optimal total transaction price function (Equation (16), as shown in the middle box in the Approximation Construction layer in Figure 8), where $a = \max\limits_{1\le k\le|N|} \frac{r(\hat{S}_k,1)}{p_k}$. Here, $|N|$ denotes the number of NFTs in the NFT project N, p_k represents the reserve price of n_k, and $r(\hat{S}_k, 1)$ is the highest valuation among active users who have valuations exceeding p_k under the influence of $\hat{S}$. The set $\hat{S}$ is the solution obtained by the continuous greedy algorithm [71] for solving NRM-QO for n_k. Based on the relationship between the total transaction price and the potential transaction prices of the offspring, we prove that the output revenue of any solution of NRM is at most $1 + c$ times of the total transaction price function (Equation (18), as shown in the rightmost box in the Approximation Construction layer in Figure 8), where $c = \frac{\lambda q_{\max} c_{\mathrm{BQ}} \mathcal{V}_{\max}}{p_{\min}}$. Here, λ is a parameter that adjusts the weighting of potential transaction prices for offspring, $q_{\max} = \max_{q_k\in Q} q_k$ represents the maximum quantity, c_{BQ} denotes the user breeding quota, $\mathcal{V}_{\max}$ is the maximum potential transaction price of offspring, and $p_{\min}$ is the minimum reserve price.

3) Combine the above results, we conclude that the approximation gap is $\frac{1}{ea(1+c)}$ (as shown in the Final Approximation Ratio layer in Figure 8).

Note that in the influence propagation of NFTs during the Airdrop stage, for each NFT n_k, its total transaction price function $TP_k(S_k, q_k)$ is independent from other NFTs. In the following, we first examine whether the total transaction price function $TP_k(S_k, q_k)$ is submodular.

Definition E.1 (Submodular function [99]). Given a ground set U, a set function $\rho : 2^U \mapsto \mathbb{R}$ is submodular if for any subsets X, Y with $X \subseteq Y$ and any element $u \in U \setminus Y$,

$$\rho(Y \cup \{u\}) - \rho(Y) \le \rho(X \cup \{u\}) - \rho(X). \tag{13}$$

Unfortunately, $TP_k(S_k, q_k)$ is non-monotonically increasing and thus not submodular.

Lemma E.3. *For each $k \in \{1, 2, \ldots, |N|\}$, the total transaction price function $TP_k(S_k, q_k)$ is neither monotonically increasing nor submodular.*

Proof. We prove this lemma by giving an instance as follows. Let the NFT project $N = \{n_1\}$, airdrop budget $b_1 = 3$, NFT quantity $q_1 = 1$, reserve price $p_1 = 1$ and the social network G be a path graph of five vertices, i.e., there are five users $u_1, u_2, \ldots, u_5$, and four edges $e_{i,i+1}$, $1 \le i \le 4$, where each edge $e_{i,i+1}$ has the activation probability of $a_{i,i+1} = 1$, as shown in Figure 9. The valuations of all users u_i for NFT n_1 are $v_{u_1,n_1}(q_1) = 1$, $v_{u_2,n_1}(q_1) = 5$, $v_{u_3,n_1}(q_1) = 1$, $v_{u_4,n_1}(q_1) = 3$, and $v_{u_5,n_1}(q_1) = 1$, respectively. In this instance, when (u_3, n_1) is chosen as the only airdrop, users u_4 and u_5 are activated, and thus u_4 acquires the NFT n_1, i.e., $TP_k(\{(u_3, n_1)\}, q_1) = 3$. However, if we choose (u_3, n_1) and (u_4, n_1) as the airdrops, only user u_5 is activated, and thus $TP_k(\{(u_3, n_1), (u_4, n_1)\}, q_1) = 1$, which implies that the revenue function $TP_k(S_1, q_1)$ is non-monotonically increasing.

To prove the non-submodularity, we consider two sets of airdrops $\{(u_1, n_1), (u_3, n_1)\}$ and $\{(u_1, n_1), (u_3, n_1), (u_4, n_1)\}$. The former set of airdrops results in $f(\{(u_1, n_1), (u_3, n_1)\}, q_1) = 5$ because u_2, u_4 and u_5 are activated, and u_2 acquires NFT n_1, and the latter results in $TP_k(\{(u_1, n_1), (u_3, n_1), (u_4, n_1)\}, q_1) = 5$ because u_2 and u_5 are activated, and u_2 acquires NFT n_1. Therefore,

$$TP_k(\{(u_1, n_1), (u_3, n_1), (u_4, n_1)\}, q_1) - TP_k(\{(u_3, n_1), (u_4, n_1)\}, q_1) = 4$$

and

$$TP_k(\{(u_1, n_1), (u_3, n_1)\}, q_1) - TP_k(\{(u_3, n_1)\}, q_1) = 2,$$

which implies that the total transaction price function $TP_k(S_1, q_1)$ is non-submodular. The lemma follows. □

For each $k \in \{1, 2, \ldots, |N|\}$, let $Act(S_k)$ denote the set of users being active in NFT n_k, and let

$$r(S_k, q_k) = \sum_{u_i \in Act(S_k), v_{u_i,n_k}(q_k) \ge p_k} v_{u_i,n_k}(q_k)$$

represent the total valuation function of users being active in NFT n_k following the transaction price constraint (i.e., $v_{u_i,n_k}(q_k) \ge p_k$).

The following lemma shows that, different from the total transaction price function $TP_k(S_k, q_k)$, the total valuation function $r(S_k, q_k)$ is submodular.

Lemma E.4. *For each $k \in \{1, 2, \ldots, |N|\}$, the total valuation function $r(S_k, q_k)$ is non-monotonically increasing but submodular in the airdrop selection.*

Proof. Since the revenue of all users being airdropped is zero, the total valuation function $r(S_k, q_k)$ is non-monotonically increasing for each $k \in \{1, 2, \ldots, |N|\}$. To prove the submodularity, we show that each function $r(S_k, q_k)$ satisfies Inequality (13). Following the proof in [92] where the submodularity of the influence function on the IC model can be reduced to that in a deterministic graph realized by flipping the coin for each edge of $G = (V, E)$, we show the submodularity of $r(S_k, q_k)$ in a deterministic graph $G' = (V, E') \subseteq G$ realized by flipping the coin for each edge of G with the activation probability. The process of influence propagation on G can be regarded as the influence propagation process upon the deterministic graph G'. Thus, for any activated user, its influence propagation is a connected subgraph of G' rooted by some airdropped user u, i.e., $(u, n_k) \in S_k$. For any set of airdrops S_k, the function $r(S_k, q_k)$

is the total valuation (excluding the valuations violating the transaction price constraint $v_{u_i,n_k}(q_k) \geq p_k$) of the union of the connected subgraphs rooted by all airdrops in S_k. Therefore, for each $k \in \{1, 2, \ldots, |N|\}$, the total valuation function $r(S_k, q_k)$ is a coverage function, which is submodular [98]. The lemma follows. □

Recall that $V(S_k, q_k)$ is the set of users holding the NFT n_k under the influence of S_k with the quantity q_k, and $Act(S_k)$ is the set of users being active in NFT n_k. Thus for each $k \in \{1, 2, \ldots, |N|\}$, we have $V(S_k, q_k) \subseteq Act(S_k)$ and $|V(S_k, q_k)| \leq q_k$, which implies

$$TP_k(S_k, q_k) \leq r(S_k, q_k). \tag{14}$$

Moreover, by Equations (10) and (1), for any q_k and q'_k with $q_k \leq q'_k$, we have $v_{u_i,n_k}(q_k) \geq v_{u_i,n_k}(q'_k)$ and thus

$$r(S_k, q_k) \geq r(S_k, q'_k). \tag{15}$$

Let (S^{opt}, Q^{opt}) denote the optimal solution of NRM, where $S^{opt} = \bigcup_{k\in\{1,2,\ldots,|N|\}} S_k^{opt}$ and $Q^{opt} = \{q_1^{opt}, q_2^{opt}, \ldots, q_{|N|}^{opt}\}$. To derive the approximation ratio, we first consider a problem similar to NRM, named NRM-QO, where the quantity constraint is removed. In NRM-QO, all active users with valuations satisfy the reserve price constraint $v_{u_i,n_k}(q_k) \geq p_k$, without the restriction that the users with the q_k highest valuations acquire the NFT n_k. The user u_i's valuation on NFT n_k is set to $v_{u_i,n_k}(1)$, and λ is set to 0. Similarly, let $\hat{S}^{opt}$ denote the optimal solution of NRM-QO, where $\hat{S}^{opt} = \bigcup_{k\in\{1,2,\ldots,|N|\}} \hat{S}_k^{opt}$ satisfies $\hat{S}_k^{opt} = \arg\max_{S_k} r(S_k, 1)$ for each $k \in \{1, 2, \ldots, |N|\}$.

Lemma E.5. *For each $k \in \{1, 2, \ldots, |N|\}$, $r(\hat{S}_k, 1) \geq \frac{1}{e} \cdot TP_k(S_k^{opt}, q_k^{opt})$ holds, where $\hat{S}_k$ is the solution found by the continuous greedy algorithn [71] to solve NRM-QO for NFT n_k.*

Proof. By Lemma E.4, the total valuation function $r(S_k, 1)$ is submodular for each $k \in \{1, 2, \ldots, |N|\}$. According to [71], the set of airdrops $\hat{S}_k$ found by the continuous greedy algorithm is a $\frac{1}{e}$-approximation solution of NRM-QO for NFT n_k, i.e., $r(\hat{S}_k, 1) \geq \frac{1}{e} \cdot r(\hat{S}_k^{opt}, 1)$. To complete the proof, for each $k \in \{1, 2, \ldots, |N|\}$, we show $r(\hat{S}_k^{opt}, 1) \geq TP_k(S_k^{opt}, q_k^{opt})$ as follows,

$$r(\hat{S}_k^{opt}, 1) \geq r(S_k^{opt}, 1) \geq r(S_k^{opt}, q_k^{opt}) \geq TP_k(S_k^{opt}, q_k^{opt}),$$

where the first, second, and last inequalities are obtained due to the optimality of $\hat{S}_k^{opt}$ to NRM-QO for NFT n_k, Inequality (15), and Inequality (14), respectively. The lemma follows. □

For each $k \in \{1, 2, \ldots, |N|\}$, let (S_k^{alg}, q_k^{alg}) denote the algorithm solution obtained by QOOA for NFT n_k. Then (S^{alg}, Q^{alg}) is the algorithm solution obtained by QOOA, where $S^{alg} = \bigcup_{k\in\{1,2,\ldots,|N|\}} S_k^{alg}$ and $Q^{alg} = \{q_1^{alg}, q_2^{alg}, \ldots, q_{|N|}^{alg}\}$.

Theorem E.6. *QOOA is $\frac{1}{ea(1+c)}$-approximation for NRM, where $a = \max_{1\leq k\leq |N|} \frac{r(\hat{S}_k,1)}{p_k}$, $c = \frac{\lambda q_{\max} c_{\mathrm{BQ}} \mathcal{V}_{\max}}{p_{\min}}$, $\mathcal{V}_{\max}$ is the maximum potential transaction price of offspring, and $p_{\min}$ is the minimum reserve price.*

Proof. To prove this theorem, we show $f(S^{alg}, Q^{alg}) \geq \frac{1}{ea(1+c)} \cdot f(S^{opt}, Q^{opt})$. For each $k \in \{1, 2, \ldots, |N|\}$, we have

$$\begin{aligned} TP_k(S_k^{alg}, q_k^{alg}) &\geq \frac{p_k}{r(\hat{S}_k, 1)} \cdot r(\hat{S}_k, 1) \\ &\geq \frac{1}{e} \cdot \frac{p_k}{r(\hat{S}_k, 1)} \cdot TP_k(S_k^{opt}, q_k^{opt}) \\ &\geq \frac{1}{ea} \cdot TP_k(S_k^{opt}, q_k^{opt}), \end{aligned} \tag{16}$$

where the first inequality follows by the fact that NFT n_k is sold with price at least p_k, and the second and third inequalities are obtained by Lemma E.5 and $a = \max_{1\leq k\leq |N|} \frac{r(\hat{S}_k,1)}{p_k}$, respectively.

We derive the relation between the total transaction price of N and the potental transaction prices of NFT offspring generated from N as follows. Let $\mathcal{V}_{\max}$ denote the maximum potential transaction price of an offspring, i.e.,

$$\mathcal{V}_{\max} = 1 \cdot e^{\eta_0 + \eta_1 \frac{1}{1} + \eta_2 |T| \frac{2^{|T|}}{2} + \eta_3 d_{\max}} = e^{\eta_0 + \eta_1 + \eta_2 |T| \cdot 2^{|T|-1} + \eta_3 d_{\max}}, \tag{17}$$

where we assume that the expected preference of users across the entire social network is 1 (i.e., the maximum possible preference), the quantity of this offspring is 1 (leading to e^{η_1}), it has $|T|$ traits, each trait is only owned by it and one of its parents, at most $2^{|T|}$ offspring are generated (leading to $e^{\eta_2 |T| \cdot 2^{|T|-1}}$), and its owner has the maximum degree, i.e., $d_{\max}$, on the social network (leading to $e^{\eta_3 d_{\max}}$). For any (S, Q) in NRM, we have

$$\begin{aligned} &\lambda \cdot OS(S, Q) \\ &\leq \lambda \cdot \left(\sum_{u_i \in \bigcup_{k=1}^{|N|} V(S_k, q_k)} c_{\mathrm{BQ}} \cdot \mathcal{V}_{\max} \right) \\ &\leq \lambda \cdot \frac{q_{\max} |N|}{|N|} \cdot \frac{c_{\mathrm{BQ}} \cdot \mathcal{V}_{\max}}{p_{\min}} \cdot p_{\min} \cdot |N| \\ &\leq c \sum_{k=1}^{|N|} p_k d_k \qquad (\text{Let } c = \frac{\lambda \cdot q_{\max} \cdot c_{\mathrm{BQ}} \cdot \mathcal{V}_{\max}}{p_{\min}}) \\ &\leq c \sum_{k=1}^{|N|} TP_k(S_k, q_k), \end{aligned}$$

where $p_{\min}$ is the minimum reserve price, and d_k is the actual number of the NFT n_k sold. Note that $\bigcup_{k=1}^{|N|} V(S_k, q_k) \leq q_{\max} |N|$ holds because at most $q_{\max} |N|$ NFTs are sold. $p_{\min} |N| \leq \sum_{k=1}^{|N|} p_k d_k$ holds since $p_{\min} |N|$ is the minimum transaction prices assuming each NFT is sold at $p_{\min}$ with only one quantity.[31] Then, for any (S, Q)

[31] To ensure that an NFT is marketable in the real world, its reserve price is typically determined according to the valuations of its intended audience.

in NRM,

$$f(S,Q) = \sum_{k=1}^{|N|} TP_k(S_k, q_k) + \lambda \cdot OS(S,Q) \tag{18}$$
$$\leq (1+c) \cdot \sum_{k=1}^{|N|} TP_k(S_k, q_k).$$

Therefore, we have

$$\begin{aligned} f(S^{alg}, Q^{alg}) &= \sum_{k=1}^{|N|} TP_k(S_k^{alg}, q_k^{alg}) + \lambda \cdot OS(S^{alg}, Q^{alg}) \\ &\geq \sum_{k=1}^{|N|} TP_k(S_k^{alg}, q_k^{alg}) \\ &\geq \frac{1}{ea} \cdot \sum_{k=1}^{|N|} TP_k(S_k^{opt}, q_k^{opt}) \\ &\geq \frac{1}{ea(1+c)} \cdot f(S^{opt}, Q^{opt}), \end{aligned}$$

where the first inequality is obtained because $OS(S^{alg}, Q^{alg})$ is non-negative by definition, and the second and third inequalities are obtained by Inequality (16) and Inequality (18), respectively. The theorem follows. □

Note that regarding a, $r(\hat{S}_k, 1)$ is at most $1 \times e^{\eta_0 + \eta_1 \cdot \frac{1}{1} + \eta_2 |T||N| + \eta_3 \cdot 0}$, which is the maximum user valuation derived from some user with the maximum personal preference 1 for some NFT with the maximum assessment. To achieve the maximum assessment, the quantity of this NFT is 1, leading to $e^{\eta_1 \cdot \frac{1}{1}}$. It possesses $|T|$ traits, each of which occurs only once in the NFT project and thus has rarity $|N|$ according to Equation (8). Hence, the rarity of this NFT is $|T|\,|N|$ according to Equation (9), leading to $e^{\eta_2 |T||N|}$. Besides, since it has not been sold to anyone, the impact imparted by the ownership history is 0, leading to $e^{\eta_3 \cdot 0}$. Hence, a is $O(\frac{e^{|T||N|}}{p_{\min}})$, where $p_{\min}$ is the minimum reserve price in the NFT project, given in the problem as the input.

Regarding c, $q_{\max} = \max\limits_{1 \leq k \leq |N|} q_k$ is the maximum quantity sold across all NFTs, which is at most $l_{\max}$, where $l_{\max}$ is given in the problem as the input and set at most to $|V|$. According to Equation (17), $\mathcal{V}_{\max} = 1 \cdot e^{\eta_0 + \eta_1 + \eta_2 |T| \cdot 2^{|T|-1} + \eta_3 d_{\max}}$ is the maximum potential transaction price of offspring, where $d_{\max}$ is the maximum degree, which is at most $|V|$. Hence, $\mathcal{V}_{\max} = O(e^{\eta_2 |T| \cdot 2^{|T|} + \eta_3 |V|})$. Therefore, c is $O(\frac{\lambda c_{\mathrm{BQ}} |V| e^{\eta_2 |T| \cdot 2^{|T|} + \eta_3 |V|}}{p_{\min}})$, where λ and c_{BQ} are given by the problem as the input.

In practice, to prevent the undervaluation of NFTs, creators of NFT projects typically set a reserve price $p_{\min}$, which is not too low. For example, the reserve price for Adidas NFT sneakers is approximately \$550.[32] For $c = \frac{\lambda q_{\max} c_{\mathrm{BQ}} \mathcal{V}_{\max}}{p_{\min}}$, as aforementioned, $q_{\max}$ is at most $l_{\max}$, which is set much smaller than $|V|$ to maintain the scarcity of NFTs. $\mathcal{V}_{\max} = 1 \cdot e^{\eta_0 + \eta_1 + \eta_2 |T| \cdot 2^{|T|-1} + \eta_3 d_{\max}}$, where $d_{\max}$ is usually much smaller than $|V|$ in a typical social network. Therefore, the performance of our algorithm depends on the number of NFTs and the number of traits within an NFT project. When these two numbers are lower, our algorithm performs better.

Recall that the NRM problem cannot be approximated within a factor of $|V|^{1/(\log\log|V|)^c}$ (Theorem 3.1). In real-world scenarios, the number of users $|V|$ on social networks is in the tens of millions, making the factor $O(\frac{1}{|V|^{1/(\log\log|V|)^c}})$ exceedingly small. This implies that NRM is difficult to approximate within any meaningful factor between $O(\frac{1}{|V|^{1/(\log\log|V|)^c}})$ and 1. However, while NRM is inapproximable within a factor of $|V|^{1/(\log\log|V|)^c}$, it is still possible to achieve an approximation ratio larger than this bound. Our algorithm, QOOA, attains an approximation ratio that exceeds $|V|^{1/(\log\log|V|)^c}$, so there is no conflict between the hardness result and the performance of QOOA.

In addition, we incorporate the confidence probability into the approximation guarantee by following [93, 139]. These studies account for the stochastic nature of influence spread by introducing parameters δ and r, where δ represents the probability bound ensuring a high-confidence estimation, and r controls the trade-off between accuracy and computational complexity. Accordingly, given $\delta, r > 0$, if we take a number of simulations (polynomial in δ, r and $|V|$) in the estimation of the influence of airdrops, then a $(\frac{1}{ea(1+c)} - \epsilon)$-approximation is obtained with probability at least $1 - \delta$, where $\epsilon = \frac{r}{a(1+c)}$, $a = \max\limits_{1 \leq k \leq |N|} \frac{r(\hat{S}_k, 1)}{p_k}$, $c = \frac{\lambda q_{\max} c_{\mathrm{BQ}} \mathcal{V}_{\max}}{p_{\min}}$, $q_{\max} = \max_{q_k \in Q} q_k$ is the maximum quantity, $\mathcal{V}_{\max}$ is the maximum potential transaction price of offspring, and $p_{\min}$ is the minimum reserve price.

E.2.4 Time Complexity.

Theorem E.7. *The time complexity of QOOA is $O(l_{\max} b_{\max} |V|\,|N|)$, where $l_{\max} = \max_{l_k \in L} l_k$ is the maximum quantity limit and $b_{\max}$ is the maximum budget in B.*

Proof. In the QAS phase, for an NFT n_k with budget b_k, it takes $O(|V|\, b_k)$ time to find the airdrops under a specific quantity. As the maximum quantity limit is $l_{\max} = \max_{l_k \in L} l_k$, it requires $O(l_{\max} b_k |V|)$ time to identify the most appropriate quantity and the corresponding airdrops for each NFT n_k. Therefore, QAS takes $O(l_{\max} b_{\max} |V|\,|N|)$ time to find an initial solution of NRM, where $b_{\max}$ is the maximum budget in B. Next, in the ORE phase, it examines $O(b_k)$ replacements of airdrops for a treasure n_k. As there are $O(|N|)$ treasures, ORE takes $O(b_{\max} |N|)$ time. Consequently, the time complexity of QOOA is $O(l_{\max} b_{\max} |V|\,|N|)$. The theorem follows. □

For time complexity, for each NFT n_k, since each active user only acquires one, $l_{\max}$ is set at most to $|V|$, as allowing a greater quantity would have no impact. On the other hand, since the number of each NFT that can be airdropped does not exceed the total number of users, $b_{\max}$ is set at most to $|V|$ as well. The time complexity of QOOA can also be rewritten as $O(|V|^3\,|N|)$, which is polynomial time.

In practice, to maintain the scarcity of NFTs, $l_{\max}$ is usually not too large. For example, the NFTs of Trump Digital Trading Card have a maximum quantity of only 10, i.e., $l_{\max} = 10$. At the same time, viral marketing aims to leverage the social influence of a small

[32] More information can be found at https://collect.adidas.com/bape/faq.

number of people to achieve promotional effects. Therefore, the budget for airdrops, i.e., $b_{\max}$, is also not very large, such as ranging from 0.3% to 0.6% [76], 0.04% to 0.3% [136], or 0.03% to 0.06% [135] of the population, because allocating a larger budget may not significantly improve the overall influence spread (potentially resulting in wasteful expenditure without commensurate promotional gains).

F Workflow and Derivations of QOOA

F.1 Workflow

Algorithm 1: QOOA

Input: NFT project N with traits T and reserve prices P, social network G, user breeding quota c_{BQ}, budgets B, quantity limits L

Output: NFT airdrops S and quantities Q

/* QAS phase */

for *each* $n_k \in N$ **do**
  $q_k^* \leftarrow null$; $S_k^* \leftarrow null$; $TP_k^* \leftarrow 0$
  for $q_k = 1, \ldots, l_k$ **do**
    if $UB_k(q_k) \le TP_k^*$ **then**
      continue
    $S_k \leftarrow \emptyset$; $TP_k \leftarrow \sum_{u_j \in V(S_k, q_k)} v_{u_j, n_k}(q_k)$
    while $|S_k| < b_k$ **do**
      $U \leftarrow \emptyset$
      for *each* $(u_i, n_k) \notin S_k$ **do**
        if $SCR_k(S_k \cup \{(u_i, n_k)\}, q_k) \ge TP_k$ **then**
          $U \leftarrow U \cup \{u_i\}$
      $u_i^* \leftarrow null$; $gain \leftarrow 0$
      for $u_i \in U$ **do**
        if $TP(S_k \cup \{(u_i, n_k)\}, q_k) - TP_k(S_k, q_k) > gain$ **then**
          $u_i^* \leftarrow u_i$;
          $gain \leftarrow TP(S_k \cup \{(u_i, n_k)\}, q_k) - TP_k(S_k, q_k)$
      if $gain > 0$ **then**
        $S_k \leftarrow S_k \cup \{(u_i^*, n_k)\}$; $TP_k \leftarrow TP_k + gain$
      else
        break
    if $TP_k > TP_k^*$ **then**
      $q_k^* \leftarrow q_k$; $S_k^* \leftarrow S_k$; $TP_k^* \leftarrow TP_k$
$S \leftarrow \bigcup_{n_k \in N} S_k^*$; $Q \leftarrow \{q_1^*, \ldots, q_{|N|}^*\}$

/* ORE phase */

$N^{\text{T}} \leftarrow$treasures of NFTs; $RTC \leftarrow$ RTCs according to N^{T}
Sort N^{T} according to the number of rarest traits possessed
for *each* $n_k \in N^{\text{T}}$ **do**
  $S'_k \leftarrow S_k^*$; $\bar{S}'_k \leftarrow \emptyset$
  while $S'_k \neq \emptyset$ **do**
    $(\underline{u}, n_k) \leftarrow \text{argmin}_{(u,n_k) \in S'_k} VOGUE_k(u, q_k^*)$
    $(u^*, n_k) \leftarrow \text{argmax}_{u \in V, (u,n_k) \notin S'_k \cup \bar{S}'_k} VOGUE_k(u, q_k^*)$
    if $VOGUE_k(\underline{u}, q_k^*) < VOGUE_k(u^*, q_k^*)$ **then**
      $S'_k \leftarrow S'_k \setminus \{(\underline{u}, n_k)\}$; $\bar{S}'_k \leftarrow \bar{S}'_k \cup \{(u^*, n_k)\}$
      $S' \leftarrow (S \setminus \{(\underline{u}, n_k)\}) \cup \{(u^*, n_k)\}$
      if $f(S', Q) > f(S, Q)$ **then**
        $S \leftarrow S'$
    else
      break
return S, Q

Algorithm 1 presents the pseudo-code of QOOA while Figure 10 illustrates QOOA.

The workflow of QOOA consists of two sequential phases: QAS and ORE. QAS initializes with the NFT project and social network as inputs (as indicated by the blue-shaded region in Figure 10), processing each of the $|N|$ NFTs. For each NFT n_k, QOOA iterates through possible for-sale quantities q_k, starting from $q_k = 1$. For each quantity, QAS first leverages VQI to verify whether $UB_k(q_k) \ge TP_k^*$ (represented by the topmost decision box). If this condition holds and the number of airdrops remains within the budget b_k (represented by the second decision box from the top), the process advances to airdrop selection. Before selecting airdrops, QOOA computes the current TP_k and SCR. It then identifies users satisfying $SCR_k \ge TP_k$ and selects the one that maximizes the gain in TP_k as the next airdrop recipient. This process iterates until the budget is exhausted (represented by the second decision box from the top). If the resulting TP_k surpasses the previously recorded TP_k^* (represented by the decision box to the right of the second one from the top), QOOA updates the best quantity and airdrops for n_k. However, if VQI fails at the initial check (represented by the topmost decision box), indicating that the current quantity cannot yield a TP_k higher than TP_k^* from prior quantities, QOOA skips to the next quantity. This process continues until reaching the quantity limit l_k, after which QAS outputs the best quantity and airdrops for each n_k, which serves as the input for ORE.

ORE refines the initial airdrops obtained from QAS by focusing specifically on treasures—NFTs with the rarest traits (as indicated by the orange-shaded region in Figure 10). This phase processes the $\left|N^{\text{T}}\right|$ treasures sequentially, prioritizing those with a greater number of rare traits. For each treasure n_i, if there remain airdrops in S_i that have not yet been evaluated for potential replacement (represented by the topmost decision box), ORE first computes $VOGUE_i$ for each user and selects an alternative airdrop candidate. If the replacement improves S_i (represented by the second decision box from the top), it is retained; otherwise, the original airdrop remains. The process continues until all airdrops have been evaluated (represented by the topmost decision box). ORE then proceeds to the next treasure, tailoring its airdrops. This iterative refinement continues until all treasures have been processed, yielding the final optimized airdrops S_i for each treasure n_i.

F.2 Derivation of RR-Rev

To find RR-Rev of an acceptor $u \in V_k^{\text{a}}(x)$ under the influence of $\hat{S}_k^x$, QAS searches for reverse reachable sets in different deterministic realized graphs of G.[33] Then, it derives the likelihood for any user $u_i \in \hat{S}_k^x$ to influence u according to the average occurrence of u_i in u's reverse reachable sets, denoted as $oc(u_i, u)$. Consequently, u's RR-Rev in n_k under the influence of $\hat{S}_k^x$, denoted as $\mathcal{R}_k(u, \hat{S}_k^x, x)$,

[33] Following [135, 136], we adopt the concept of *live-edge graph*, where a deterministic realized graph of $G = (V, E)$ consisting of V and the set of live-edges. An edge $e_{i,j} \in E$ is declared to be a "live-edge" if flipping a biased random coin with probability $a_{i,j}$ returns success. A reverse reachable set of a node u_i in the deterministic realized graph contains the nodes that have a path to u_i in this graph.

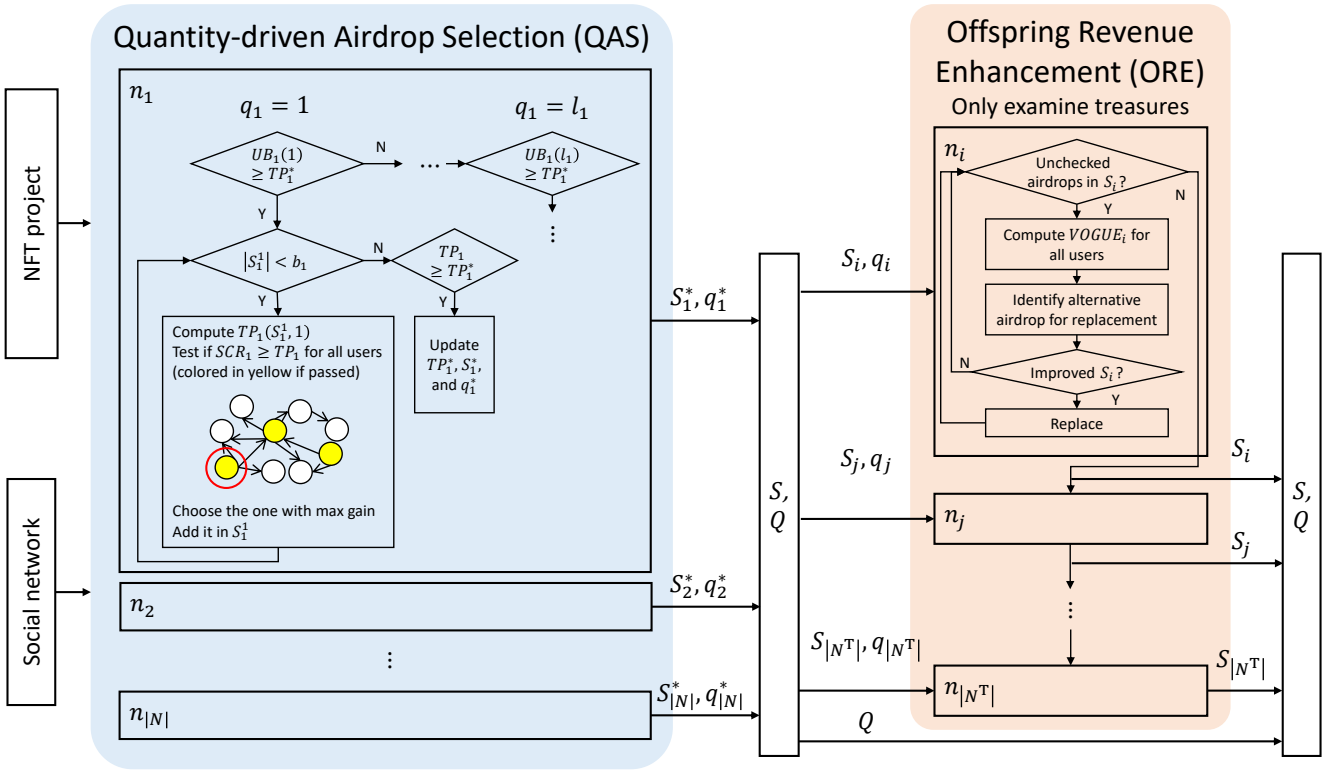

Figure 10: The workflow of QOOA.

based on the likelihood for every user in $\hat{S}_k^x$ to influence u is formulated as follows.

$$\mathcal{R}_k(u, \hat{S}_k^x, x) = v_{u,n_k}(x) \cdot \min\{1, \sum_{(u_i,n_k)\in\hat{S}_k^x} oc(u_i, u)\}, \quad (19)$$

where the sum of average occurrences of users in $\hat{S}_k^x$ upper bounds the probability of u being successfully influenced by $\hat{S}_k^x$ (with a maximum value of 1), since different users in $\hat{S}_k^x$ may concurrently occur in u's reverse reachable sets, leading to duplicate counts and thus overestimating the probability of successful influence by $\hat{S}_k^x$. Accordingly, RR-Rev of u in NFT n_k can serve as the upper bound of u's expected revenue in NFT n_k.

F.3 Derivation of VQI

Let $W_k(y)$ denote the y-th largest user preference for n_k. For $W_k(y)$, the corresponding user is a *valid acceptors* if her valuation is no smaller than the reserve price p_k, i.e.,

$$\begin{aligned} W_k(y) \cdot A(n_k, q_k) &= W_k(y) \cdot e^{\eta_0+\eta_2\Phi(n_k)+\eta_3\cdot 0} \cdot e^{\frac{\eta_1}{q_k}} \quad (20)\\ &= W_k(y) \cdot \eta^* \cdot e^{\frac{\eta_1}{q_k}} \quad (\text{Let } \eta^* = e^{\eta_0+\eta_2\Phi(n_k)}) \\ &\geq p_k. \end{aligned}$$

Accordingly, VQI rewrites Inequality (20) to determine the minimum preference for n_k that ensures users with a preference higher than this value are valid acceptors.

$$W_k(y) \geq \frac{p_k}{\eta^*} \cdot e^{-\frac{\eta_1}{q_k}}. \quad (21)$$

Note that for an NFT n_k, $\frac{p_k}{\eta^*}$ remains constant regardless of variations in q_k. Hence, QAS can efficiently derive the exact number of acceptors under various quantities by examining how many users with preferences for n_k satisfy Inequality (21).

F.4 Derivation of B-Index

Specifically, B-Index is designed to prioritize users based on their likelihood to participate in breeding and their contribution to offspring assessment. It considers i) breeding and siring probabilities, which represent a user's inclination to engage in breeding, ii) user impact, capturing the effect of ownership on the offspring's assessment when bred by this user, and iii) aggregated valuation of n_k under their influence, ensuring that prioritizing this user does not significantly reduce TP.

To comprehensively capture third factor, we first introduce *Cascaded TP (CTP)*. Inspired by [131], CTP accounts not only for a user u_i's own transaction price of n_k, but also for the aggregated transaction prices of their influenced neighbors. It is achieved through the iterative multiplication of activation probabilities and transaction prices, thereby effectively integrating the cascading effects of influence propagation within the network.

Let $\mathbf{V}$ be the valuation matrix, where each element $\mathbf{V}_{i,k}$ represents the transaction prices of user u_i for NFT n_k under its quantity q_k, i.e.,

$\mathbf{V}_{i,k} = v_{u_i,n_k}(q_k)$ if $v_{u_i,n_k}(q_k) \geq p_k$ and $\mathbf{V}_{i,k} = 0$ otherwise, where p_k is the reserve price of n_k. Let $\mathbf{A}$ denote the adjacency matrix of the social network, where $\mathbf{A}_{i,j}$ represents the activation probability of user u_i influencing user u_j, i.e., $\mathbf{A}_{i,j} = a_{i,j}$. Cascaded TP (CTP) is defined as follows.

$$\boldsymbol{\kappa}_{n_k}(q_k) = \sum_{\xi=0}^{\xi_{\max}} \rho^{\xi} \mathbf{A}^{\xi} \mathbf{v}_k, \tag{22}$$

where $\mathbf{v}_k = \mathbf{V}_{:,k}$ is the valuation vector of n_k under its quantity q_k, $\xi_{\max}$ is the number of iterations capturing high-order influence, and $\rho \in (0, 1]$ is a decay factor to control the diminishing impact of distant neighbors.[34] $\mathbf{A}^{\xi}\mathbf{v}_k$ represents the propagation of user transaction prices through the social network over ξ iterations, reflecting both direct and indirect influence in determining the final CTP vector $\boldsymbol{\kappa}_{n_k}(q_k)$.

By integrating CTP into the B-Index, it mitigates concerns regarding potential TP loss when adjusting airdrops, as it prioritizes users who contribute not only to OS but also to maintaining overall TP. The design enables a more balanced selection strategy, effectively optimizing overall revenue.

Hence, the B-Index of an acceptor u_a for n_k, denoted as $\mathcal{B}_k(u_a, S, Q)$, is defined according to u_a's breeding probability, impact, CTP of n_k, siring probability, and the number of treasures held by u_a. It focuses on two cases: 1) Targeting RTCs with fewer treasures than c_{BQ} to evaluate their potential to individually breed valuable offspring. 2) Targeting the friends of RTCs who either lack treasures or hold more than c_{BQ} in treasures to evaluate their potential to provide siring-ready NFTs that facilitate collaborative breeding of their friends (RTCs) for valuable offspring.

$$\mathcal{B}_k(u_a, S, Q) = \begin{cases} \beta_a I_a \kappa_{u_a,n_k}(q_k), & \text{if } 1 \leq \Theta(u_a, S, Q) < c_{\text{BQ}} \\ \beta_c \gamma_a \kappa_{u_a,n_k}(q_k), & \text{else if an RTC } u_c \text{ is } u_a\text{'s friend} \\ 0, & \text{otherwise} \end{cases}, \tag{23}$$

where $\Theta(u_a, S, Q)$ is the number of treasures held by u_a given S and Q, and I_a is the impact of u_a. For the first case where u_a is an RTC holding fewer treasures than c_{BQ}, prioritizing u_a for purchasing n_k can enhance the likelihood of u_a breeding valuable offspring. B-Index is evaluated by u_a's breeding probability (β_a), impact (I_a), and CTP of n_k ($\kappa_{u_a,n_k}(q_k)$) in order to increase the expected assessments of offspring without significantly compromising the total transaction price. For the second case, where u_a either lacks treasures or holds an excessive amount, and it has a friend u_c who is an RTC, prioritizing u_a for purchasing n_k can enable u_a to provide n_k for siring, thereby increasing the likelihood for u_c to breed valuable offspring. B-Index is evaluated by u_c's breeding probability β_c to represent the likelihood of u_c requesting u_a to provide siring-ready NFTs, u_a's siring probability (γ_a) and CTP of n_k ($\kappa_{u_a,n_k}(q_k)$).[35]

[34] A larger $\xi_{\max}$ captures higher-order influence but increases computational complexity. Since distant neighbors contribute less significantly, setting $\xi_{\max}$ too high offers diminishing returns [79, 87]. A moderate value balances accuracy and efficiency. In addition, the decay factor ρ controls the weight of high-order influence [87]. A lower ρ reduces the impact of distant neighbors, while a higher ρ allows influence to propagate further.

[35] If u_a has multiple RTCs as friends, B-Index refers to the one with the highest breeding probability among them to ensure the importance of targeting u_a is not underestimated.

F.5 Details on ORE's Design Idea

ORE optimizes expected revenue by increasing the probability of breeding rare offspring through its main design the Breeding Index (B-Index) and Valuable Offspring Generation Utility Estimation (VOGUE), rather than assuming deterministic user behavior. An alternative airdrop is selected only if it improves the expected revenue; otherwise, the current airdrop remains unchanged, ensuring that each adjustment in ORE consistently optimizes overall expected revenue.

First, B-Index is specifically designed to evaluate a user's potential to generate rare and valuable offspring when acquiring additional treasures, i.e., NFTs that possess the rarest traits. In particular, according to Equation (12), the expected revenue of offspring considers both the probability that offspring will be bred and their assessed value. B-Index addresses the above two important aspects as follows. 1) *If the user to be evaluated is a Rare Trait Collector (RTC)*: Since RTCs are users who hold treasures, when they acquire additional treasures, the probability that these treasures will be utilized for breeding within a limited breeding quota increases, thereby enhancing the expected offspring assessment. The evaluated user with a higher breeding probability is more likely to initiate breeding. Moreover, the evaluated user with a greater impact contributes more significantly to the value of the offspring, as NFTs are assessed in part by the reputation of their owners. 2) *If the user to be evaluated is a friend of RTCs*: Acquiring additional treasures increases the likelihood that these treasures will be used for siring, enabling their RTC friends to initiate collaborative breeding. This, in turn, increases the probability that these treasures will be utilized for breeding within a limited breeding quota, enhancing the expected offspring assessment. The evaluated user with a higher siring probability is more likely to contribute a treasure for siring, thereby increasing the chance of successful breeding. In addition, the evaluated user with a RTC friend who has a higher breeding probability is more likely to have their treasure used to initiate breeding.

In summary, B-Index enhances both the probability of offspring being bred and their assessed value. It achieves this goal by considering the breeding probability of RTCs and the siring probability of their friends to increase the likelihood of successful breeding. Meanwhile, by prioritizing RTCs and their friends in acquiring treasures and accounting for RTCs' impact, it ensures higher offspring assessment.

Equipped with the above ideas, ORE is designed to improve the expected revenue by identifying alternative airdrops that are more likely to influence users with high B-Index (i.e., maximizing the expected total B-Index). VOGUE evaluates a user's potential to influence those with high expected total B-Index, facilitating the identification of alternative airdrops. It explicitly accounts for the constraint of limited quantity supply, ensuring that high VOGUE is not created by influencing a large number of users with low B-Index. More importantly, an alternative airdrop is only selected if it improves the expected revenue; otherwise, the current airdrop remains unchanged, ensuring that alternative airdrops do not reduce the expected revenue due to insufficient improvement in the expected revenue from offspring.

Specifically, Offspring Revenue Enhancement refines the initial solution (obtained by QAS) by considering the total revenue, incorporating both TP and OS, to ensure a comprehensive evaluation. In Algorithm 1, each time ORE identifies an alternative airdrop through VOGUE for potential tailoring (Line 30), it evaluates the revenue function f before and after tailoring (Line 33). If the tailored airdrop results in an improved revenue, the original airdrop is replaced with the alternative (Line 34). In this process (i.e., Line 33), ORE considers both TP and OS rather than explicitly targeting OS alone. This is because ORE has already preselected alternatives that have the potential to improve OS. Although these alternatives may significantly enhance OS, they could also reduce TP, as the original airdrops were chosen by QAS based on TP. To ensure a more balanced evaluation, ORE assesses whether the overall revenue f improves before finalizing the airdrop adjustment.

G Extensions and Discussions of QOOA

G.1 Support for Various Breeding Mechanisms

Here we show that QOOA is capable of supporting various breedings, including *Only Individual Breeding* and *Booster*.

- For *Only Individual Breeding*, ORE no longer takes into account the influence on friends of RTCs providing siring-ready NFTs. It modifies B-Index by discarding the second case.

$$\mathcal{B}_k(u_\mathrm{a}, S, Q) = \begin{cases} \beta_\mathrm{a} I_\mathrm{a} \kappa_{u_\mathrm{a}, n_k}(q_k), & \text{if } 1 \le \Theta(u_\mathrm{a}, S, Q) < c_\mathrm{BQ} \\ 0, & \text{otherwise} \end{cases}.$$

- For *Booster* that raises the inheritance probability of a specified trait by c_BT, ORE modifies B-Index to account for the number of boosters possessed by an RTC as follows.

$$\mathcal{B}_k(u_\mathrm{a}, S, Q) = \begin{cases} (1 + \frac{\psi_\mathrm{a}}{\psi_\mathrm{max}}) \beta_\mathrm{a} I_\mathrm{a} \kappa_{u_\mathrm{a}, n_k}(q_k), & \text{if } 1 \le \Theta(u_\mathrm{a}, S, Q) < c_\mathrm{BQ} \\ \beta_c \gamma_\mathrm{a} \kappa_{u_\mathrm{a}, n_k}(q_k), & \text{else if an RTC } u_c \text{ is } u_\mathrm{a}\text{'s friend} \\ 0, & \text{otherwise} \end{cases},$$

  where ψ_j is the number of boosters possessed by u_j, ψ_max is the maximum number of boosters possessed by users in the social network, and $\frac{\psi_j}{\psi_\mathrm{max}}$ indicates the increment in B-Index attributable to the possession of boosters.

Equipped with the modified B-Index, ORE evaluates VOGUE of users and tailors airdrops accordingly.

G.2 Extension for Dynamic Social Networks

In the real world, the social network within NFT marketplaces is often dynamic, with users' social connections and preferences evolving over time. Moreover, past marketing strategies influence subsequent promotions. For instance, a user's ownership of already-released NFTs may affect her subsequent breeding, and the total number of released NFTs impacts their value, thereby altering user valuations. Consequently, at each time t, QOOA first re-assess the value of each NFT at time t based on the total number of NFTs previously released, denoted as $q_k^{(<t)}$, and the number of NFTs decided to be released at time t, denoted as $q_k^{(t)}$, i.e.,

$$A^{(k)}(n_k, q_k^{(t)}) = e^{\eta_0 + \eta_1 \frac{1}{q_k^{(<t)} + q_k^{(t)}} + \eta_2 \Phi(n_k) + \eta_3 h_k}.$$

Since network changes are typically not drastic, to quickly determine the best quantity and airdrops at time t, QOOA begins with the quantity from the previous time $t-1$, i.e., $q_k^{(t)} = q_k^{(t-1)}$. Due to changes in NFT assessments and user preferences, QOOA first re-identifies the reserve-price acceptors based on updated user valuations. Then, QOOA adjusts the airdrops from the previous time $t-1$, denoted as $S_k^{(t-1)}$, by replacing airdrop recipients with non-recipients who have higher SCR to achieve higher TP_k at time t.

Specifically, for each user $u \in V$, QOOA evaluates its SCR, denoted as $SCR_k^{(k)}(\{u\}, q_k^{(t)})$. Let $\bar{u}$ denote the non-recipient at time $t-1$ with the highest SCR among all non-recipients, and let $LS_k^{(k-1)}$ denote the set of all recipients in $S_k^{(t-1)}$ whose SCR is lower than that of $\bar{u}$, i.e., $\forall u_\mathrm{s} \in LS_k^{(k-1)}, SCR_k^{(k)}(\{\bar{u}\}, q_k^{(t)}) > SCR_k^{(k)}(\{u_\mathrm{s}\}, q_k^{(t)})$. QOOA examines each $u_\mathrm{s} \in LS_k^{(k-1)}$ and replaces u_s with $\bar{u}$ to maximize TP_k, ensuring that the resulting TP_k is higher than $TP_k(S_k^{(t-1)}, q_k^{(t)})$. Regardless of whether $\bar{u}$ successfully replaces any u_s, QOOA proceeds to consider the next non-recipient with the highest SCR among all remaining non-recipients as the new $\bar{u}$, updates $LS_k^{(k-1)}$ according to $SCR_k^{(k)}(\{\bar{u}\}, q_k^{(t)})$, and repeats the replacement examination. This process continues until the new $\bar{u}$ has a lower SCR than all recipients, i.e., $LS_k^{(k-1)} = \emptyset$. The final set of airdrop recipients after these replacements is $S_k^{(t)}$.

Next, QOOA examines the upper bounds of TP_k for other quantities, i.e., UB_k, based on the updated user preferences, and sequentially adjusts the airdrops from the previous time's airdrops following the aforementioned process, prioritizing quantities with higher UB_k. Once all quantities with UB_k greater than the current TP_k have been evaluated, QOOA identifies the quantity and the corresponding airdrops that yield the highest TP_k as the solution, i.e., $q_k^{(t)}$ and $S_k^{(t)}$.

Finally, QOOA leverages ORE to adjust $S_k^{(k)}$ in order to improve revenue from breeding. Since prior marketing efforts may have already resulted in the existence of offspring, it is necessary to re-assess treasures based on all NFTs and offspring present at time t. Subsequently, the airdrops for each treasure are adjusted to incentivize RTCs and their friends to hold as many treasures as possible. Note that RTCs are also re-identified based on the newly determined treasures.

G.3 Discussion on Practical and Ethical Issues

G.3.1 Additional Marketing Channels. As most NFT research [91, 107, 125] predominantly focuses on online marketing, with limited attention to other channels [64], we have concentrated on online marketing in this paper. However, following the viral marketing research that explores additional marketing channels, we can extend our approach accordingly. These studies typically involve augmenting the influence network by adding additional nodes and edges to represent influences from other channels, leaving the fundamental mathematical problem unchanged. By modifying the input graph to include

offline events, direct partnerships, and media outreach, QOOA can adapt to these channels without fundamental modifications.

1) *Direct partnerships* for NFTs involve collaborations between NFT projects and external brands, companies, or other NFT projects to expand reach. To account for their influence, the partner's audience can be modeled as an additional layer within a multilayer network. This new layer encapsulates the partner's audience, where each node corresponds to an individual member. Within this layer, edges signify interactions or relationships among audience members. To accurately capture the influence dynamics, inter-layer edges must also be incorporated. These edges connect nodes from the original network to nodes in the partner's audience layer. Such connections illustrate the relationships or influence pathways between the two groups. For instance, an inter-layer edge may represent a platform user following the partner on social media or purchasing a product recommended by the partner.

This augmented multilayer network, with the added audience layer and the inter-layer edges, can then be combined with the original input graph for QOOA. For instance, Lv et al. [108] introduce the PR_BIS centrality measure to evaluate the importance of both nodes and layers for seed selection in multilayer networks. Similarly, Rao et al. [123] propose identifying communities, evaluating users' edge weight sums, and employing a quota-based approach to select top users from each community.

2) Regarding *offline events*, their influence can be modeled by incorporating location-based interactions into the propagation process within QOOA. Specifically, offline events introduce new nodes representing physical venues, such as conference centers, retail stores, or exhibition spaces, where interactions occur. Edges are then established to capture the influence dynamics, such as i) *user-to-event edges*: represent user attendance at an offline event, indicating direct exposure to promotional content; ii) *user-to-user edges*: capture in-person interactions between attendees, enabling influence propagation through word-of-mouth; iii) *event-to-online edges*: connect offline events to online platforms, representing users who share event-related content or engage with digital promotions after attending.

To effectively model influence propagation, GNNs and graph transformers, such as HGT [86] and HINormer [111], are utilized to capture the dependencies among various interactions, generating node representations that encode multi-faceted relationships within the network. These representations are then leveraged to derive activation probabilities, which serve as inputs for QOOA. In particular, Shi et al. [130] present a location-driven propagation model that describes online influence triggered by offline events, while Yang et al. [147] design a double-layer information propagation scheme to capture both online and offline behaviors.

3) The influence of *media outreach*, spanning both online and traditional channels, can be modeled by integrating a media interaction layer into the graph structure. This layer captures the relationship between media outlets and content, offering a more comprehensive view of influence propagation. It consists of media outlet nodes, representing sources such as newspapers, TV channels, radio stations, magazines, press agencies, online blogs, and outdoor advertising platforms, and content nodes, representing NFT-related articles, TV segments, radio interviews, press releases, blog posts, or outdoor ad campaigns. Edges include outlet-to-content connections, linking media outlets to the content they produce, with weights reflecting outlet reach and content prominence. This framework forms a multilayer network, comprising the original user-user social network and the media outreach layer. Inter-layer edges, connecting content to users who engage with it, represent different types of interactions (e.g., sharing, liking, viewing) and account for both online engagement (e.g., social shares, website visits) and traditional media exposure (e.g., estimated readership, TV ratings, and radio listenership).

The social connections and media influence can be integrated to allow QOOA to refine activation probabilities based on users' media exposure, effectively modeling the role of media outreach in shaping influence propagation. For example, Guo et al. [80] proposed a multi-scale propagation framework that incorporates both shallow propagation via meta-paths and deep propagation through graph neural networks for link prediction, effectively capturing influence in heterogeneous networks. Deng et al. [67] introduced the measuring influence model, which quantifies user influence based on heterogeneous factors such as interactions, social relationships, tags, and topics to integrate multi-faceted influence estimation into a network structure, demonstrating the importance of considering diverse media exposure channels in influence propagation.

G.3.2 Airdrop Hunters. The issue of airdrop hunters — individuals who exploit airdrop campaigns to accumulate free tokens without genuine engagement — poses a significant challenge in this paper and previous IM/RM/PM [54, 55, 61, 66, 72, 73, 82, 88, 90, 103, 113, 129, 137, 138, 141, 148]. These actors can undermine the effectiveness of marketing strategies by misrepresenting their influence to obtain airdrops, despite lacking meaningful engagement or impact. This problem is similar to fake influencers in e-commerce viral marketing. It has appeared in previous IM as preprocessing strategies by using 1) established bot detection algorithms from viral marketing, and 2) practical strategies to filter out candidate fake influencers used by e-commerce platforms. We could adopt those strategies before our main algorithm starts. Specifically, established bot detection algorithms are usually based on the following strategies. i) *Network structure* [105, 128, 145, 150]: Leverage community detection, clickstream clustering, centrality analysis, and registration graph analysis based on feature similarity derived from multi-faceted user attributes, including activity-based connections represented in a hypergraph model, to identify anomalous user accounts indicative of bot or fraudulent activity; ii) *Engagement and behavior* [84, 95]: Learn user embeddings from structural information (e.g., influencer engagement networks), textual data (e.g., comments), and profile metadata (including followers/following counts and profile descriptions), which are then analyzed using deep learning models, such as LSTMs for textual data and hybrid architectures for combined numerical and textual features, to detect abnormal patterns indicative of bot or fraudulent activity; iii) *Content and sentiment* [124]: Calculate post similarity using fuzzy concept analysis and topic extraction to identify irrelevant users; iv) *Friendship preference analysis* [114]: Analyze the characteristics of an account's social connections, comparing them to random connections within the network, to identify deviations indicative of bot or fraudulent activity. Practical strategies to filter fake influencer include: i) *Engagement ratios*: A low ratio between followers and likes/comments (e.g., 10,000 followers but

only 10 likes) suggests low-quality or artificial engagement; ii) *Follower quality*: High proportions of inactive or generic profiles (e.g., no posts or photos) may suggest ghost accounts or bots; iii) *Follower growth*: Gradual growth is typical. Sudden spikes may point to purchased followers; iv) *Engagement consistency*: Fluctuating interactions are normal; highly uniform engagement suggests automation or manipulation.

G.3.3 Ethical Implications. The ethical implications of aggressive airdropping strategies in the NFT ecosystem mirror those observed in e-commerce viral marketing. Such strategies can inadvertently perpetuate 1) biases and 2) disparities within the network. Specifically, algorithms that prioritize highly connected users for airdrops may exclude marginalized communities, thereby reinforcing existing network inequalities. To mitigate bias in seed selection, researchers have proposed i) rebalancing the seed group using feature-aware seeding methods [133] or ii) optimizing with equality constraints solvable via Mixed Integer Linear Programming [70]. Additionally, the focus on maximizing overall influence spread often results in unequal distribution of influence, disproportionately benefiting certain groups while leaving others—such as underrepresented demographics like females—unaffected. To address this disparity in influence spread, approaches such as i) learning the optimal balancing ratio with disparity seeding [140] or ii) applying multi-objective optimization with diversity constraints [142] have been proposed. Implementing these strategies within the NFT ecosystem could help mitigate similar ethical concerns arising from aggressive airdropping practices.

H Details on Experiments

H.1 Experimental Settings

Datasets. We conduct experiments on four NFT projects and three social networks. The NFT projects include i) Defimons Characters (Defi) [18]: The NFTs are the identities in the pixel world of Defimons, with traits like genders and locations. ii) Lascaux (Las) [25]: The NFTs record the art and performance of the artist Lascaux, with traits like utility and series. iii) Timpers Pixelworks (Tim) [46]: The NFTs are artworks by Timpers and top guest artists, with traits like artists. iv) Gutter Cat Gang (GCG) [22]: The NFTs are Gutter Cat Gang's premier level of membership, with traits like necklaces and hats. Table 4 summarizes the statistics of the NFT projects. To ensure a robust evaluation of NFT marketing strategies, we select these NFT projects with diverse rarity distributions. We analyze three key aspects—trait rarity, NFT rarity, and the ratio of NFTs with the rarest trait—to capture the broad spectrum of rarity structures across different datasets. 1) *Trait rarity*: Trait rarity measures the frequency of specific attributes within an NFT project, influencing user perception and demand. A broader range indicates greater diversity, with GCG displaying the widest variation, while Tim has the narrowest, suggesting more uniform traits. The remaining datasets fall in between. This diversity ensures that our evaluation encompasses both collections with highly exclusive traits and those where traits are more evenly distributed. 2) *NFT rarity*: NFT rarity, defined as the sum of an NFT's trait rarities, reflects its uniqueness within a project. Greater variation signifies a stronger distinction between common and rare NFTs. GCG exhibits the widest spread, followed by Las, while Tim and Defi display more uniform rarity distributions. This range ensures our experiments cover both highly stratified and balanced projects. 3) *Ratio of NFTs with the rarest trait*: This metric indicates the exclusivity of the rarest traits within each project. GCG has the lowest ratio, making its rarest traits highly exclusive, while Tim has the highest, suggesting broader accessibility. The remaining datasets offer intermediate levels of exclusivity. These differences ensure that our evaluation covers a wide range of rarity structures, from highly exclusive projects to those with more widely distributed rare traits.

The social networks based on NFT transactions include a) NBA (NBA Top Shot transactions) [29]: It contains 245K users and 2.6M relationships derived from 2.63M transactions. b) EthereumWAX [115] (collected primarily from Ethereum and WAX): It contains 269K users and 2.8M relationships derived from 7M transactions. c) Moralis [51] (collected via the Web3 APIs of the Moralis platform):[36] It contains 5.1M users and 30.6M relationships derived from 77M transactions. We follow [89, 149] to propagate social influence and follow [102, 106, 138] to set user preferences and activation probabilities. Following [115], the breeding and siring probabilities of a user u_i, β_i and γ_i, are set based on her activity strength. Following existing NFT projects, e.g., Trump Digital Trading Card [11] and MODragon [27], the quantity limit $l_k = 10$ for each n_k and the user breeding quota $c_{\mathrm{BQ}} = 5$ for each user. Following OpenSea [24], the reserve price p_k of each n_k is set to 1. Following [115], λ is set as 0.2 based on the proportion of NFTs successfully sold by current holders.

Baselines. We compare QOOA with five state-of-the-art approaches: Dysim [141], BGRD [54], RMA [82], TipTop [103], and AG [72]. Table 5 summarizes the characteristics of the baselines. The selected baselines for comparison capture different aspects of NRM, making them meaningful benchmarks for evaluation. Below, we outline key characteristics of NRM and identify which baselines incorporate these elements. 1) *Multiple items*: NRM optimizes airdrop selection across multiple NFTs rather than treating them as a single homogeneous entity, ensuring that each NFT has a distinct set of seed users. Among the baselines, Dysim, BGRD, and RMA also consider multiple items but in different contexts—Dysim optimizes influence across user-item-time triples, BGRD maximizes social welfare across different items, and RMA selects seed users for multiple advertisers. 2) *Different benefits per item or user*: In NRM, the value of an NFT varies across both NFTs and users, as different users may have distinct valuations for different NFTs. This characteristic reflects real-world variations in user preferences and market demand. Among the baselines, RMA accounts for different benefits across advertisers, TipTop considers different benefits per user, and AG models benefits at the edge level. 3) *Limited supply*: A key distinction of NRM is the supply constraint on each NFT, ensuring that only a fixed quantity of NFTs can be sold. This aspect sets NRM apart from traditional influence/revenue maximization problems, which typically assume unlimited supply. While none of the baselines explicitly incorporate supply constraints, we extend them by identifying seed users under different quantity settings and selecting the configuration that yields the highest revenue.

[36] https://moralis.io.

Table 4: Summary of NFT projects.

NFT project	#NFTs	#Traits	Min. trait rarity	Max. trait rarity	Min. NFT rarity	Max. NFT rarity	Ratio of NFTs with the rarest trait
Defi	16	10	2	16	2.29	10.29	18.75%
Las	17	10	1.21	17	4.05	39.89	23.53%
Tim	7	3	1.4	7	1.4	7	28.57%
GCG	3000	117	3.40	272.73	25.57	486.1	0.73%

Table 5: Summary of baselines.

Baseline	Optimization goal	Output	Multiple items	Limited supply	Different benefits per item or user
QOOA	Revenue	An airdrop group (users) for each NFT	✓	✓	✓
Dysim	Influence	A seed group (triples of user-item-time)	✓	✗	✗
BGRD	Social welfare	A seed group (users)	✓	✗	✗
RMA	Revenue	A seed group (users) for each advertiser	✓(advertisers)	✗	✓(each advertiser with its benefit)
TipTop	Benefit	A seed group (users)	✗	✗	✓(each user with its benefit)
AG	Benefit	A seed group (users)	✗	✗	✓(each edge with its benefit)

Specifically, for Dysim, RMA, and TipTop, the seeding cost is 1 for all users to be consistent with QOOA. For RMA, the cost-per-engagement of each advertiser is set to 1. Note that TipTop and AG aim to maximize the benefits of users and edges, respectively. The benefits are the gains of influencing either individual users or both end users of edges, instead of being uniform for every user as in Dysim, BGRD, and RMA. We thus set the benefits in relation to user valuations to better accommodate NRM. Moreover, as TipTop and AG typically focus on a single item, to facilitate breeding, we apply NFT recommendation based on trait similarity in [121] to encourage them to prioritize influencing users to hold multiple NFTs. For TipTop, the benefit to a user is set to the product of her valuation of n_k and the similarity between n_k and the NFTs she possesses, while that for AG is set to the product of the average valuation of n_k from both end users and the average similarity of the NFTs they hold. Since all baselines do not decide the quantities of NFTs for sale, we evaluate various quantities to find the one with the highest revenue.

Metrics. The performance metrics include i) revenue $f(S, Q)$, ii) the total transaction price $TP(S, Q)$, iii) the potential transaction prices of offspring $OS(S, Q)$, and iv) the execution time. We perform a series of sensitivity tests regarding 1) the budgets B, 2) the quantity limits L, 3) the reserve prices P, and 4) the user breeding quota c_{BQ}. We conduct a case study on different breeding mechanisms to gain deeper insights, as well as an ablation study on QOOA to evaluate the efficacy of SCR-based pruning, VQI-based pruning, and ORE.

We conduct all experiments on an HP DL580 server with an Intel 2.10GHz CPU and 1TB RAM. Each simulation result is averaged over 100 samples.

H.2 Additional Experiments

H.2.1 Large-scale NFT Project. In this section, we present a comparison between QOOA and baselines in promoting the large-scale NFT project, GCG, with 3000 NFTs and 117 traits on the *NBA* social network with 245K users. Following GCG's floor price [22], we set the reserve price to 870 to reflect the real-world total volume of GCG, where the total volume is the cumulative transaction prices of all GCG NFTs traded in the marketplace.

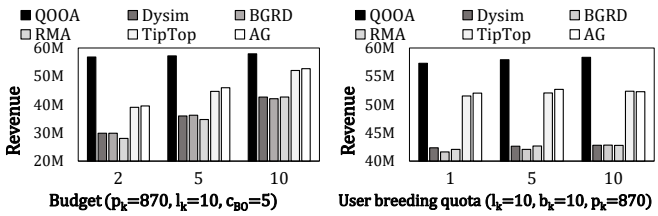

(a) f vs B. (b) f vs c_{BQ}.

Figure 11: Additional experimental results on large-scale NFT project (GCG-*NBA*).

Figure 11(a) compares the revenue across different budgets. QOOA consistently achieves the highest revenue, particularly when the budget is low. Since QOOA accounts for quantity constraints when identifying airdrops, it effectively targets users with the highest valuations and maximizes revenue. In contrast, the baselines focus on all influenced users, implying that under limited budgets, users with the highest valuations may not have a sufficiently high probability of being influenced, resulting in lower revenue. Compared to TipTop and AG, which prioritize users with high valuations, Dysim, BGRD, and RMA focus solely on maximizing the number of influenced users without considering their transaction prices. As a result, they may target users with low valuations who are unable to meet the high reserve price, thereby limiting revenue growth even as the budget increases.

Figure 11(b) further evaluates revenue under varying user breeding quotas. Baselines achieve relatively higher revenue compared to their performance on Defi-*NBA* (as shown in Figure 4(a)). This difference arises because GCG comprises 3000 NFTs, whereas Defi contains only 16, increasing the likelihood of users engaging in collaborative breeding with friends. In contrast, QOOA consistently generates high revenue across both datasets by effectively adjusting airdrops to facilitate both individual and collaborative breeding, thereby maximizing overall revenue. However, since the baselines do not strategically select airdrops to encourage friend groups to collectively acquire rare-trait NFTs, they fail to generate a substantial number of valuable offspring, leading to relatively lower revenue.

Table 6: Comparison of factors in BGRD, RMA, and QOOA.

	Breeding	Distinct airdrops under diff. quantities	Distinct airdrops for diff. NFTs
BGRD	✗	✗	✗
RMA	✗	✗	✓
QOOA	✓	✓	✓

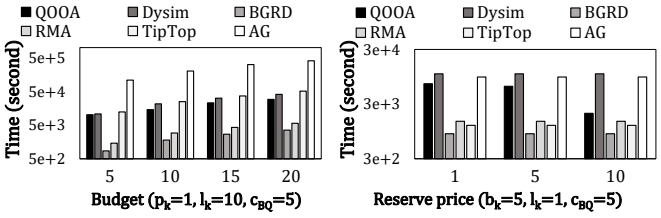

(a) Time vs B (Defi-*NBA*). (b) Time vs P ((Defi-*NBA*).

Figure 12: Additional experimental results for execution time.

Moreover, as c_{BQ} increases, QOOA achieves a moderate increase in revenue by incorporating the constraint of c_{BQ} when tailoring airdrops to maximize the value of bred offspring. A more relaxed quota provides greater flexibility for QOOA to optimize the airdrops. In contrast, the baselines remain largely unaffected by variations in c_{BQ}, as they do not optimize for breeding, resulting in minimal impact from changes in the breeding quota.

H.2.2 Execution Time Comparison. Figures 12(a) and 12(b) compare the execution time Defi-*NBA* under different budgets and reserve prices, respectively. QOOA requires slightly more time than some baselines since it carefully determines the airdrops to encourage RTCs and their friends to purchase multiple NFTs with rare traits. Additionally, QOOA carefully examines various quantities to determine the best airdrops that maximize revenue. Nevertheless, BGRD and RMA exhibit faster performance by considering fewer factors, as summarized in Table 6. Specifically, both methods entirely neglect breeding. BGRD selects only the most influential users for airdrops, assigning them to promote all NFTs indiscriminately. Although RMA allocates different airdrops for distinct NFTs, it fails to account for variations in user valuations across NFTs, often resulting in suboptimal revenue outcomes. Moreover, neither BGRD nor RMA considers that user valuations may vary with different quantities; consequently, they identify the same airdrops regardless of the quantity q_k chosen for each n_k, thereby eliminating the need to repeatedly evaluate airdrops across varying quantities and significantly reducing computational overhead. In summary, the quantity-agnostic baselines (i.e., Dysim, BGRD, and RMA) do not spend time in identifying airdrops with various potential quantities. BGRD usually requires the least time since it does not perform separate searches for airdrops corresponding to different NFTs. RMA and TipTop are more efficient than Dysim and AG, respectively, by leveraging reverse influence sampling to identify airdrops.

As shown in Figure 12(a), when more budgets are allocated, all approaches require more time. This is because a larger airdrop budget increases the number of potential recipients, leading to a longer search. However, QOOA leverages SCR to mitigate the overhead, resulting in a less pronounced increase in execution time compared to other baselines as the budget grows. On the other hand, in Figure 12(b), as the reserve price increases, the efficacy of VQI becomes more pronounced, leading to more effective pruning in QOOA. Hence, the execution time of QOOA decreases with higher reserve prices. In contrast, all baselines do not account for reserve prices; thus, they cannot leverage reserve prices to reduce execution time.

H.3 Case Study

In the case study, we configure the parameters according to the specifications of Defimons Characters [18]. The floor price (1.86) is used as the reserve price, while the issuance quantity, ranging from 15 to 2800, serves as the respective quantity limit. Following [1, 27], the airdrop budget is set at 1% of each NFT's issuance quantity, i.e., ranging from 1 to 28, and the user breeding quota c_{BQ} is set to 5.

H.3.1 Empirical Results. Figure 13(a) compares the revenue from original NFTs (TP) and offspring (OS) across different approaches on the *NBA* social network. QOOA consistently outperforms all baselines in TP, OS, and overall revenue. It is important to note that QOOA assigns a quantity of 5 and 4 to the rarest NFTs, `Apollo` and `Nova`, respectively, while setting a quantity of 3 for the second-rarest NFT, `Leo`. For the remaining NFTs, half are assigned a quantity of 2, and the other half a quantity of 1. The rationale for the quantity determination is that the three rarest NFTs, `Apollo`, `Nova`, and `Leo`, possess the rarest traits, inherently conferring higher value within the Defimons Characters project. Although increasing the for-sale quantity can slightly reduce scarcity, the intrinsic value of these NFTs remains relatively high, enabling a larger user base to acquire them at favorable transaction prices and thereby generating higher overall revenue. In contrast, NFTs lacking rare traits are of lower value; increasing their quantity would further depress user valuations for them, potentially causing it to fall below the reserve price. Consequently, QOOA assigns higher quantities to rare NFTs to enhance availability while maintaining value, whereas it limits the quantity of lower-value NFTs to prevent excessive depreciation, effectively balancing scarcity with widespread adoption. In contrast, TipTop and AG assign a quantity of 2 only to the rarest NFTs, `Apollo` and `Nova`, while all other NFTs are set to 1. Since user valuation decreases as the quantity increases and they do not incorporate quantity constraints, they tend to set most quantities to 1 to maximize revenue. Similarly, Dysim, BGRD, and RMA, which focus solely on influence spread and remain unaffected by quantity variations, set the quantity of all NFTs to 1.

Beyond quantity determination, we observe that QOOA effectively leverages ORE to tailor airdrops and further enhance revenue. During the ORE step, QOOA adjusts airdrops for the three treasures: `Apollo`, `Nova`, and `Leo`. The first adjustment occurs in `Apollo`, where QOOA examines 71% of airdrops for potential replacement (i.e., their VOGUE is lower than that of non-airdrop users), and among them, 85% are ultimately replaced with alternative airdrops. As QAS of QOOA does not consider breeding and thus prioritizes users who contribute to high TP, ORE then evaluates users based on B-Index to jointly consider their contributions to both TP and OS,

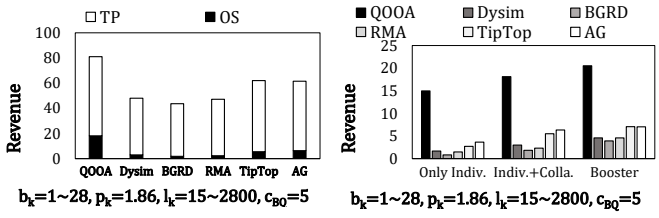

(a) *TP* vs *OS*. (b) *OS* vs breeding.

Figure 13: Case study (Defi-*NBA*).

thereby effectively identifying suitable airdrop alternatives. The second adjustment involves Nova. Since the prior adjustment to Apollo has already facilitated both individual and collaborative breeding, QOOA efficiently narrows the evaluation scope to only 14% of Nova's airdrops by utilizing VOGUE, among which 75% are replaced. These results further validate that the alternative airdrops selected by ORE, i.e., those with high VOGUE, consistently lead to a greater likelihood of achieving higher revenue compared to the original airdrops, demonstrating the efficacy of the VOGUE and B-Index design. Finally, due to the preceding adjustments, all airdrops of Leo exhibit higher VOGUE than non-airdrop users, terminating ORE without further modifications.

In addition to *Individual and Collaborative Breeding* (Indiv.+Colla.), we additionally evaluate other breeding: *Only Individual Breeding* (Only Indiv.) and *Booster*. Figure 13(b) compares the potential transaction prices of offspring (*OS*) across various approaches on *NBA*. QOOA consistently outperforms baselines. As *Booster* boosts the likelihood of inheriting rare traits, QOOA tailors airdrops for treasures by giving priority to RTCs with a booster to acquire them. It increases the probability of breeding offspring with rare traits, ultimately resulting in the highest *OS* among all mechanisms. In contrast, *Only Individual Breeding* limits breeding to individual ownership, reducing the flexibility of QOOA in tailoring airdrops and resulting in the lowest *OS* among the three mechanisms. By favoring users who may possess similar NFTs, TipTop and AG tend to facilitate airdrops that lead to more offspring generation compared to other baselines. However, they fail to maximize the pairing of rare-trait NFTs to produce offspring with rarer traits, resulting in low-value offspring. Consequently, they still achieve significantly lower *OS* compared to QOOA. In contrast, other baselines prioritize airdrops that maximize influence spread without taking breeding into consideration, thus resulting in negligible *OS*.

H.3.2 Case Analysis. In this case study, we observe that the selection of airdrop recipients may vary depending on the quantity. For User #1589: when using QOOA, if the quantity is set to 1, the probability of being selected as an airdrop recipient for Nova is only 0.12, as the likelihood of influencing User #91620 (who has the highest valuation for Nova at 5.67) is nearly zero. Under this condition, airdrop selection is primarily concentrated among the 2-hop friends of User #91620. However, when the quantity increases to 4, the probability of airdropping Nova to User #1589 rises to 0.49. This increase is driven by the presence of two 1-hop friends, User #8837 and User #81, who exhibit relatively high valuations for Nova at 2.51 and 2.39, respectively. Additionally, User #1589 has activation probabilities of 0.8 and 0.84 toward these users. As a result, selecting User #1589 under a quantity of 4 leads to an expected revenue of at least 4.02.

In contrast, when using BGRD, with a quantity of 1, User #1589 is selected as the airdrop recipient for Nova with a probability of 0.02, as the expected number of influenced users across the entire social network is 9.4. When the quantity increases to 4, their selection probability remains unchanged at 0.02, since the expected number of influenced users does not vary with quantity.

Similarly, when using TipTop, with a quantity of 1, User #1589 is selected with a probability of 0.06. Although they are expected to influence 9.4 users, the valuations of these users are relatively high (e.g., User #8837 and User #81), resulting in an expected revenue of 26 across the entire social network. In contrast, another user, User #549, who is also expected to influence 9.4 users, primarily influences those with valuations below the reserve price, yielding an expected revenue close to 0. As a result, their probability of being selected for the airdrop is nearly 0. When the quantity increases to 4, User #1589's selection probability remains at 0.06. Although the increase in quantity reduces their expected revenue to 12.6, the expected revenue of all users declines proportionally, resulting in an unchanged selection probability.

Besides, we observe that different breeding mechanisms result in varied outcomes. For User #77, who is likely to acquire the NFT Apollo (featuring the rarest trait Luck with a rarity of 16) through QAS's airdrops, ORE's adjustments lead to different results under different breeding mechanisms.

1) In *Only Individual Breeding*, since User #77 has a breeding probability of 0.8 and an impact of 0.68 (evaluated by PageRank), ORE is inclined to influence them to acquire an additional NFT Nova (featuring Hidden Village with a rarity of 16). While their initial probability of generating offspring is nearly zero, it now stands at about 0.64 due to their acquisition of enough NFTs for breeding. Furthermore, the generated offspring has a 0.12 probability of inheriting the rarest trait (Luck or Hidden Village), resulting in a significant increase in *OS*. In contrast, although TipTop also selects airdrops that are highly likely to influence User #77 to acquire Apollo, its airdrop of Nova has only a 0.04 probability of leading to User #77's adoption, as TipTop prioritizes influencing a larger group of users with high valuations.

2) In *Individual and Collaborative Breeding*, users can utilize their friends' siring-ready NFTs to breed offspring together. User #77's friend, User #1062, with a siring probability of 0.6, becomes highly likely to acquire the NFT Nova as well after ORE. As User #1062 is likely to provide Nova for siring, the chance of User #77 to generate offspring inheriting the rarest trait (Luck or Hidden Village) becomes 0.12, since collaborative breeding allows User #77 to breed. Consequently, by adjusting airdrops to influence the friends of RTCs, ORE can enhance the likelihood of achieving higher *OS*. By contrast, while Dysim's airdrop of Apollo and Nova may also influence User #1062 to acquire both NFTs, their breeding probability is only 0.1, resulting in a 0.01 probability of producing offspring. Note that, as previously discussed, Dysim assigns a quantity of 1 to all NFTs, making the likelihood of User #1062 and User #77 each acquiring a different NFT (necessary for collaborative breeding) extremely low.

3) In *Booster* (which increases the inheritance probability of the rarest trait by introducing an additional independent trial, ensuring

that the trait is inherited if at least one of the two attempts is successful), when User #77 possesses a booster, ORE tends to encourage User #77's friend, User #847, who has a siring probability of 0.8, to also acquire Apollo for siring. It assists User #77 in breeding offspring with the rarest trait Luck, boosting the inheritance probability from 0 to 0.23 due to collaborative breeding and the booster. While collaborative breeding allows User #77 to breed offspring with a 0.12 probability of inheriting the rarest trait, the booster increases the probability to 0.23. This demonstrates that ORE, by encouraging the friends of RTCs with boosters to purchase rare-trait NFTs, effectively increases OS. By contrast, since BGRD's airdrops influence User #77 to acquire NFTs with the rarest traits (i.e., Apollo, Nova, and Leo) with probabilities of only 0.13, 0.02, and 0.06, respectively, their likelihood of engaging in breeding remains low. Consequently, even if the booster increases the probability of offspring inheriting the rarest trait, the overall expected revenue from the offspring remains negligible.